The GOES-15 Science Test:
Imager and Sounder Radiance and Product Validations

Editors:

Donald W. Hillger[1] and Timothy J. Schmit[3]

Other Contributors:

Americo Allegrino[6], A. Scott Bachmeier[4], Andrew Bailey[6], Eric Brunning[10], Hyre Bysal[13], Jerry Cantril[16], Lawrence Carey[15], Jaime M. Daniels[5], Prasanjit Dash[2], Michael Grotenhuis[6], Mathew M. Gunshor[4], Jay Hanna[12], Andy Harris[10], Michael P. Hiatt[2], John A. Knaff[1], Jun Li[4], Daniel T. Lindsey[1], Eileen M. Maturi[9], Kevin Micke[2], Jon Mittaz[10], Debra Molenar[1], James P. Nelson III[4], Walt Petersen[14], Robert Potash[11], Elaine Prins[17], Gordana Rancic[6], Dale G. Reinke[2], Christopher C. Schmidt[4], Anthony J. Schreiner[4], Christopher Schultz[15], Dustin Sheffler[12], Dave Stettner[4], William Straka III[4], Chris Velden[4], Gary S. Wade[3], Steve Wanzong[4], Dave Watson[2], Xiangqian (Fred) Wu[7], and Fangfang Yu[8]

Affiliations:

[1]StAR/RAMMB (SaTellite Applications and Research/Regional and Mesoscale Meteorology Branch)
[2]CIRA (Cooperative Institute for Research in the Atmosphere), Colorado State University, Fort Collins

[3]StAR/ASPB (SaTellite Applications and Research/Advanced Satellite Products Branch)
[4]CIMSS (Cooperative Institute for Meteorological Satellite Studies)
University of Wisconsin, Madison

[5]StAR/OPDB (SaTellite Applications and Research/Operational Products Development Branch)
[6]I.M. Systems Group, Inc. (IMSG), Rockville, Maryland

[7]StAR/SPB (SaTellite Applications and Research/Sensor Physics Branch)
[8]ERT, Inc., Annapolis Junction, MD

[9]StAR/SOCD (SaTellite Applications and Research/Satellite Oceanography and Climatology Division)
[10]CICS (Cooperative Institute for Climate Studies)
University of Maryland, College Park
[11]Science Systems and Applications, Inc. (SSAI)

[12]NOAA/NESDIS Satellite Analysis Branch (SAB)
[13]NOAA/NESDIS Office of Satellite and Product Operations (OSPO)

[14]NASA/MSFC (Marshall Space Flight Center), Earth Sciences Office
[15]University of Alabama, Huntsville, Department of Atmospheric Science

[16]Columbus, Inc.

[17]CIMSS – Consultant, Grass Valley, CA

TABLE OF CONTENTS

LIST OF TABLES

LIST OF FIGURES

Executive Summary of the GOES-15 NOAA Science Test

The Science Test for GOES-15 produced several results and conclusions:

- GOES-15 Imager and Sounder data were collected during the six-week NOAA Science Test that took place during August/September 2010 while the satellite was stationed at 89.5ºW longitude. Additional pre-Science Test data, such as the first visible and IR images, were collected in April 2010.

- Imager and Sounder data were collected for a host of schedules, including rapid scan imagery. The GOES Variable (GVAR) data stream was stored at several locations for future access.

- Data collected through Keep Out Zones (KOZ) were tested to ultimately provide additional imagery affected by solar contamination. These data are being used in a stray-light correction and notification algorithm that is being considered for operational implementation.

- Initial Infrared Atmospheric Sounding Interferometer (IASI) and Atmospheric Infrared Sounder (AIRS) high-spectral-resolution inter-calibrations with both the Imager and Sounder were verified for good radiometric accuracy, although biases were seen for bands 3 and 6 of the Imager.

- These Imager biases have been reduced by modifying, and operationally implementing, the updated system Spectral Response Functions (SRFs) for Imager bands 3 and 6.

- The GOES Sounder instrument noise was comparable to the other GOES-N/O/P Sounders, after the Sounder patch temperature was controlled at the low level. Some striping remains, especially in band-15.

- Many Level 2 products were generated (atmospheric profiles and derived parameters, Atmospheric Motion Vectors (AMVs), cloud-top properties, Clear Sky Brightness Temperature (CSBT), Lifted Index (LI), Sea Surface Temperature (SST), total column ozone, surface insolation products, etc.) and validated.

- Various application areas, such as precipitation, volcanoes and fires, were also investigated.

- Many GOES-15 images and examples were posted on the Web in near real-time.

- Special rapid-scan imagery was acquired, which offers a glimpse into the possibilities of the next generation geostationary imagers.

Instrument related results and conclusions:

- The detector size of the Imager 13.3 μm band (band-6) was changed from 8 km to 4 km by incorporating two detectors instead of one. The GVAR format was modified, similar to the GOES-14 changes, to accommodate the extra detector.

- In order to operate the instruments (Imager and Sounder) during the eclipse periods and KOZ periods, improved spacecraft batteries and partial-image frames were utilized. Improved instrument performance means there will no longer be the required health and safety related KOZ outages.

- Colder patch (detector) temperatures were noted due to the new spacecraft design. In general, Imager and Sounder data from GOES-13 through GOES-15 are improved considerably in quality (noise level) to that from GOES-8 through GOES-12.

- The image navigation and registration with GOES-13 through GOES-15 are much improved, especially in comparison to GOES-8 through GOES-12.

- There is a potential reduction in detector-to-detector striping to be achieved through increasing the Imager scan-mirror dwell time on the blackbody from 0.2 s to 2 s.

- During the GOES-15 Post-Launch Science Test (PLT), from 11 August 2010 to 22 September 2010, the Imager patch temperature was controlled at low-level. Imager calibration related telemetries were all functioning normally.

- The Sounder, however, had the so-called "blanket-heating" problem when the spacecraft was oriented in the upright position. During these two upright position periods, the Sounder patch temperature could not be controlled at low-level and experienced diurnal variations. These floating patch temperatures caused large detector noise, especially for the detectors at the longwave bands.

- The Sounder patch control issue was characterized as due to the additional heat reflection from a dislocated insulation blanket. This issue will be mitigated with satellite yaw-flips twice a year around each equinox.

- Compared to GOES-11/12, GOES-N/O/P satellites have much better quality of visible data in terms of reduced noise.

1. Introduction

The latest Geostationary Operational Environmental Satellite (GOES), GOES-P, was launched on 4 March 2010, and reached geostationary orbit at 89.5°W on 16 March 2010 to become GOES-15. The plans are to use the GOES-15 Imager and Sounder operationally as the Western GOES beginning in December of 2011. GOES-15 is the third, and final, of the three GOES-N/O/P series spacecraft.

The National Oceanic and Atmospheric Administration (NOAA)/National Environmental Satellite, Data, and Information Service (NESDIS) conducted a six-week GOES-15 Science Test that began 11 August 2010 and ended officially on 22 September 2010. The first three weeks of the Science Test were integrated within the National Aeronautics and Space Administration (NASA) GOES-15 Post-Launch Test (PLT) schedule. An additional three weeks of the Science Test were performed under NOAA/NESDIS control.

GOES-15 has an Imager and Sounder similar to those on GOES-8/12, but GOES-15, like GOES-13 and GOES-14, is on a different spacecraft bus. The new bus allows improvements both to navigation and registration, as well as the radiometrics. Due to larger spacecraft batteries, the GOES-N/O/P system is able to supply data through the eclipse periods, thereby addressing one of the major limitations of eclipse and related outages. Outages due to Keep Out Zones (KOZ) are also minimized. In terms of radiometric improvements, a colder patch (detector) temperature results in the GOES-13/14/15 instruments (Imager and Sounder) being less noisy. In addition, there is a potential reduction in detector-to-detector striping to be achieved through increasing the Imager scan-mirror dwell time on the blackbody from 0.2 s to 2 s. Finally, the navigation was improved due to the new spacecraft bus and the use of star trackers (as opposed to the previous method of edge-of-earth sensors). In general, the navigation accuracy (at nadir) improved from between 4-6 km with previous Imagers, to less than 2 km with those on the GOES-N/O/P satellites.

Figure 1.1: GOES-P/15 spacecraft decal.

This report describes the NOAA/NESDIS Science Test portion only. The Imager and Sounder are covered, while the solar/space instruments are not. System performance and operational testing of the spacecraft and instrumentation was performed as part of the PLT. During the Science Test, GOES-15 was operated in a special test mode, where the default schedule involved routine emulation of either GOES-East or GOES-West operations. Numerous other scan schedules and sectors were constructed and used for both the Imager and the Sounder. GOES-15 was then placed into standby mode on 25 October 2010. At the time of the GOES-15 Science Test, GOES-13 was operating in the GOES-East position, and GOES-11 was operating in the GOES-West position.

1.1. Goals for the GOES-15 Science Test

First goal: To assess the quality of the GOES-15 radiance data. This evaluation was accomplished through comparison to data from other satellites or by calculating the signal-to-noise ratio compared to specifications, as well as assessing the striping in the imagery due to multiple detectors.

Second goal: To generate products from the GOES-15 data stream and compare to those produced from other satellites. These products included several Imager and Sounder products: land skin temperatures, temperature/moisture retrievals, Total Precipitable Water (TPW), Lifted Index (LI), cloud-top pressure, Atmospheric Motion Vectors (AMVs), surface insolation, and Sea Surface Temperatures (SSTs). Validation of these products was accomplished through comparisons to products generated from other satellites or through comparisons to radiosondes and ground-based instruments.

Third goal: To collect nearly-continuous rapid-scan imagery of interesting weather cases at temporal resolutions as fine as every 30 seconds, a capability of rapid-scan imagery from GOES-R that is not implemented operationally on the current GOES. The rapid-scan data may augment radar and lightning data, collected at special networks, to investigate the potential for improving severe weather forecasts.

Fourth goal: To monitor the impact of any instrument changes. Changes included the finer spatial resolution (detector sizes from 8 km to 4 km) for the Imager 13.3 μm band (band-6) which began on GOES-14. Other improvements which began with GOES-13 include: better navigation, improved calibration, and the capabilities of the GOES-N series to operate through eclipse, when the satellite is in the shadow of the earth, as well as to minimize outages due to KOZ, when the sun can potentially contaminate imagery by being within the Field Of View (FOV) of the instruments (Imager and Sounder).

Finally, the GOES-15 Imager and Sounder data were received via direct downlink at the following sites: (1) CIRA, Colorado State University, Fort Collins CO; (2) Space Science and Engineering Center (SSEC), University of Wisconsin-Madison, Madison WI; and (3) NOAA/NESDIS, Suitland/Camp Springs MD. Each site ingested, archived, and made the data available on its own internal network in McIDAS (Man computer Interactive Data Access System) format, as well as to other sites as needed. The NOAA-NESDIS Regional and

Mesoscale Meteorology Branch (RAMMB) at CIRA also made the GOES-15 imagery available over the internet via RAMM Advanced Meteorological Satellite Demonstration and Interpretation System (RAMSDIS) Online. Image and product loops were also made available on the Cooperative Institute for Meteorological Satellite Studies (CIMSS) Web site. See Appendix A for the appropriate URLs for these and many other GOES-15 related Web sites. Other sites, such as NASA Goddard Space Flight Center (GSFC) also directly received the GOES-15 data stream.

This report documents results from these various activities undertaken by NOAA/NESDIS and it's Cooperative Institutes during the Science Test. Organizations which participated in these GOES-15 Science Test activities included the: NOAA/NESDIS SaTellite Applications and Research (StAR), NOAA/NESDIS Office of Satellite and Product Operations (OSPO), Cooperative Institute for Meteorological Satellite Studies (CIMSS), Cooperative Institute for Research in the Atmosphere (CIRA), NOAA/NESDIS Satellite Analysis Branch (SAB), and NASA Marshall Space Flight Center (MSFC). The GOES-15 NOAA Science Test was co-led by D. Hillger and T. Schmit, both of NOAA/NEDSIS/StAR.

NOAA Technical Reports similar to this one were produced for the **GOES-11** (Daniels et al. 2001), **GOES-12** (Hillger et al. 2003), **GOES-13** (Hillger and Schmit, 2007 and 2009), and **GOES-14** (Hillger and Schmit 2010) Science Tests. The reference/bibliography section contains articles related to the GOES-15 Science Test.

2. Satellite Schedules and Sectors

A total of eight schedules involving numerous predefined Imager and Sounder sectors were constructed for the GOES-15 Science Test. The choice of Imager and Sounder sectors was a result of input from the various research and development groups participating in the Science Test. Most of these schedules are similar to those run during the previous (GOES-14) Science Test (Hillger and Schmit 2010).

Thanks to dedicated support provided by the NOAA/NESDIS/Satellite Operations Control Center (SOCC) and the Office of Satellite and Product Operations (OSPO), a significant amount of flexibility existed with respect to switching and activating the schedules on a daily basis. The ease with which the schedules could be activated was important for capturing significant weather phenomena of varying scales and locations during the Science Test.

A brief summary of the eight schedules is provided in Table 2.1. The C5RTN and C4RTN schedules, emulating GOES-East and GOES-West operations respectively, were the default schedules if no other schedule was requested at the cutoff of one hour before the 1630 UTC daily schedule change time. For the Sounder, the default schedules also emulated normal GOES-East and GOES-West operations.

The C1CON schedule was mainly for emulating the temporal aspects of the GOES-R Advanced Baseline Imager (ABI) data, where five-minute images will be routine over the Continental United States (CONUS). The C2SRSO and C3SRSO schedules, with images at 1-minute and 30-second intervals respectively, were prepared to provide the ability to call up Super Rapid Scan Operations (SRSO) during the Science Test. It should be noted that the 30-second interval schedule was not executed, in part to better maximize capturing the rapidly-changing

phenomena. This change is due to the fact that the 30-second scans cover a much smaller area than the 1-minute scans. The C6FD schedule allowed continuous 30-minute interval full-disk imaging of the entire hemisphere, although the ABI will be able to scan the full disk every 15 minutes. The C7MOON schedule provided specialized datasets of the moon, and the C8HUR sector allowed a special 5-minute CONUS-sized hurricane sector, with a specified center point. Finally, the alternate C59RTN schedule contained partial-image frames that will be available to users during KOZ, to avoid solar contamination radiances and the detrimental effect on image products.

The daily implementation of the various schedules during the entire Science Test is presented in Table 2.2. The GOES-15 daily call-up began on 11 August 2010 and continued through 21 September 2010. GOES-15 continued to collect imagery for five more weeks, through 25 October 2010, before the GOES-15 Imager and Sounder were turned off.

Table 2.1: Summary of Science Test schedules for GOES-15.

Test Schedule Name	Imager	Sounder	Purpose
C1CON	Continuous 5-minute CONUS sector	26-minute CONUS sector every 30 minutes	Test navigation, ABI-like (temporal) CONUS scans
C2SRSO	Continuous 1-minute rapid-scan (with center point specified for storm analysis)	26-minute CONUS sector every 30 minutes	Test navigation, ABI-like (temporal) mesoscale scans
C3SRSO	Continuous 30-second rapid-scan (with center point specified for storm analysis)	26-minute CONUS sector every 30 minutes	Coordination with lightning detection arrays in Huntsville AL, Norman OK, and Washington DC areas[1]
C4RTN	Emulation of GOES-**West** routine operations[2]	Emulation of GOES-**West** routine operations[2]	Radiance and product comparisons
C5RTN (and C59RTN)[4]	Emulation of GOES-**East** routine operations	Emulation of GOES-**East** routine operations	Radiance and product comparisons
C6FD	Continuous 30-minute Full Disk (including off-earth measurements)	Sectors on both east and west limbs every hour (including off-earth measurements)[3]	Imagery for noise, striping, etc.
C7MOON (depends on moon availability)[4]	Capture moon off edge of earth (when possible) for calibration purposes	Inserted into current schedule	Test ABI lunar calibration concepts
C8HUR	Continuous 5-minute CONUS-size hurricane sector	Emulation of GOES-East routine operations	Hurricane monitoring for tropical cyclone field experiments[5]

[1]Including the Hazardous Weather Testbed in North Alabama (centered at Huntsville AL, 34.72°N, 86.65°W), the Oklahoma Lightning Mapping Array (centered at Norman OK, 35.28°N, 97.92°W), and the Washington DC lightning mapping array (centered over Falls Church VA, 38.89°N, 77.17°W).
[2]During the C4RTN and C5RTN schedules, special stray-light test sectors for both the Imager and Sounder were taken between 0400 and 0800 UTC starting 23 August 2010 [Julian Day 235].
[3]Limb sectors similar to GOES Sounder scans during previous GOES Science Tests.
[4]Successive images of the moon were captured on 26 April, 30 July, and 27 August 2010.
[5]In un-official support of two large field campaigns (NASA GRIP and NSF PREDICT).

Table 2.2: Daily implementation of GOES-15 Science Test schedules (Daily starting time: 1630 UTC).

Starting Date [Julian Day] (Day of Week)	Science Test Schedule Name	Imager	Sounder	Purpose
Start of 6-week Science Test				
August 11 [223] (Wednesday)	C1CON	Continuous 5-minute CONUS sector	26-minute CONUS sector every 30 minutes	ABI-like (temporal) CONUS scans
August 12 [224] (Thursday)	C1CON	Continuous 5-minute CONUS sector	26-minute CONUS sector every 30 minutes	ABI-like (temporal) CONUS scans
August 13 [225] (Friday)	C1CON	Continuous 5-minute CONUS sector	26-minute CONUS sector every 30 minutes	ABI-like (temporal) CONUS scans
August 14 [226] (Saturday)	C5RTN	Emulation of GOES-**East** routine operations	Emulation of GOES-**East** routine operations	Radiance and product comparisons
August 15 [227] (Sunday)	C5RTN	Emulation of GOES-**East** routine operations	Emulation of GOES-**East** routine operations	Radiance and product comparisons
August 16 [228] (Monday)	C1CON	Continuous 5-minute CONUS sector	26-minute CONUS sector every 30 minutes	ABI-like (temporal) CONUS scans
August 17 [229] (Tuesday)	C1CON	Continuous 5-minute CONUS sector	26-minute CONUS sector every 30 minutes	ABI-like (temporal) CONUS scans
August 18 [230] (Wednesday)	C5RTN	Emulation of GOES-**East** routine operations	Emulation of GOES-**East** routine operations	Radiance and product comparisons
August 19 [231] (Thursday)	C5RTN	Emulation of GOES-**East** routine operations	Emulation of GOES-**East** routine operations	Radiance and product comparisons
August 20 [232] (Friday)	C5RTN	Emulation of GOES-**East** routine operations	Emulation of GOES-**East** routine operations	Radiance and product comparisons
August 21 [233] (Saturday)	C6FD	Continuous 30-minute Full Disk	Sectors on both east and west limbs every hour	Imagery for noise, striping, etc.
August 22 [234] (Sunday)	C6FD	Continuous 30-minute Full Disk	Sectors on both east and west limbs every hour	Imagery for noise, striping, etc.
August 23 [235] (Monday)	C8HUR	Continuous 5-minute CONUS-size hurricane sector	Emulation of GOES-East routine operations	Hurricane monitoring
August 24 [236] (Tuesday) starting 0900 UTC	C2SRSO[1]	Continuous 1-minute rapid-scan (center point 18°N, 46°W)	26-minute CONUS sector every 30 minutes	Hurricane (Danielle) monitoring
August 24 [236] (Tuesday) starting 2100 UTC	C8HUR	Continuous 5-minute CONUS-size hurricane sector	Emulation of GOES-East routine operations	Hurricane monitoring

August 25 [237] (Wednesday)	C4RTN	Emulation of GOES-**West** routine operations	Emulation of GOES-**West** routine operations	Radiance and product comparisons
August 26 [238] (Thursday)	C4RTN	Emulation of GOES-**West** routine operations	Emulation of GOES-**West** routine operations	Radiance and product comparisons
August 27 [239] (Friday)	C4RTN	Emulation of GOES-**West** routine operations	Emulation of GOES-**West** routine operations	Radiance and product comparisons
August 27 [239] (Friday) ~1900 to ~2045 UTC	C7MOON	Capture moon off edge of earth	Inserted into current schedule	Test ABI lunar calibration concepts
August 28 [240] (Saturday)	C8HUR[2]	Continuous 5-minute CONUS-size hurricane sector	Emulation of GOES-East routine operations	Hurricane monitoring
August 29 [241] (Sunday)	C8HUR	Continuous 5-minute CONUS-size hurricane sector	Emulation of GOES-East routine operations	Hurricane monitoring
August 30 [242] (Monday)	C8HUR	Continuous 5-minute CONUS-size hurricane sector	Emulation of GOES-East routine operations	Hurricane monitoring
August 31 [243] (Tuesday) ~1715 to ~2130 UTC [Day 244]	Yaw Flip Maneuver	Not specified	Not specified	Due to yaw flip, no Science Test schedule available
September 1 [244] (Wednesday) starting ~2230 UTC	C8HUR	Continuous 5-minute CONUS-size hurricane sector	Emulation of GOES-East routine operations	Hurricane (Earl) monitoring
September 2 [245] (Thursday)	C1CON	Continuous 5-minute CONUS sector	26-minute CONUS sector every 30 minutes	ABI-like (temporal) CONUS scans, including Hurricane (Earl) monitoring
September 3 [246] (Friday) 0945 UTC to ~0045 UTC [Day 247]	C2SRSO	Continuous 1-minute rapid-scan (center point 39°N, 72°W)	26-minute CONUS sector every 30 minutes	Hurricane (Earl) monitoring
September 4 [247] (Saturday) starting 0045 UTC	C6FD	Continuous 30-minute Full Disk	Sectors on both east and west limbs every hour	Imagery for noise, striping, etc.
September 5 [248] (Sunday) starting 0045 UTC	C6FD	Continuous 30-minute Full Disk	Sectors on both east and west limbs every hour	Imagery for noise, striping, etc.
September 6 [249] (Monday) starting 0045 UTC	C5RTN	Emulation of GOES-**East** routine operations	Emulation of GOES-**East** routine operations	Radiance and product comparisons

September 7 [250] (Tuesday)	C1CON	Continuous 5-minute CONUS sector	26-minute CONUS sector every 30 minutes	ABI-like (temporal) CONUS scans
September 8 [251] (Wednesday)	C5RTN	Emulation of GOES-**East** routine operations	Emulation of GOES-**East** routine operations	Radiance and product comparisons
September 9 [252] (Thursday)	C5RTN	Emulation of GOES-**East** routine operations	Emulation of GOES-**East** routine operations	Radiance and product comparisons
September 10 [253] (Friday)	C5RTN	Emulation of GOES-**East** routine operations	Emulation of GOES-**East** routine operations	Radiance and product comparisons
September 11 [254] (Saturday)	C2SRSO	Continuous 1-minute rapid-scan (center point 35°N, 87°W)	26-minute CONUS sector every 30 minutes	Huntsville AL lightning mapping array
September 12 [255] (Sunday)	C5RTNS	Emulation of GOES-**East** routine operations	Emulation of GOES-**East** routine operations	Special Sounder sectors for striping analysis/abatement
September 13 [256] (Monday)	C2SRSO	Continuous 1-minute rapid-scan (center point 18°N, 51°W)	26-minute CONUS sector every 30 minutes	Hurricane (Igor) monitoring
September 13 [256] (Monday) starting 2200 UTC	C8HUR	Continuous 5-minute CONUS-size hurricane sector	Emulation of GOES-East routine operations	Hurricane (Igor) monitoring
September 14 [257] (Tuesday)	C8HUR	Continuous 5-minute CONUS-size hurricane sector	Emulation of GOES-East routine operations	Hurricane monitoring
September 15 [258] (Wednesday)	C8HUR	Continuous 5-minute CONUS-size hurricane sector	Emulation of GOES-East routine operations	Hurricane monitoring
September 16 [259] (Thursday)	C8HUR	Continuous 5-minute CONUS-size hurricane sector	Emulation of GOES-East routine operations	Hurricane monitoring
September 17 [260] (Friday) 1145 UTC to ~0045 UTC [Day 261]	C2SRSO[3]	Continuous 1-minute rapid-scan (center point 20°N, 96°W)	26-minute CONUS sector every 30 minutes	Hurricane (Karl) monitoring
September 18 [261] (Saturday) starting 0045 UTC	C8HUR	Continuous 5-minute CONUS-size hurricane sector	Emulation of GOES-East routine operations	Hurricane monitoring
September 19 [262] (Sunday)	C8HUR	Continuous 5-minute CONUS-size hurricane sector	Emulation of GOES-East routine operations	Hurricane monitoring
September 20 [263] (Monday)	C2SRSO	Continuous 1-minute rapid-scan (center point 39°N, 114°W)	26-minute CONUS sector every 30 minutes	Western fires and fog burnoff
September 21 [264] (Tuesday) starting 1245 UTC	C2SRSO	Continuous 1-minute rapid-scan (center point 41°N, 90°W)	26-minute CONUS sector every 30 minutes	Potential severe weather

End of 6-week Science Test				
Starting September 22 [265] (Wednesday)	**GOES-15 continued to operate through 24/25 October 2010 [Day 297/298]**, but with only two schedule options, either C5RTN or a C5RTN schedule with occasional hurricane sectors. At that point the Imager and Sounder were put into storage mode.			
September 23 and 24 [266 and 267] (Thursday and Friday) ~1900 to ~2045 UTC	C7MOON	Capture moon off edge of earth	Inserted into current schedule	Test ABI lunar calibration concepts

[1]There is a gap in the intended C2SRSO collection, between ~1445 and ~1839 UTC [Day 236].
[2]There is a large gap in the intended C8HUR collection, between ~1622 and ~0245 UTC [Day 241].
[3]There is a delay in the start of the C2SRSO collection, from ~1145 to ~1415 UTC [Day 260].

3. Changes to the GOES Imager from GOES-8 through GOES-15

The differences in spectral bands between the two versions of the GOES Imager (Schmit et al. 2002a) are explained in Table 3.1. Each version has five bands. The Imagers on GOES-8 through GOES-11 contain bands 1 through 5. The Imagers on GOES-12, 13, 14, and 15 contain bands 1 through 4 and band-6.

Table 3.1: GOES Imager band nominal wavelengths (GOES-8 through GOES-15).

GOES Imager Band	Wavelength Range (μm)	Central Wavelength (μm)	Meteorological Objective
1	0.53 to 0.75	0.65 (GOES-8/12) 0.63 (GOES-13/15)	Cloud cover and surface features during the day
2	3.8 to 4.0	3.9	Low cloud/fog and fire detection
3	6.5 to 7.0 5.8 to 7.3	6.75 (GOES-8/11) 6.48 (GOES-12/15)	Upper-level water vapor
4	10.2 to 11.2	10.7	Surface or cloud-top temperature
5	11.5 to 12.5	12.0 (GOES-8/11)	Surface or cloud-top temperature and low-level water vapor
6	12.9 to 13.7	13.3 (GOES-12/15)	CO_2 band: Cloud detection

The differences in the nominal spatial resolution between the more recent GOES Imager are explained in Table 3.2. The east-west over-sampling is not included in the table. The increased resolution of band-6 necessitated a change in the GOES Variable (GVAR) format to include an additional block of data associated with two detectors instead of only one detector.

Table 3.2: GOES Imager band nominal spatial resolution (GOES-12 through GOES-15).

GOES Imager Band	Central Wavelength (µm)	Spatial Resolution (km)	Number of Detectors
1	0.65	1	8
2	3.9	4	2
3	6.48	4	2
4	10.7	4	2
6	13.3	8 (GOES-12/13) 4 (GOES-14/15)	1 (GOES-12/13) 2 (GOES-14/15)

Figures 3.1 and 3.2 show the nominal region of the atmosphere sensed by each Imager and Sounder band on GOES-15. Note these are representative of clear-skies and a nadir view.

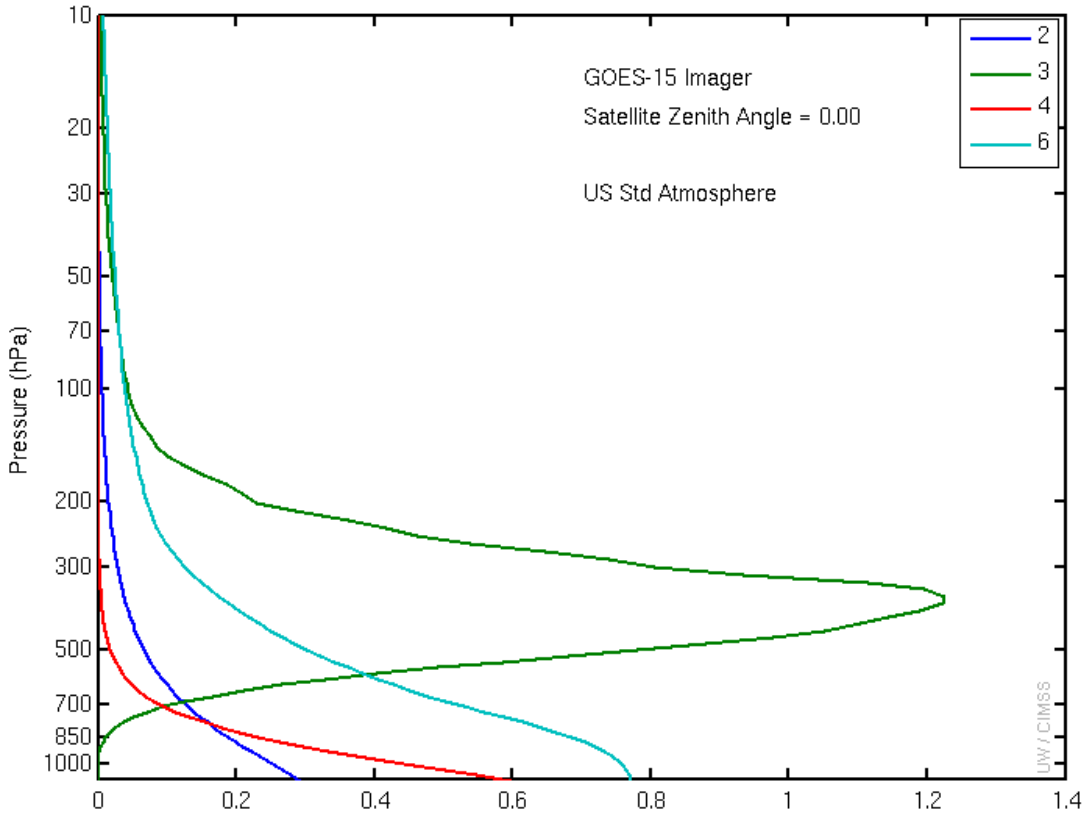

Figure 3.1: The GOES-15 Imager weighting functions.

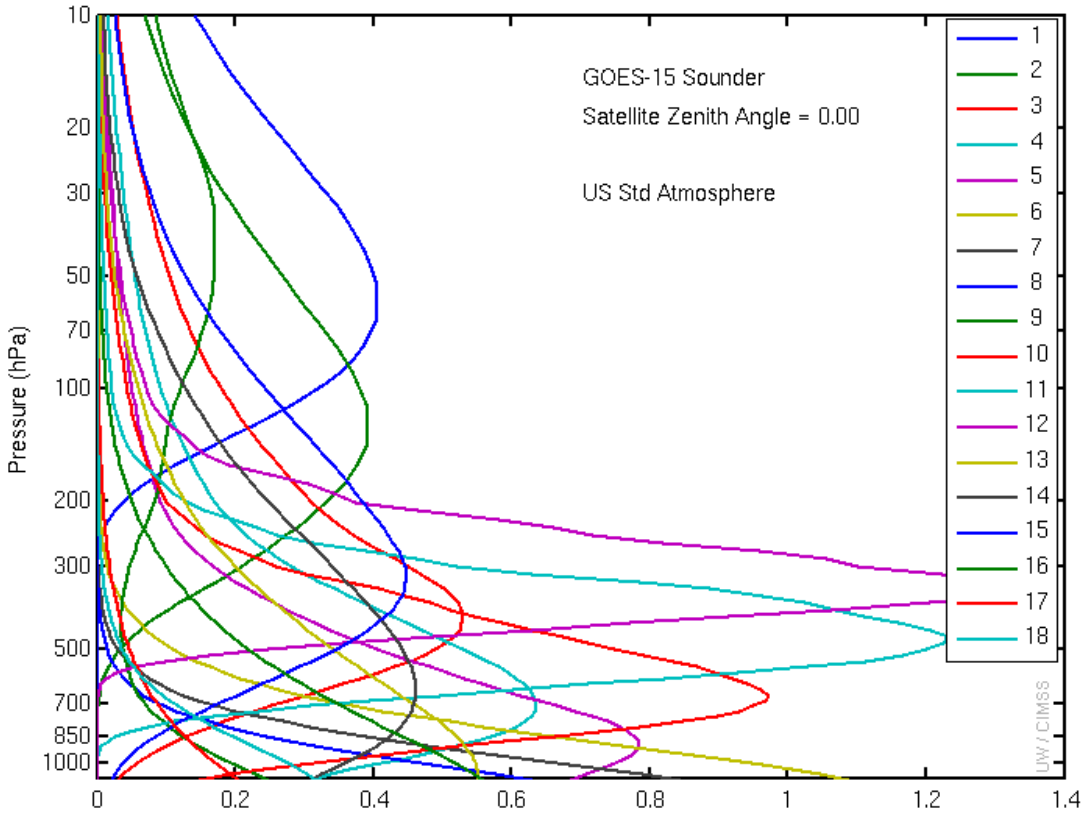

Figure 3.2: The GOES-15 Sounder weighting functions.

4. GOES Data Quality

4.1. First Images

The first step to ensure quality products is to verify the quality of the radiances that are used as inputs to the product generation. This process begins with a visual inspection of the images at a number of spatial resolutions.

4.1.1. Visible

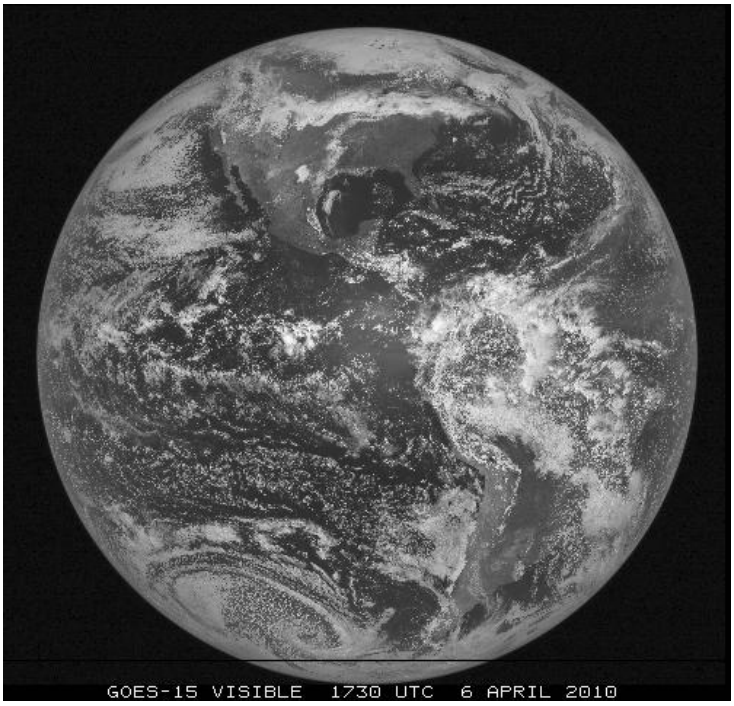

Figure 4.1: The first visible (0.63 µm) image from the GOES-15 Imager occurred on 6 April 2010 starting at approximately 1730 UTC.

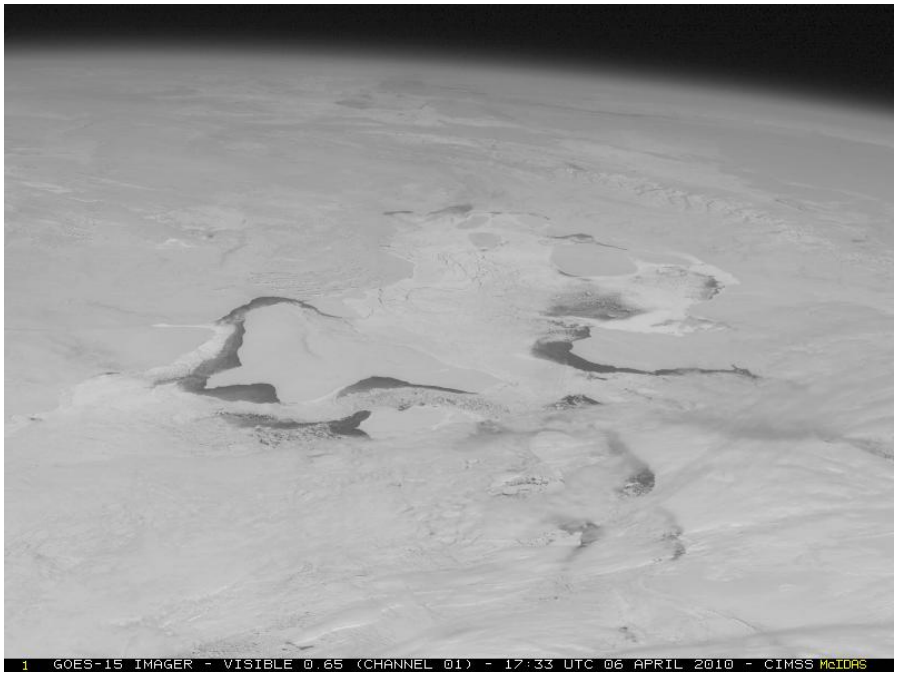

Figure 4.2: A GOES-15 visible image on 6 April 2010 showing a close-up view centered on Northern Hudson Bay and the Canadian Arctic Archipelago (showing some areas of ice-free water).

4.1.2. Infrared (IR)

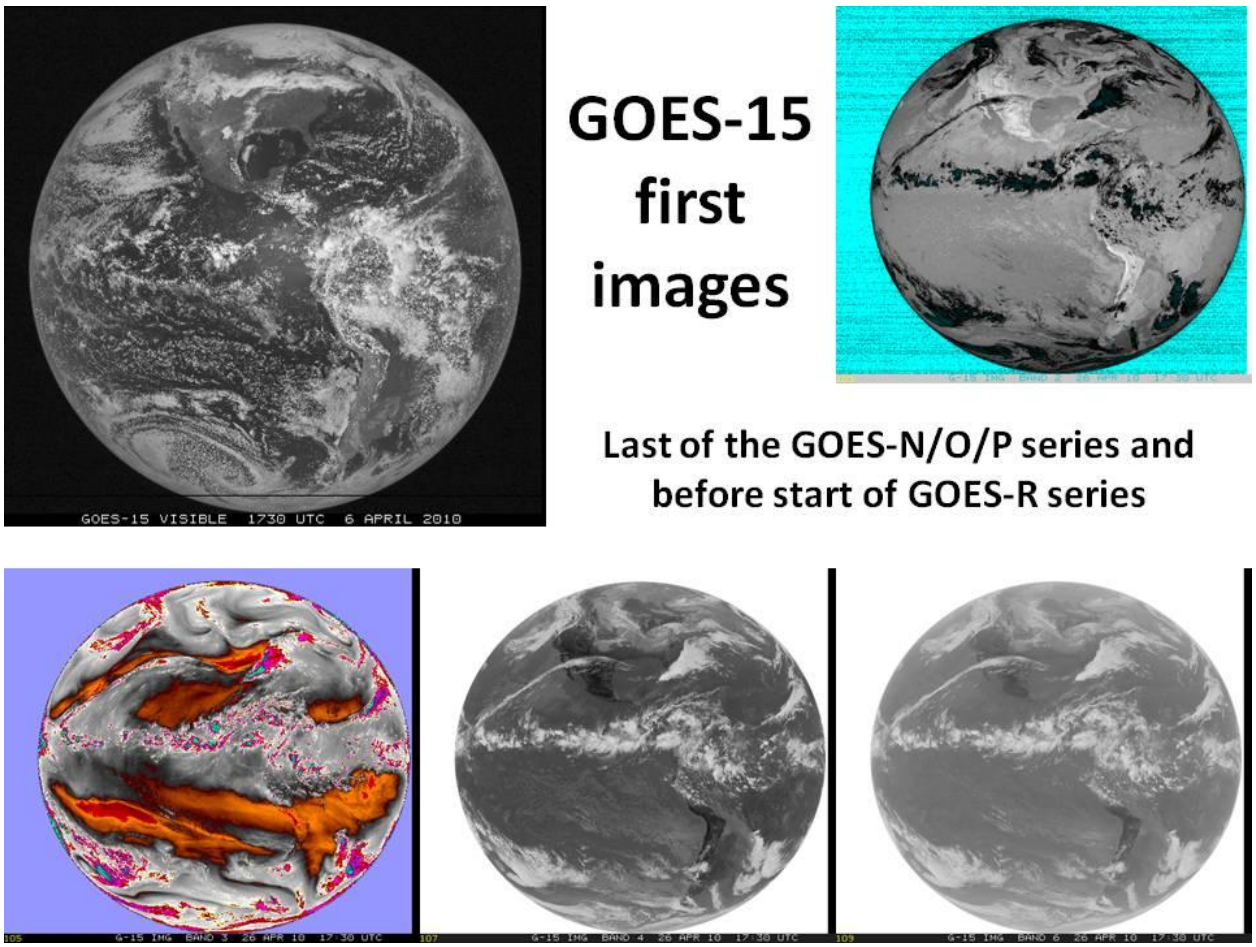

Figure 4.3: First GOES-15 full-disk visible (from 6 April 2010) and IR images (from 26 April 2010).

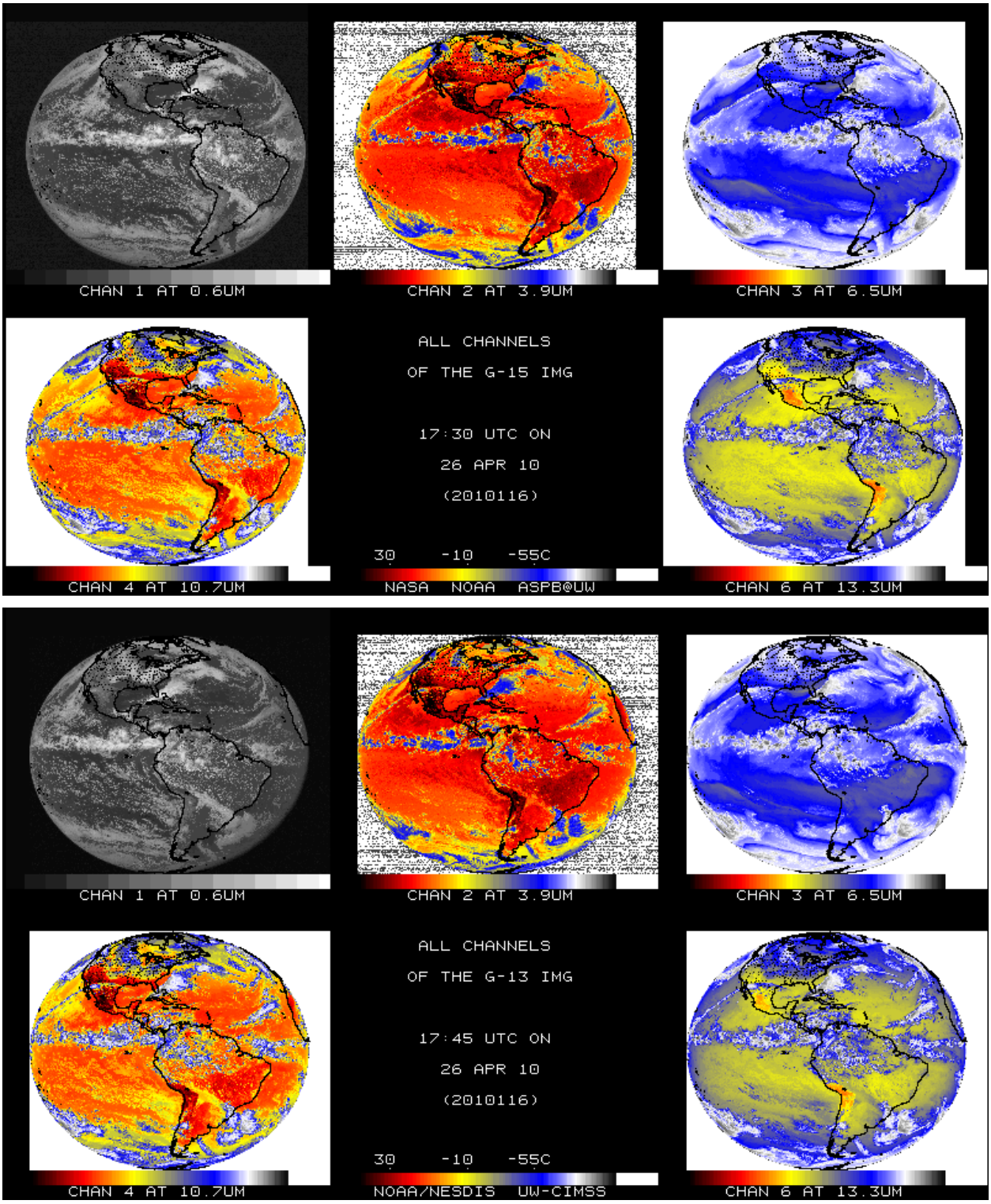

Figure 4.4: GOES-15 Imager bands (top) and the corresponding GOES-13 Imager bands (bottom). Both sets of images are shown in their native projections.

The images in Figure 4.4 have been sub-sampled. The pixel sub-sampling is necessary, in part, due to the fact that the first GOES-15 Imager full-disk images were too wide.

4.1.3. Sounder

The first GOES-15 Sounder images showed good qualitative agreement with GOES-12.

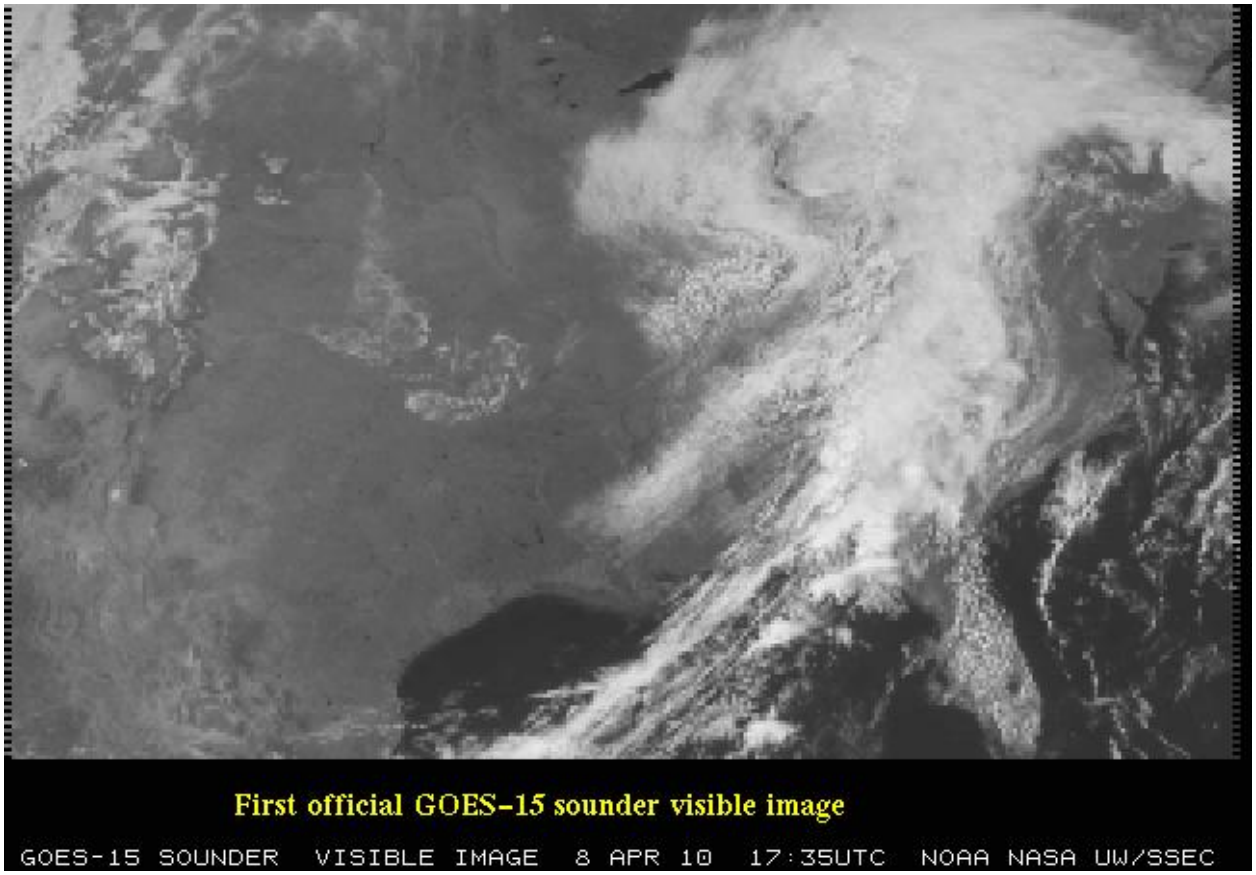

Figure 4.5: The visible (band-19) image from the GOES-15 Sounder shows data from 8 April 2010. The west and east 'saw-tooth' edges are due to the geometry of collecting the pixels.

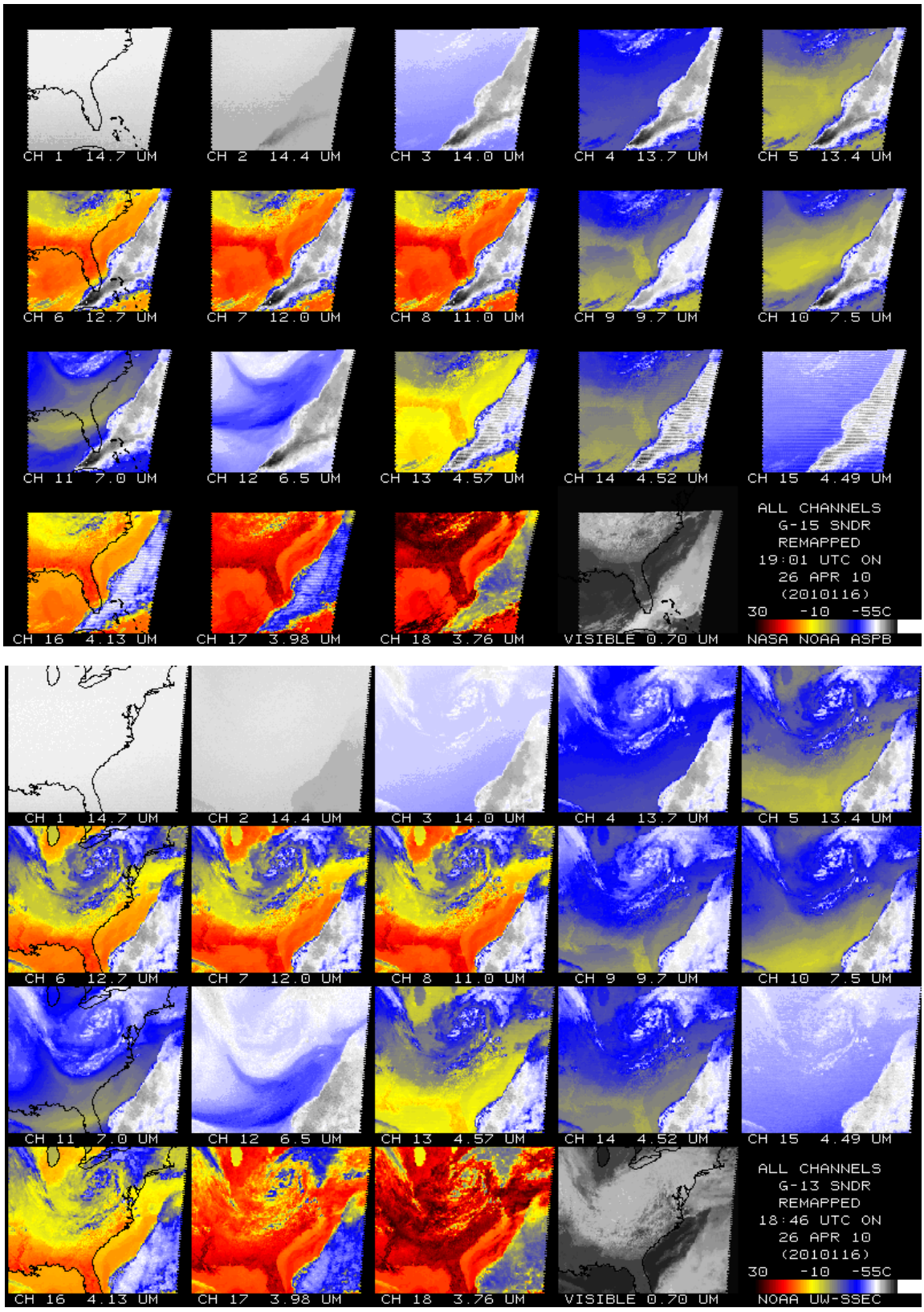

Figure 4.6: The first IR Sounder images for GOES-15 from 26 April 2010 (top) compared to GOES-13 (bottom). Both sets of images have been remapped to a common projection.

4.2. Spectral Response Functions (SRFs)

4.2.1. Imager

The GOES Spectral Response Functions (SRFs) for the GOES series Imagers can be found at http://www.oso.noaa.gov/goes/goes-calibration/goes-imager-srfs.htm and are plotted in Figure 4.7. Note that while there are several versions of the GOES-15 Imager SRF, the Rev. H version should be used. The GOES-15 Imager is spectrally similar to the GOES-12 Imager in that it has the spectrally-wide 'water vapor' band and a 13.3 μm band (band-6) has replaced the 12 μm band (band-5). Information about the GOES calibration can be found in Weinreb et al. (1997).

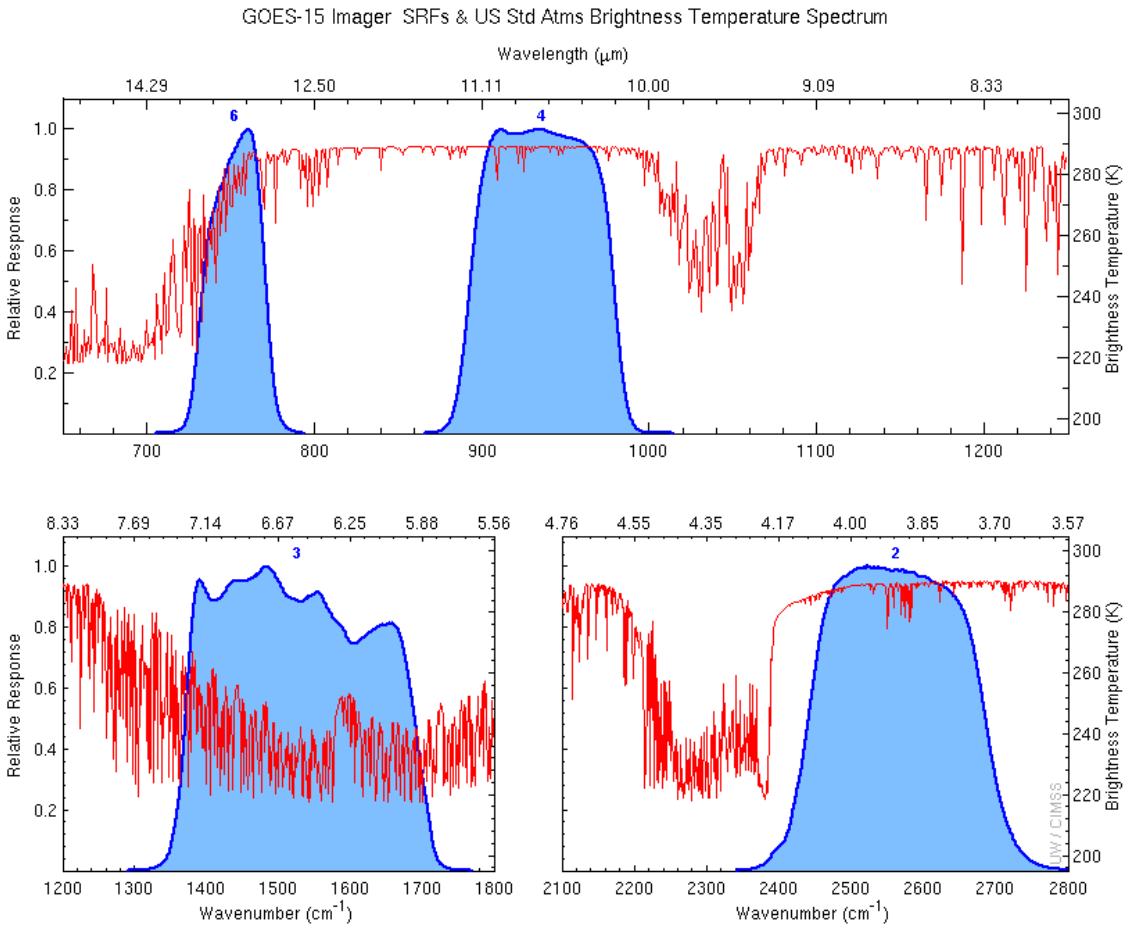

Figure 4.7: The four GOES-15 Imager IR-band SRFs super-imposed over the calculated high-resolution earth-emitted U.S. Standard Atmosphere spectrum. Absorption due to carbon dioxide (CO_2), water vapor (H_2O), and other gases are evident in the high-spectral-resolution earth-emitted spectrum. These are the 'shifted' Rev. H set (see Section 4.11).

4.2.2. Sounder

The GOES SRFs for the GOES series Sounders can be found at http://www.oso.noaa.gov/goes/goes-calibration/goes-sounder-srfs.htm and are plotted in Figure 4.8. The overall band selection is unchanged from previous GOES Sounders (Schmit et al. 2002b). As before, the carbon dioxide (CO_2), ozone (O_3), and water vapor (H_2O) absorption bands are indicated in the calculated high-spectral-resolution earth-emitted U.S. Standard Atmosphere spectrum. The central wavenumbers (wavelengths) of the spectral bands range from 680 cm^{-1} (14.7 μm) to 2667 cm^{-1} (3.75 μm) (Menzel et al. 1998).

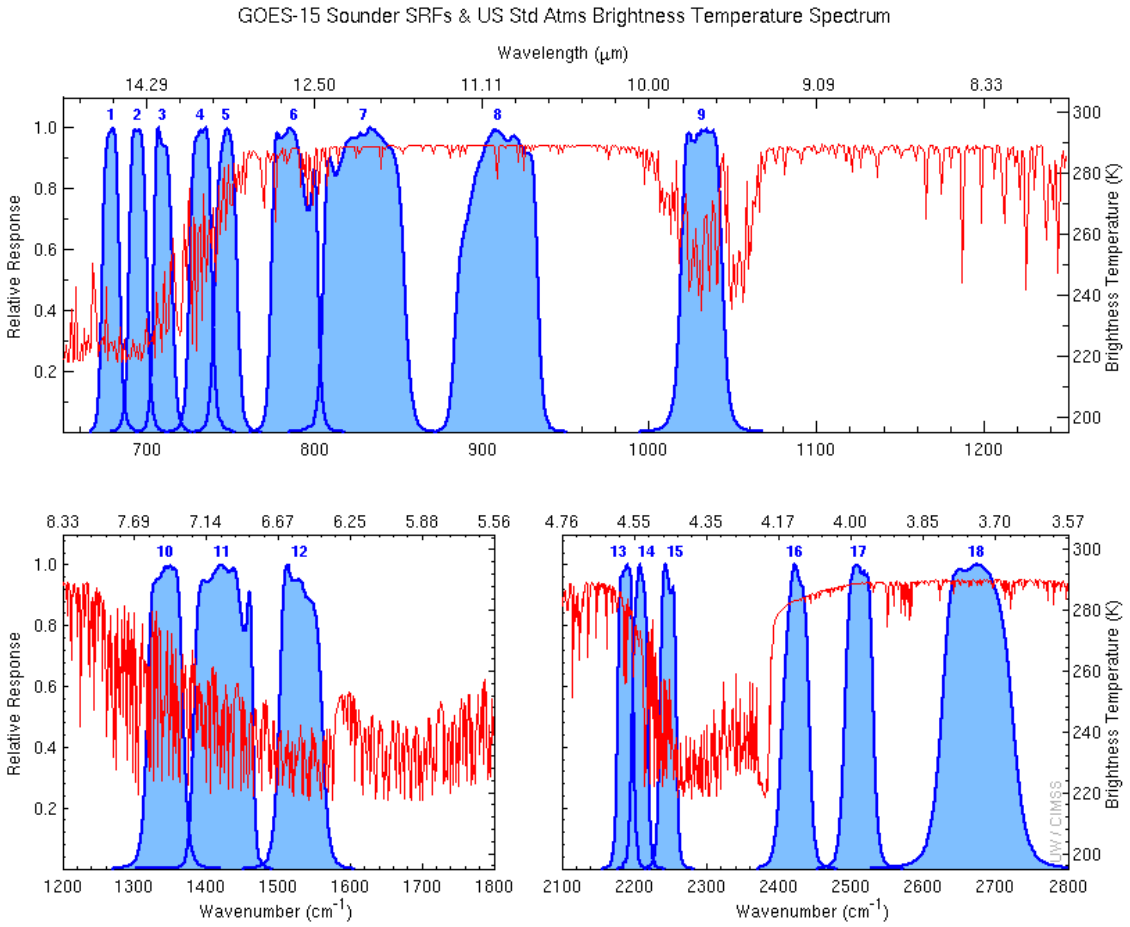

Figure 4.8: The eighteen GOES-15 Sounder IR-band SRFs (Rev. F) super-imposed over the calculated high-resolution earth-emitted U.S. Standard Atmosphere spectrum.

4.3. Random Noise Estimates

Band noise estimates for the GOES-15 Imager and Sounder were computed using two different approaches. In the first approach, the band noise levels were determined by calculating the variance (and standard deviation) of radiance values in a space-look scene. The second approach involved performing a spatial structure analysis (Hillger and Vonder Haar 1988). Both

approaches yielded nearly identical band noise estimates. Results of both approaches are presented below.

4.3.1. Imager

Full-disk images for the Imager provided off-earth space views and allowed noise levels to be determined. Estimated noise levels for the GOES-15 Imager were averaged over time for both east and west-limb space views for 48 hours of data starting at 1645 UTC on 21 August 2010 and ending at 1615 UTC on 23 August 2010. Results are presented in Table 4.1 in radiance units. The limb-averaged noise levels (second to last column) compared well with those from simpler variance (standard deviation) analysis (last column), the values of which were computed on a smaller dataset on Julian days 247-248 in 2010.

Table 4.1: GOES-15 Imager noise levels
(In radiance units, from 48 hours of limb/space views on Julian days 233-235 in 2010).

Imager Band	Central Wavelength (μm)	East Limb	West Limb	Limb Average	Variance Analysis
		mW/(m^2·sr·cm^{-1})			
2	3.9	0.0024	0.0023	**0.0024**	0.0023
3	6.5	0.022	0.022	**0.022**	0.022
4	10.7	0.095	0.102	**0.099**	0.094
6	13.3	0.22	0.22	**0.22**	0.22

A further comparison of the noise levels from the GOES-15 Imager with those from previous GOES Imagers is presented in Table 4.2. In this table the noise levels are given in temperature units. In general, noise levels were much improved over those for older GOES Imagers, with both GOES-13 and GOES-14 in particular having lower noise in most bands as compared to GOES-8 through GOES-12.

Keep in mind as well, the finer pixel size for band-6 images (from 8 km to 4 km) on both GOES-14 and GOES-15 compared to GOES-13 could be expected to result in an increase in noise. But the noise levels for GOES-14 and GOES-15 band-6 are only slightly higher than they were for GOES-13.

Table 4.2: Summary of the noise for GOES-8 through GOES-15 Imager bands
(In temperature units; the specification (SPEC) values are also listed).

Imager Band	Central Wavelength (μm)	GOES-15	GOES-14	GOES-13	GOES-12	GOES-11	GOES-10	GOES-9	GOES-8	SPEC
		K @ 300 K, except band-3 @ 230 K								
2	3.9	**0.063**	0.053	0.051	0.13	0.14	0.17	0.08	0.16	1.4
3	6.5 / 6.7	**0.17**	0.18	0.14	0.15	0.22	0.09	0.15	0.27	1.0
4	10.7	**0.059**	0.060	0.053	0.11	0.08	0.20	0.07	0.12	0.35
5	12.0	-	-	-	-	0.20	0.24	0.14	0.20	0.35
6	13.3	**0.13**	0.11	0.061	0.19	-	-	-	-	0.32

Band noise estimates for the GOES-15 Imager and Sounder **visible** band were also monitored at the GOES-15 Instrument Performance Monitoring (IPM) system. The visible band noise was evaluated with the standard deviation (1-sigma) of filtered space-view raw count ingested from the daytime GOES-15 GVAR Block 11 data. For the Imager, the statistics of space-view data were examined before and after the space clamp events. Since the Sounder is clamped with a filter wheel, the detector noise of the Sounder visible band was assessed with the space-view statistics at every two minutes. The results are shown in Figure 4.9 together with the noise values for the Imagers and Sounders onboard GOES-11 through GOES-14. In general, the noise levels of the GOES-15 visible band are comparable to the visible bands on GOES-13 and GOES=14. Compared to those from GOES-11/12, the visible data from the GOES-13/14/15 instruments have much better quality in terms of reduced noise.

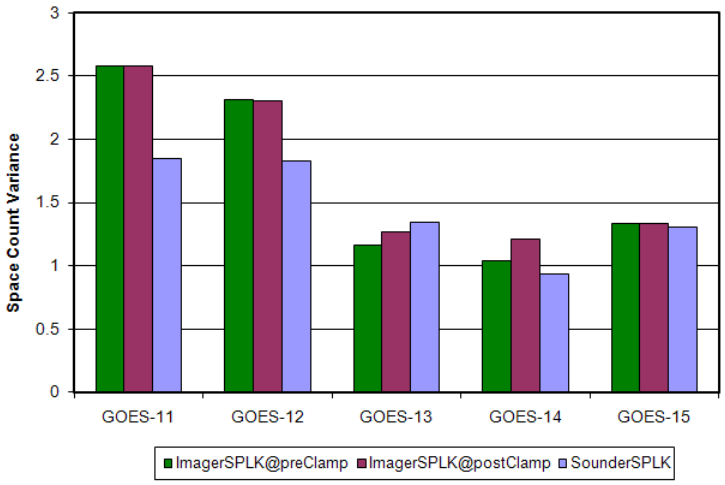

Figure 4.9: The mean standard deviation of the Imager space-view count before and after the Imager space clamp events, and Sounder space-view count for GOES-11 through GOES-15.

Figure 4.10 shows the standard deviation values of the eight Imager visible detectors from 21 August 2010 to 23 August 2010. As shown in the figures, detector #3 (in green) of the Imager visible band is noisier than the other detectors at both pre-clamp and post-clamp space views.

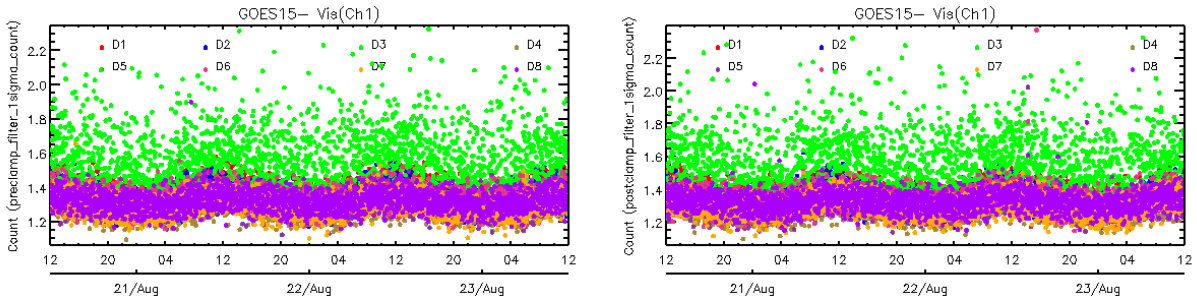

Figure 4.10: Times series of the standard deviations of space-view count for the eight detectors of GOES-15 Imager visible band from 20 August 2010 at 1200 UTC – 23 August 2010 at 1200 UTC (left: pre-clamp space-view statistics, right: post-clamp space-view statistics).

The noise in the GOES-15 IR bands was monitored using Noise Equivalent delta Radiance (NEdR) and Noise Equivalent delta Temperature (NEdT) of the blackbody scan data with the GOES IPM system. GOES-15 Imager IR band noise in temperature units is compared to the rest of the GOES series (GOES-8 through GOES-14) in Table 4.3. The data clearly show that the noise levels of all the GOES Imager Infrared (IR) bands are well below their specifications. The noise levels of the four GOES-15 IR bands are comparable with those of other GOES-N/O/P instruments and band-6 seems to be the noisiest among the four similar instruments.

Table 4.3: Summary of the noise for GOES-8 through GOES-15 Imager IR band (In temperature units; the specification (SPEC) noise levels are also listed).

Imager Band	Central Wave-length (μm)	GOES -15	GOES -14	GOES -13	GOES -12	GOES -11	GOES -10	GOES -9	GOES -8	SPEC
		K @ 300 K, except band-3 @ 230 K								
2	**3.9**	0.064	0.057	0.059	0.102	0.123	0.090	0.094	0.092	1.4
3	**6.5**	0.186	0.197	0.170	0.149	0.265	0.149	0.134	0.160	1.0
4	**10.7**	0.044	0.051	0.045	0.073	0.073	0.061	0.055	0.173	0.35
5	**12.0**	-	-	-	-	0.176	0.112	0.123	0.172	0.35
6	**13.3**	0.118	0.106	0.067	0.102	-	-	-	-	0.32

Figure 4.11 clearly shows that the noise of each GOES-15 Imager IR detector is well below the specification and no significant NEdT trend can be observed.

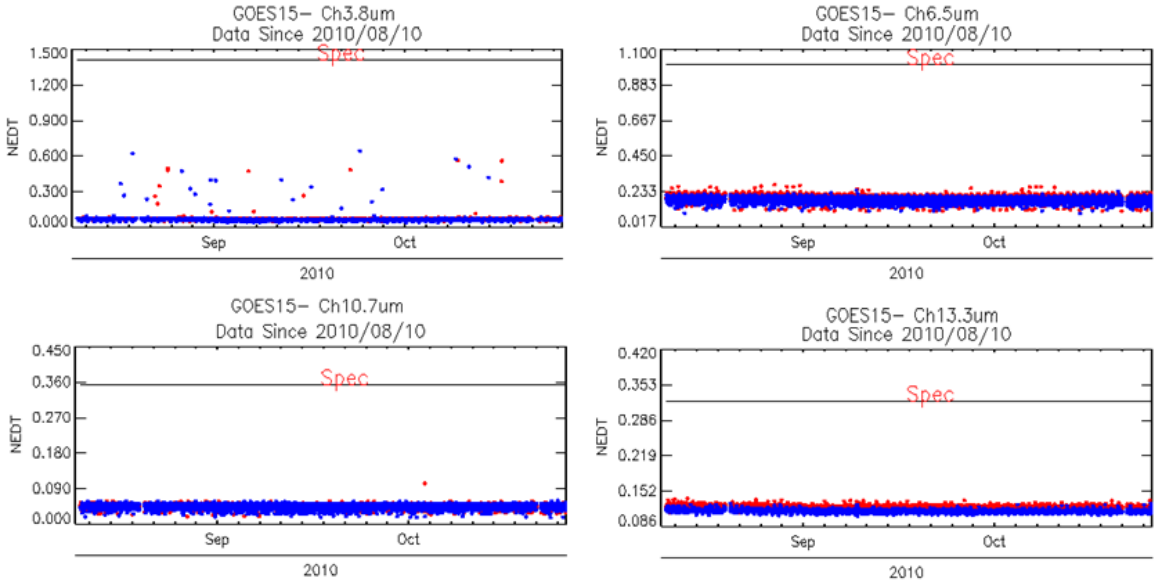

Figure 4.11: Time series of the GOES-15 Imager NEdT calculated @ 300 K, except band-3 @ 230 K, compared to the specifications. The color of the points refers to the detector number.

4.3.2. Sounder

Special GOES-15 limb-view Sounder sectors allow noise values to be determined by the scatter of radiance values looking at uniform off-earth space views. Noise values were computed for both west-limb and east-limb space-view data and averaged over the 32 hour period from 1630 UTC on 4 September 2010 through 0030 UTC on 6 September 2010. The limb-averaged values in Table 4.4 (second to last column) compare well to those from a simpler variance analysis (last column). Note that time frames with stray light were not included.

Table 4.4: GOES-15 Sounder noise levels

(In radiance units, from 32 hours of limb/space views on Julian days 247-248).

Sounder Band	Central Wavelength (μm)	East Limb	West Limb	Limb Average	Variance Analysis
		$mW/(m^2 \cdot sr \cdot cm^{-1})$			
1	14.71	0.23	0.23	**0.23**	0.27
2	14.37	0.21	0.21	**0.21**	0.25
3	14.06	0.22	0.21	**0.22**	0.25
4	13.64	0.17	0.17	**0.17**	0.21
5	13.37	0.15	0.15	**0.15**	0.18
6	12.66	0.066	0.069	**0.068**	0.087
7	12.02	0.044	0.048	**0.046**	0.063
8	11.03	0.053	0.061	**0.057**	0.067
9	9.71	0.064	0.069	**0.067**	0.077
10	7.43	0.036	0.037	**0.037**	0.044
11	7.02	0.024	0.024	**0.024**	0.031
12	6.51	0.030	0.029	**0.030**	0.037
13	4.57	0.016	0.011	**0.014**	0.012
14	4.52	0.019	0.013	**0.016**	0.014
15	4.46	0.017	0.013	**0.015**	0.013
16	4.13	0.010	0.0064	**0.0082**	0.0079
17	3.98	0.0067	0.0042	**0.0055**	0.0059
18	3.74	0.0024	0.0014	**0.0019**	0.0027

A further comparison of the noise levels for the GOES-15 Sounder with those from previous GOES Sounders is presented in Table 4.5. Noise levels are, in general, much improved over those for older GOES Sounders, with GOES-13 through GOES-15 having lower noise in most bands compared to GOES-8 through GOES-12.

Table 4.5: Summary of the noise for GOES-8 through GOES-15 Sounder bands (In radiance units; the specification (SPEC) values are also listed).

Sounder Band	Central Wavelength (μm)	GOES-15	GOES-14	GOES-13	GOES-12	GOES-11	GOES-10	GOES-9	GOES-8	SPEC
		mW/(m^2·sr·cm^{-1})								
1	14.71	**0.23**	0.29	0.32	0.77	0.67	0.71	1.16	1.76	0.66
2	14.37	**0.21**	0.24	0.25	0.61	0.51	0.51	0.80	1.21	0.58
3	14.06	**0.22**	0.21	0.23	0.45	0.37	0.41	0.56	0.98	0.54
4	13.64	**0.17**	0.16	0.18	0.39	0.36	0.41	0.46	0.74	0.45
5	13.37	**0.15**	0.15	0.18	0.34	0.34	0.36	0.45	0.68	0.44
6	12.66	**0.068**	0.073	0.095	0.14	0.17	0.16	0.19	0.32	0.25
7	12.02	**0.046**	0.053	0.086	0.11	0.11	0.09	0.13	0.20	0.16
8	11.03	**0.057**	0.076	0.10	0.11	0.14	0.12	0.09	0.13	0.16
9	9.71	**0.067**	0.068	0.11	0.14	0.13	0.10	0.11	0.16	0.33
10	7.43	**0.037**	0.039	0.081	0.099	0.09	0.07	0.08	0.08	0.16
11	7.02	**0.024**	0.025	0.046	0.059	0.06	0.04	0.05	0.07	0.12
12	6.51	**0.030**	0.029	0.063	0.11	0.11	0.07	0.09	0.11	0.15
13	4.57	**0.014**	0.0035	0.0061	0.0062	0.006	0.007	0.008	0.012	0.013
14	4.52	**0.016**	0.0035	0.0064	0.0062	0.007	0.005	0.007	0.010	0.013
15	4.46	**0.015**	0.0033	0.0055	0.0066	0.006	0.005	0.006	0.009	0.013
16	4.13	**0.0082**	0.0019	0.0030	0.0024	0.003	0.003	0.003	0.004	0.008
17	3.98	**0.0055**	0.0016	0.0026	0.0022	0.003	0.002	0.003	0.004	0.008
18	3.74	**0.0019**	0.00074	0.0011	0.00094	0.001	0.001	0.001	0.002	0.004

Figure 4.12 shows the standard deviation values of the four Sounder visible detectors from 7 October 2010 to 9 October 2010. The four Sounder visible detectors have a similar standard deviation magnitude of the filtered space view.

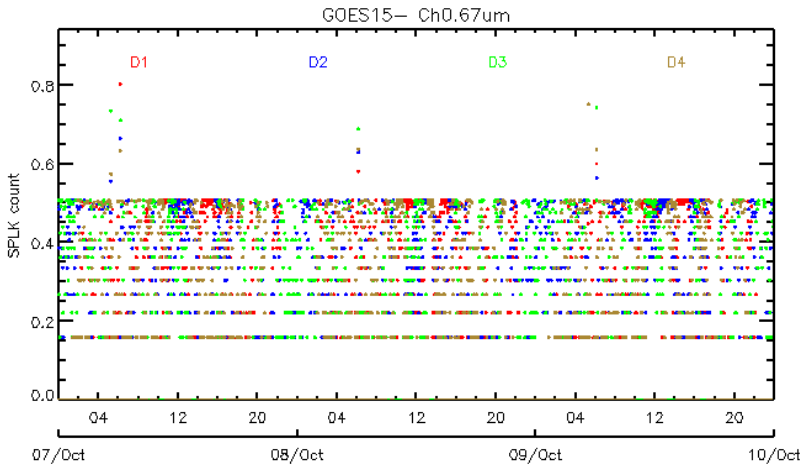

Figure 4.12: Standard deviations of space-view count for the four GOES-15 Sounder visible detectors from 0 UTC on 7 October 2010 to 0 UTC on 9 October 2010.

Comment on Figure 4.12: The outlier data are due to stray light just prior to local midnight (0600 UTC) during late eclipse. The standard deviation may decrease considerably if these outliers are disregarded.

GOES-15 Sounder noise was monitored with NEdR and NEdT of the blackbody scan data with the measured blackbody temperature; the results are available on the GOES-15 IPM Web page. Tables 4.6 and 4.7 summarize the noise levels for GOES-8 through GOES-15. In general, the GOES-14 and GOES-15 Sounder noise levels are improved compared to previous GOES Sounders.

Table 4.6: GOES-15 Sounder NEdR compared to those from GOES-8 through GOES-14 and the specification (SPEC) noise values.

Sounder Band	Central Wave-length (μm)	GOES-15	GOES-14	GOES-13	GOES-12	GOES-11	GOES-10	GOES-9	GOES-8	SPEC
		mW/(m^2·sr·cm^{-1})								
1	14.71	0.282	0.268	0.288	0.326	0.300	0.645	0.563	0.998	0.66
2	14.37	0.263	0.221	0.230	0.282	0.247	0.441	0.455	0.755	0.58
3	14.06	0.265	0.188	0.211	0.221	0.186	0.347	0.344	0.685	0.54
4	13.64	0.212	0.142	0.167	0.200	0.179	0.360	0.294	0.512	0.45
5	13.37	0.184	0.141	0.169	0.185	0.175	0.338	0.275	0.495	0.44
6	12.66	0.073	0.064	0.080	0.076	0.092	0.147	0.127	0.223	0.25
7	12.02	0.043	0.042	0.054	0.056	0.058	0.079	0.080	0.144	0.16
8	11.03	0.053	0.044	0.097	0.127	0.137	0.096	0.079	0.129	0.16
9	9.71	0.073	0.054	0.127	0.184	0.132	0.120	0.113	0.161	0.33
10	7.43	0.041	0.033	0.096	0.129	0.107	0.077	0.716	0.082	0.16
11	7.02	0.027	0.020	0.054	0.075	0.070	0.048	0.044	0.071	0.12
12	6.51	0.032	0.027	0.076	0.138	0.134	0.091	0.079	0.111	0.15
13	4.57	0.005	0.0028	0.0046	0.024	0.0045	0.006	0.006	0.008	0.013
14	4.52	0.005	0.0029	0.0049	0.023	0.0056	0.004	0.005	0.008	0.013
15	4.46	0.005	0.0025	0.0042	0.025	0.0044	0.004	0.005	0.008	0.013
16	4.13	0.003	0.0016	0.0023	0.009	0.0023	0.002	0.002	0.003	0.008
17	3.98	0.002	0.0013	0.0020	0.008	0.0021	0.002	0.002	0.002	0.008
18	3.74	<0.0001	<0.0001	<0.0001	0.0033	0.0010	<0.0001	0.001	0.002	0.004

Table 4.7: GOES-15 Sounder NEdT compared to those from GOES-8 through GOES-14.

Sounder Band	Central Wave-length (μm)	GOES -15	GOES -14	GOES -13	GOES -12	GOES -11	GOES -10	GOES -9	GOES -8
		K @ blackbody temperature							
1	14.71	0.167	0.158	0.170	0.193	0.178	0.383	0.333	0.591
2	14.37	0.154	0.129	0.135	0.165	0.147	0.259	0.267	0.443
3	14.06	0.154	0.109	0.123	0.128	0.108	0.201	0.199	0.398
4	13.64	0.122	0.082	0.096	0.115	0.103	0.208	0.169	0.295
5	13.37	0.105	0.081	0.097	0.106	0.100	0.194	0.158	0.283
6	12.66	0.042	0.036	0.046	0.043	0.053	0.084	0.072	0.127
7	12.02	0.025	0.024	0.031	0.032	0.033	0.045	0.046	0.082
8	11.03	0.031	0.026	0.057	0.074	0.081	0.056	0.047	0.076
9	9.71	0.047	0.035	0.082	0.118	0.104	0.077	0.072	0.103
10	7.43	0.042	0.034	0.097	0.130	0.108	0.078	0.071	0.082
11	7.02	0.032	0.023	0.063	0.088	0.083	0.056	0.052	0.084
12	6.51	0.048	0.039	0.112	0.206	0.201	0.135	0.116	0.165
13	4.57	0.042	0.023	0.038	0.195	0.038	0.047	0.045	0.084
14	4.52	0.048	0.026	0.043	0.205	0.050	0.035	0.046	0.067
15	4.46	0.052	0.025	0.042	0.248	0.043	0.037	0.046	0.075
16	4.13	0.047	0.027	0.038	0.147	0.040	0.038	0.039	0.056
17	3.98	0.047	0.028	0.045	0.186	0.047	0.042	0.054	0.085
18	3.74	<0.001	<0.001	<0.001	0.119	0.037	<0.001	0.038	0.064

Figure 4.13 shows the time series of the NEdT for the four detectors at each IR band in mid-September 2010. The NEdT is very consistent over the two-day period, and the noise of each GOES-15 Sounder IR band is well below its specification when the patch temperature was controlled at low-level.

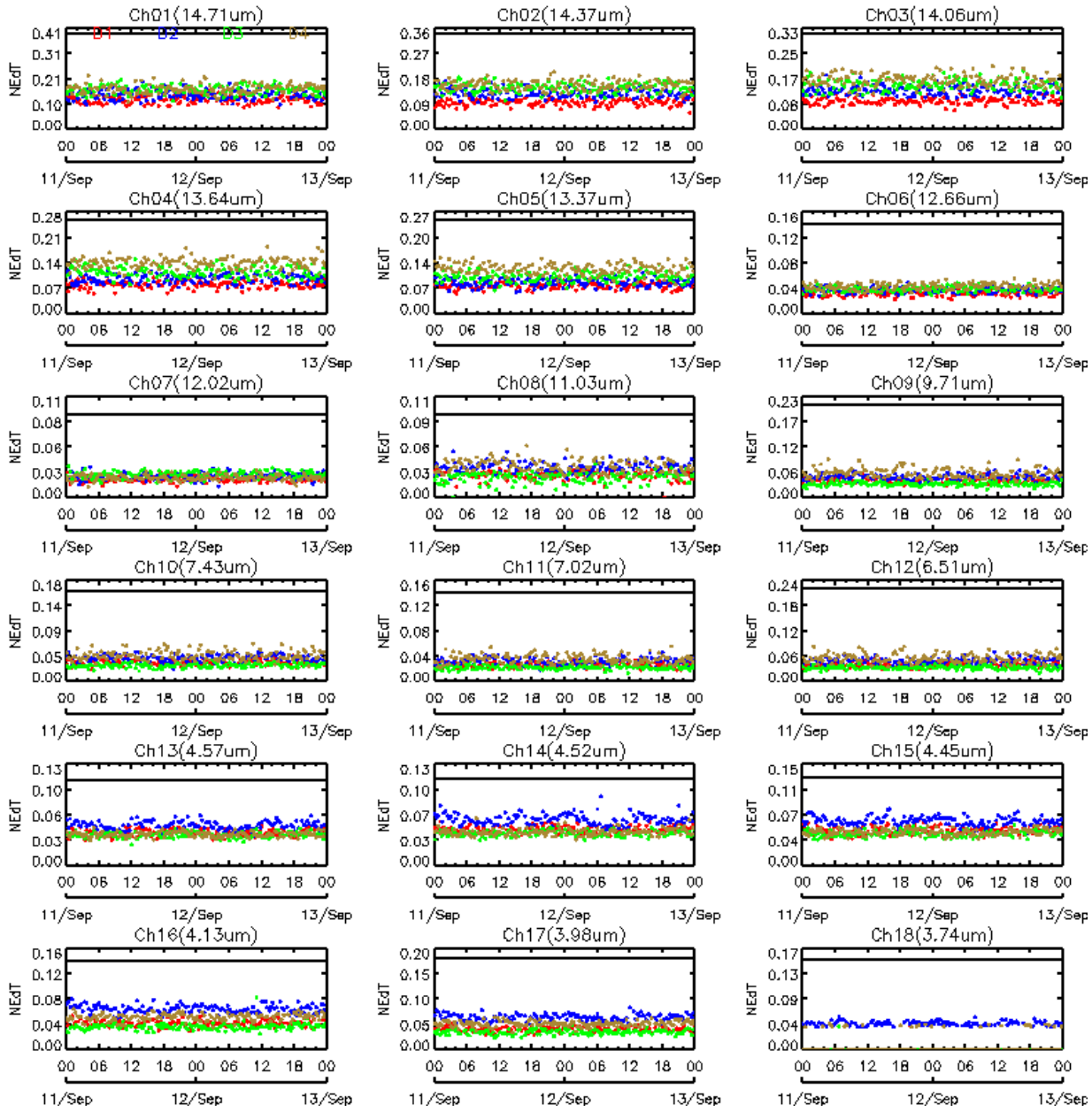

Figure 4.13: Diurnal variation in GOES-15 Sounder NEdT between 11 September 2010 and 12 September 2010. The solid line in each IR band plot is the specification value. The colors correspond to the 4 detectors.

4.4. Striping Due to Multiple Detectors

For the GOES Imager there are two detectors per spectral band, and for the GOES Sounder there are four detectors for each spectral band. Differences between the measurements in these detectors can cause striping in GOES images. Striping becomes more obvious as random noise decreases, allowing the striping to dominate the random noise. Striping is defined as the difference between the average values for each detector from the average value in all detectors.

4.4.1. Imager

Full-disk images from the Imager provide off-earth space views allowing both noise levels (reported above) and detector-to-detector striping to be determined in an otherwise constant signal situation. Table 4.8 gives estimates of GOES-15 Imager detector-to-detector striping for a 24 hour period starting at 1645 UTC on 21 August 2010 and ending at 1615 UTC on 23 August 2010. Striping was computed from off-earth space-view measurements on each side of the earth (columns 3 and 4). The limb averages (third to last column) are then determined and compared to the noise level (second to last column). A ratio of striping to noise is also computed (last column). All the ratios are less than 1, indicating that the striping is less than the noise. Because the noise has decreased with the latest GOES series, the striping can be more noticeable than for earlier GOES, as will be seen in some of the Sounder images presented later in this report.

Table 4.8: GOES-15 Imager detector-to-detector striping
(In radiance units, from 48 hours of limb/space views on Julian days 233-235).

Imager Band	Central Wavelength (μm)	East Limb	West Limb	Limb Average	Noise	Striping/Noise Ratio
		$mW/(m^2 \cdot sr \cdot cm^{-1})$				
2	3.9	0.00103	0.00063	**0.00083**	0.0024	**0.35**
3	6.5	0.0026	0.0023	**0.0025**	0.022	**0.11**
4	10.7	0.025	0.026	**0.026**	0.099	**0.26**
6	13.3	0.024	0.0095	**0.017**	0.22	**0.076**

4.4.2. Sounder

Detector-to-detector striping for the Sounder is documented in Table 4.9 from measurements taken from the same off-earth space-view sectors used for the noise analysis for the Sounder for the 32 hour period from 1630 UTC on 4 September 2010 through ~0030 UTC on 6 September 2010. The limb-averaged values (third from last column) are compared to the noise levels (second to last column), with the ratio of striping to noise in the last column. Values larger than one (sometimes much larger) indicate that striping is much more significant than noise for several of the Sounder bands. However, the largest ratios, for the longwave IR bands, do not mean that striping is obvious in the images from these bands, because the inherent signal is also very large in these window bands.

Table 4.9: GOES-15 Sounder detector-to-detector striping (In radiance units, from 32 hours of limb/space views on Julian days 247-248).

Sounder Band	Central Wavelength (μm)	East Limb	West Limb	Limb Average	Noise	Striping/Noise Ratio
		mW/(m^2·sr·cm^{-1})				
1	14.71	0.48	0.81	**0.65**	0.23	**2.8**
2	14.37	0.42	0.74	**0.58**	0.21	**2.8**
3	14.06	0.52	0.92	**0.72**	0.22	**3.3**
4	13.64	0.71	1.22	**0.97**	0.17	**5.7**
5	13.37	0.80	1.31	**1.06**	0.15	**7.0**
6	12.66	1.08	1.79	**1.44**	0.068	**21.1**
7	12.02	1.06	1.77	**1.42**	0.046	**30.8**
8	11.03	0.95	1.44	**1.20**	0.057	**21.0**
9	9.71	0.42	0.66	**0.54**	0.067	**8.1**
10	7.43	0.17	0.29	**0.23**	0.037	**6.2**
11	7.02	0.10	0.19	**0.15**	0.024	**6.0**
12	6.51	0.043	0.061	**0.052**	0.030	**1.7**
13	4.57	0.031	0.034	**0.033**	0.014	**2.3**
14	4.52	0.020	0.017	**0.019**	0.016	**1.2**
15	4.46	0.017	0.011	**0.014**	0.015	**0.9**
16	4.13	0.015	0.017	**0.016**	0.0082	**2.0**
17	3.98	0.016	0.012	**0.014**	0.0055	**2.5**
18	3.74	0.0083	0.014	**0.011**	0.0019	**5.9**

4.5. Initial Post-launch Calibration for the GOES-15 Imager Visible Band

Due to the lack of an on-board calibration devices for the GOES visible band, vicarious calibration is needed to derive accurate post-launch calibrated radiance/reflectance for the visible bands. Currently, the post-launch operational calibration of the GOES Imager visible band is based on the inter-calibration between GOES and Earth Observation System (EOS) Terra Moderate Resolution Imaging Spectroradiometer (MODIS) band-1 data (Wu and Sun 2005). The calibration correction of the post-launch GOES-15 Imager visible band data can be written as:

$$R_{post} = R_{pre} * C$$

Where R_{post} is the post-launch calibration reflectance/radiance for GOES-15 Imager visible band; R_{pre} is the pre-launch calibration reflectance/radiance (http://www.star.nesdis.noaa.gov/smcd/spb/fwu/homepage/GOES_Imager_Vis_PreCal.php); and C is the correction factor, C = 1.082 (±0.017). This result was derived based on the collocated GOES-15 and EOS-Terra MODIS pixels acquired in 2010 on the following Julian days: 228, 244, 248, 253, 273, 276, 278, 285, 289, and 294.

4.6. GEO to GEO Comparisons

During the PLT period, GOES-15 was orbiting at (89.5°W) between GOES-11 (135°W) and GOES-13 (75°W) to emulate the GOES-11 and GOES-13 scan patterns. The comparison of reflectance or emissivity (radiance/brightness temperature) over the collocated regions offers a unique opportunity to evaluate the consistency of the same product retrieved from two different GOES satellites. Similar collocation criteria as the Geostationary Earth Orbit (GEO)-Low Earth Orbit (LEO) inter-calibration was applied to identify the GEO-GEO collocation scenes, including: 1) the distance between the centers of two GEO pixels should be within the radius of the nominal spatial resolution at nadir (spatial collocation), 2) the time difference between the two observations should be less than 5 minutes (temporal collocation) for Imagers and 15 minutes for Sounders, and 3) the difference in the cosine of the viewing zenith angle should be within 1% (viewing geometry match).

Figure 4.14 shows the spatial distribution of collocation pixels of GOES-15 vs. GOES-13 Imagers (left) and GOES-15 vs. GOES-11 Imagers (right) in the Northern Hemisphere. The narrow regions of comparisons result from the constraint to approximately match the zenith angles from the two GOES. Due to the closer sub-satellite locations, the collocation pixels of GOES-15 vs. GOES-13 have a much wider spatial distribution than GOES-15 vs. GOES-11, covering from the Equator to about 50° in latitude and centered around 82.25°W (±2°). The GOES-15 vs. GOES-11 collocation pixel distribution is centered around 112.25°W (±0.6°). The high frequency and large amount of collocation scenes provides an excellent opportunity to directly inter-compare the radiance from these two satellites. All the GEO-GEO inter-calibration results are based on the analysis of collocation data from 26 September 2010 to 28 September 2010 for GOES-15 vs. GOES-13 and from 26 August 2010 to 28 August 2010 for GOES-15 vs. GOES-11.

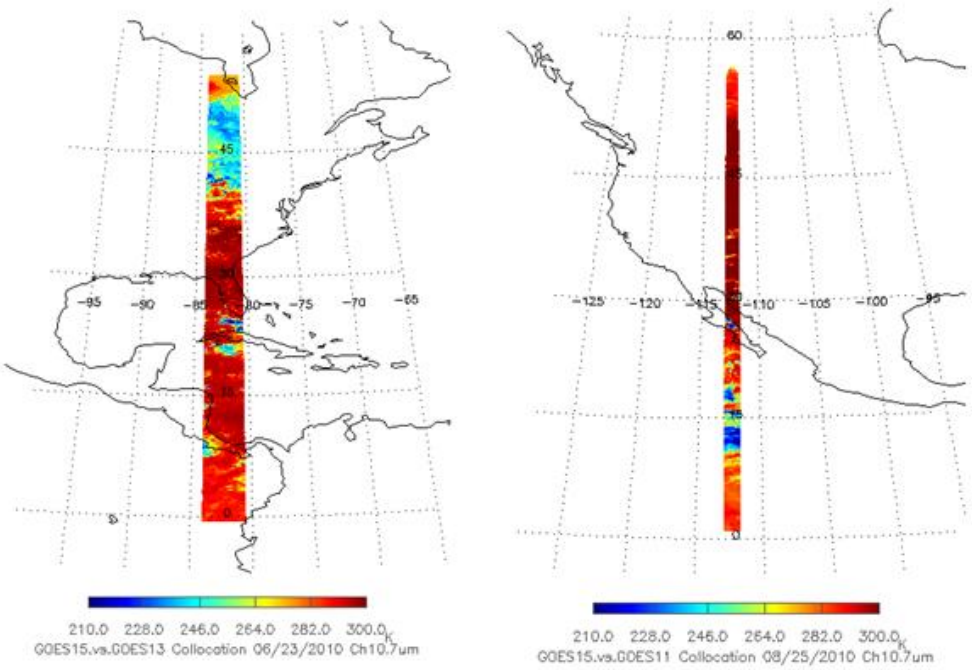

Figure 4.14: Spatial distribution of GOES-15 Imager band-4 Tb values for the collocation scenes between GOES-13 (left) and GOES-11 (right).

Figure 4.15 shows the difference in the post-launch calibrated visible reflectance between GOES-15 and GOES-13 (left) and the histogram distribution of the visible reflectance difference (right). On average, the GOES-15 visible reflectance is about 1.0% higher than GOES-13 and 2.1% lower than GOES-11 (not shown). The small visible reflectance difference between these radiometers indicates that the operational post-launch calibration corrections can reduce the "seam" feature along the overlapped areas. Causes of the difference include the SRF difference (Figure 4.16), the bidirectional reflectance function distribution (BRDF), and the operational calibration uncertainty. Note the large SRF differences between GOES-8/11 compared to GOES-13/15. These differences then cause differences in the reflection from vegetative surfaces, given the sharp transition zone near 7.2 μm (not shown).

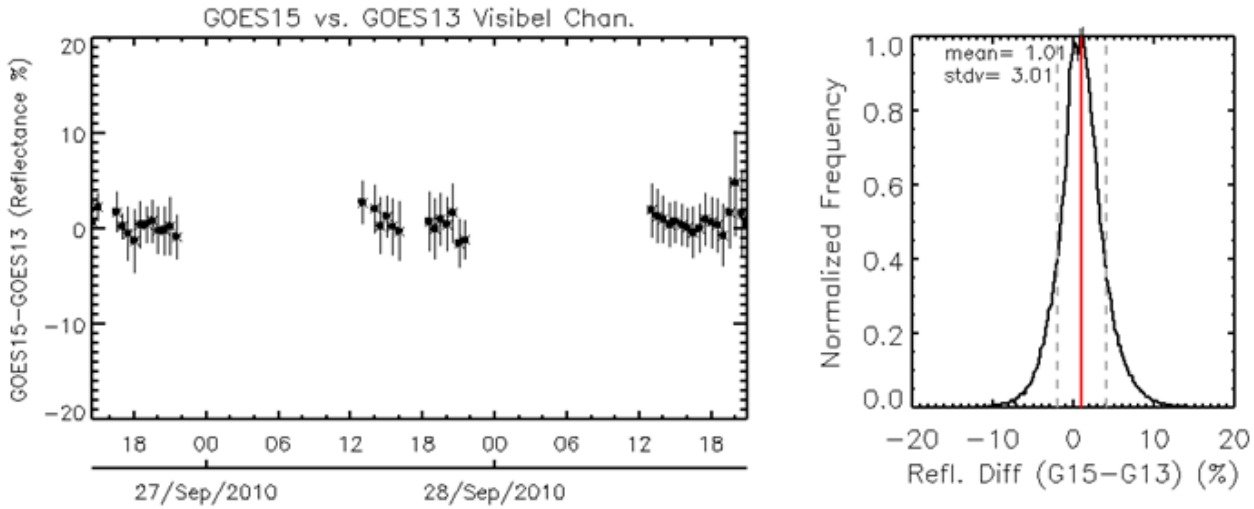

Figure 4.15: Time series of GOES-15 vs. GOES-13 post-launch calibrated visible reflectance difference (left) and the histogram of the visible reflectance difference (right).

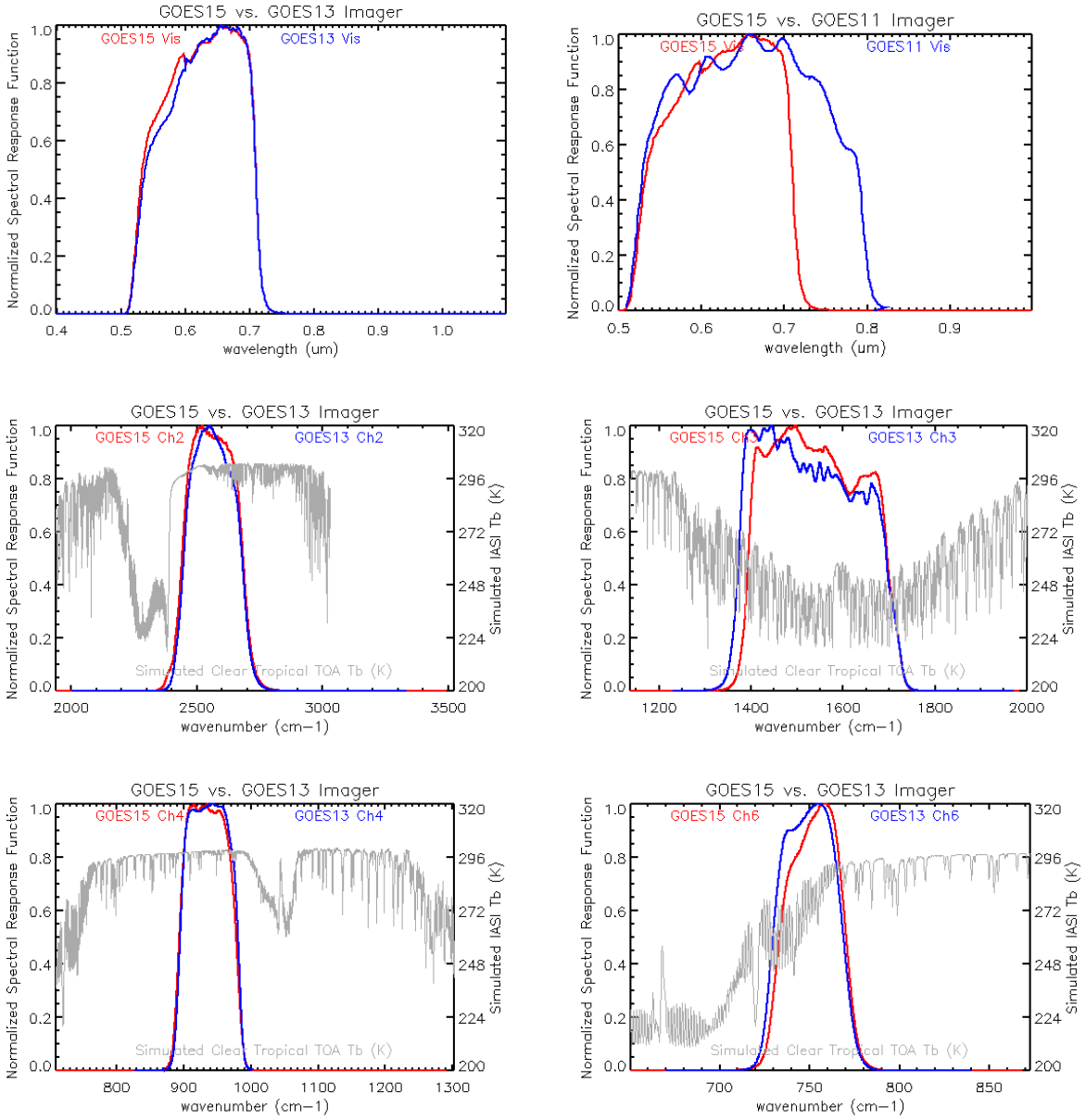

Figure 4.16: SRF of the visible bands at GOES-15 vs. GOES-13 (top left) and GOES-15 vs. GOES-11 (top right). SRF of GOES-13 and GOES-15 four IR bands (red: GOES-15, blue: GOES-13). The simulated clear tropical TOA Tb values (in gray) are also plotted for the four IR bands.

The distribution of the SRF plays a dominant role in determining the Tb difference of this direct GEO-GEO inter-comparison in this study, especially for the absorptive band-3 (6.5 μm) and band-6 (13.3 μm). Figure 4.16 shows the SRF of the four Imager IR bands on GOES-13 and GOES-15. The simulated clear tropical Top-of-Atmosphere (TOA) Tb values using the IASI spectra are also plotted for the four IR bands.

GOES-15 data were also evaluated by comparing pixel temperatures of a 10 x 10 pixel box in a Mercator projection centered at 40˚N / 82.25˚W for bands 2, 3, 4, and 6 to a similar domain on

the operational GOES-East satellite (GOES-13). This location was chosen to keep the satellite zenith angle consistent between GOES-13 and GOES-15. All results were plotted in a two-dimensional smoothed histogram approach which allows for a better representation of data in dense areas (Eilers and Goeman 2004). Additionally, numerous statistics were calculated in order to determine the performance of the GOES-15 Imager bands compared to the respective Imager bands on GOES-13.

GOES-15 testing began at SAB on 11 August 2010 and was completed on 18 October 2010. This testing period resulted in sample sizes of over 180,000 pixels for all bands tested. This analysis was completed before the GOES-15 Imager bands 3 and 6 were spectrally shifted. Figure 4.17 shows two-dimensional smoothed histograms of GOES-13 vs. GOES-15 pixel temperatures taken from a 10 x 10 domain centered at 40˚N / 82.25˚W for bands 2, 3, 4, and 6. A dashed line representing the perfect fit line with numerous performance statistics is included on the graphs. A nearly perfect degree of correlation ($r > 0.98$) was observed between GOES-13 and GOES-15 pixel temperatures for all tested bands. On bands 2 and 4, no significant biases were detected in the data. Mean Absolute Errors (MAE) were less than or equal to roughly 1.5 K for bands 2 and 4. For bands 3 and 6, SAB did note a modest cold bias of roughly 1.2 K for GOES-15 band-3 data and a more significant warm bias of 2.7 K for GOES-15 band-6 data. MAEs for the band-3 and 6 pixel temperatures nearly matched the magnitude of the observed biases which suggests very few instances where GOES-15 pixel temperatures deviated from their respective observed bias. It is noted that the observed biases of the band-3 and 6 data are consistent with central wavelength shifts for both band-3 and 6 data on GOES-15, although the magnitude of band-6 data are larger than what SAB expected considering the small wavelength shift. This result is consistent with the LEO-GEO comparisons that showed a large bias in bands 3 and 6. Root Mean Square Errors (RMSE) in most cases were similar to their respective MAEs, implying that the number of large errors were minimal. Any large errors that were observed were manually investigated, and most were determined to be a function of slight navigational errors near cloud edges.

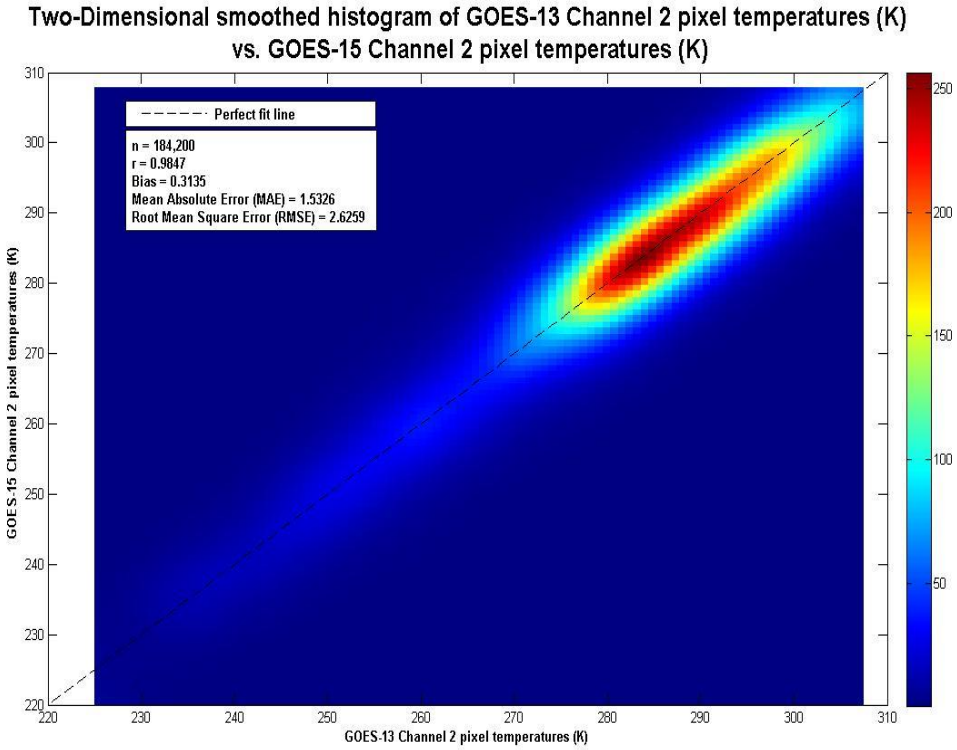
Two-Dimensional smoothed histogram of GOES-13 Channel 2 pixel temperatures (K)
vs. GOES-15 Channel 2 pixel temperatures (K)
Perfect fit line
n = 184,200
r = 0.9847
Bias = 0.3135
Mean Absolute Error (MAE) = 1.5326
Root Mean Square Error (RMSE) = 2.6259
GOES-15 Channel 2 pixel temperatures (K)
GOES-13 Channel 2 pixel temperatures (K)
220
230
240
250
260
270
280
290
300
310
50
100
150
200
250

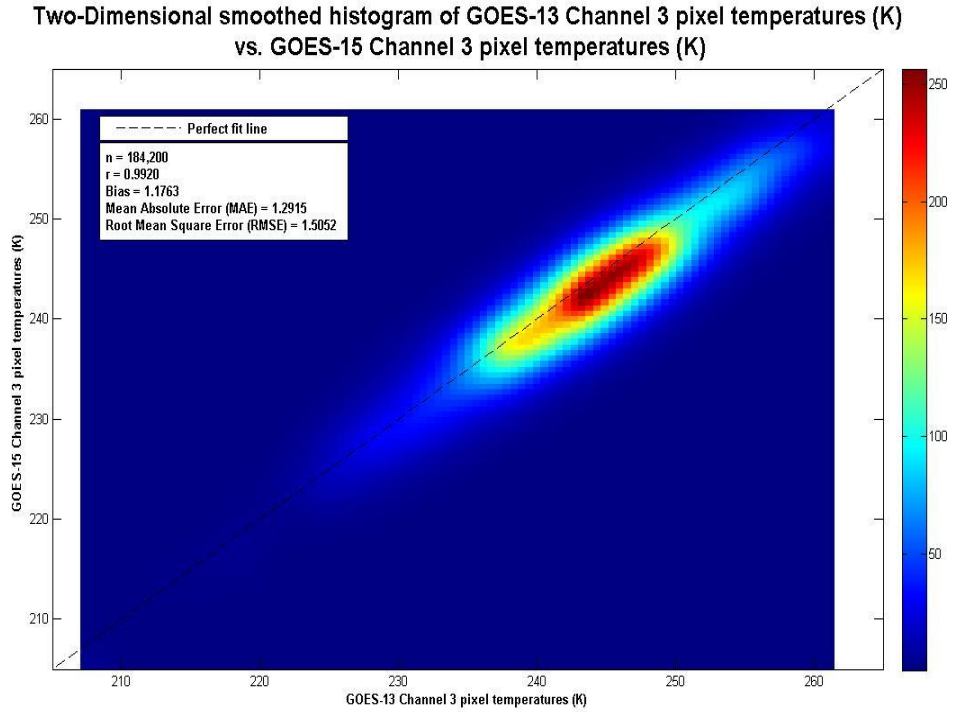
Two-Dimensional smoothed histogram of GOES-13 Channel 3 pixel temperatures (K)
vs. GOES-15 Channel 3 pixel temperatures (K)
Perfect fit line
n = 184,200
r = 0.9920
Bias = 1.1763
Mean Absolute Error (MAE) = 1.2915
Root Mean Square Error (RMSE) = 1.5052
GOES-15 Channel 3 pixel temperatures (K)
GOES-13 Channel 3 pixel temperatures (K)
210
220
230
240
250
260
50
100
150
200
250

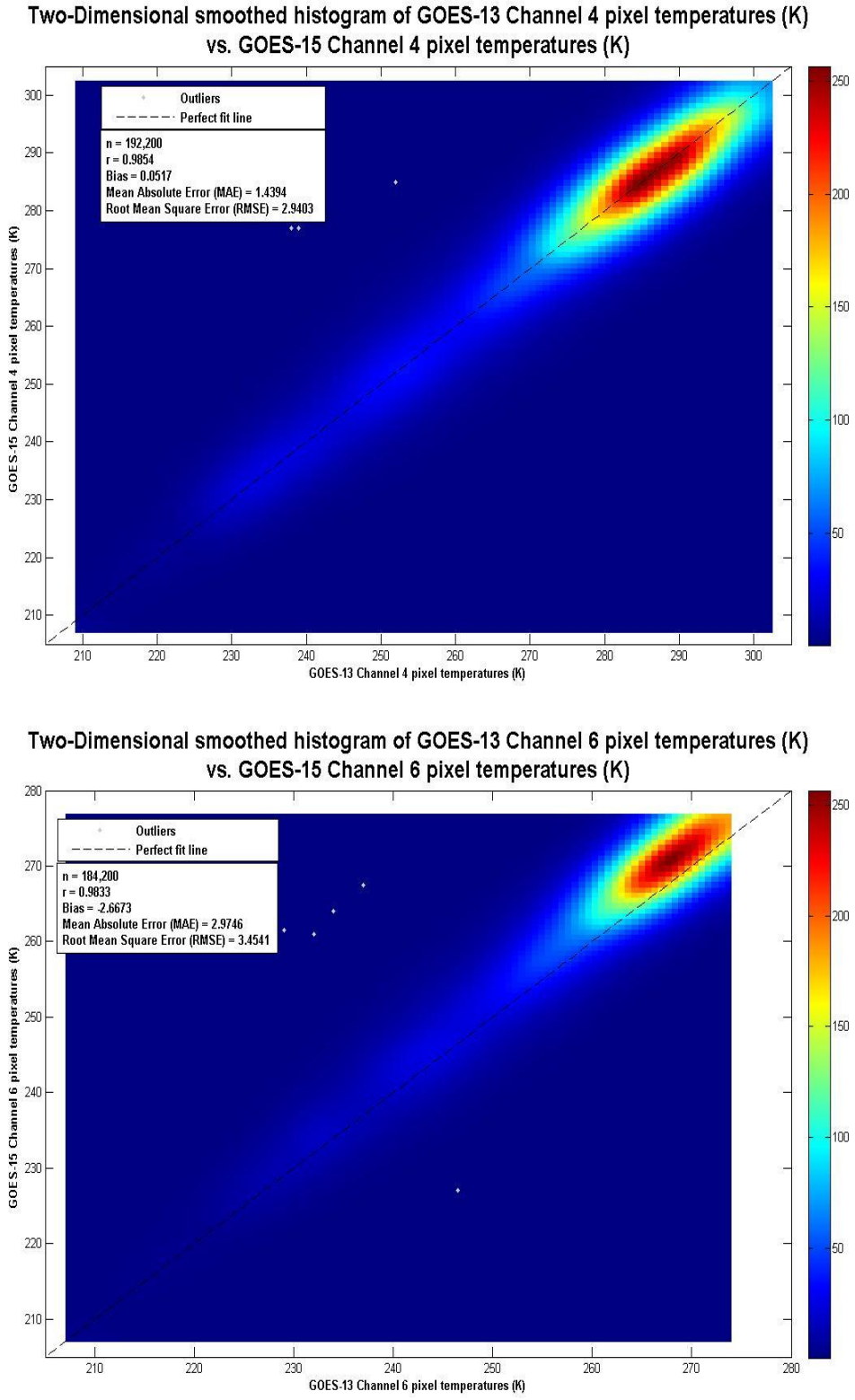

Figure 4.17: Two-Dimensional smoothed histogram of GOES-13 band-2, 3, 4, and 6 pixel temperatures (K) vs. GOES-15 band-2, 3, 4, and 6 pixel temperatures.

Figure 4.18 shows the mean Tb difference (black dots) and standard deviation (gray line segments) between GOES-13 and GOES-15 for the four IR bands at half-hour time bins from 24 to 26 June 2010. Since band-2 (3.9 μm) can also receive reflected solar radiation, a large variation in daytime Tb difference statistics are expected as the two satellites always view the collocated pixels from different directions and the surface is usually characterized with directional reflectance. The small variation in Tb difference around midnight indicates there is still some Midnight Blackbody Calibration Correction (MBCC) calibration residual, although the correction in general performs well in this band for both satellites. The mean Tb difference between GOES-15 and GOES-13 is -0.30 (±0.19) K (Table 4.10).

The Tb difference and statistics are very consistent for band-3 (6.5 μm) as the atmospheric water vapor detected by this band is relatively homogenous. The mean Tb difference between these two satellites is -0.05 (±0.06) K over the three-day study. Considering that GOES-15 has ~2 K Tb difference compared to AIRS/IASI and GOES-13 has <0.2 K Tb difference compared to these two hyperspectral radiometers, the large discrepancy of the GEO-LEO and GEO-GEO inter-calibration results is a result of the sensitivity of the radiometric calibration of the absorptive bands to the SRF distribution and SRF calibration uncertainty. Further work is needed to account for the difference in the SRF.

The mean Tb difference in band-4 (10.7 μm) between GOES-15 and GOES-13 is 0.08 (±0.15) K. The small, consistent daytime Tb difference, together with the small Tb bias compared to AIRS/IASI of these two instruments, indicates that band-4 on both GOES-15 and GOES-13 is well-calibrated. The large Tb variation around midnight is associated with the MBCC calibration residuals at these bands.

A large Tb difference can be observed for band-6 (13.3 μm). The mean Tb difference is 2.94 (±0.27) K. This large bias in band-6 was one of the reasons that the SRF was shifted. The discrepancy between the GEO-GEO and GEO-LEO inter-calibration is mainly due to the different SRFs for GOES-15 and GOES-13. More research is needed to understand the Tb variation between 1000-1800 UTC as this variation is unlikely related to the MBCC calibration residuals. Note that this analysis was done with the SRF available during the NOAA Science Test.

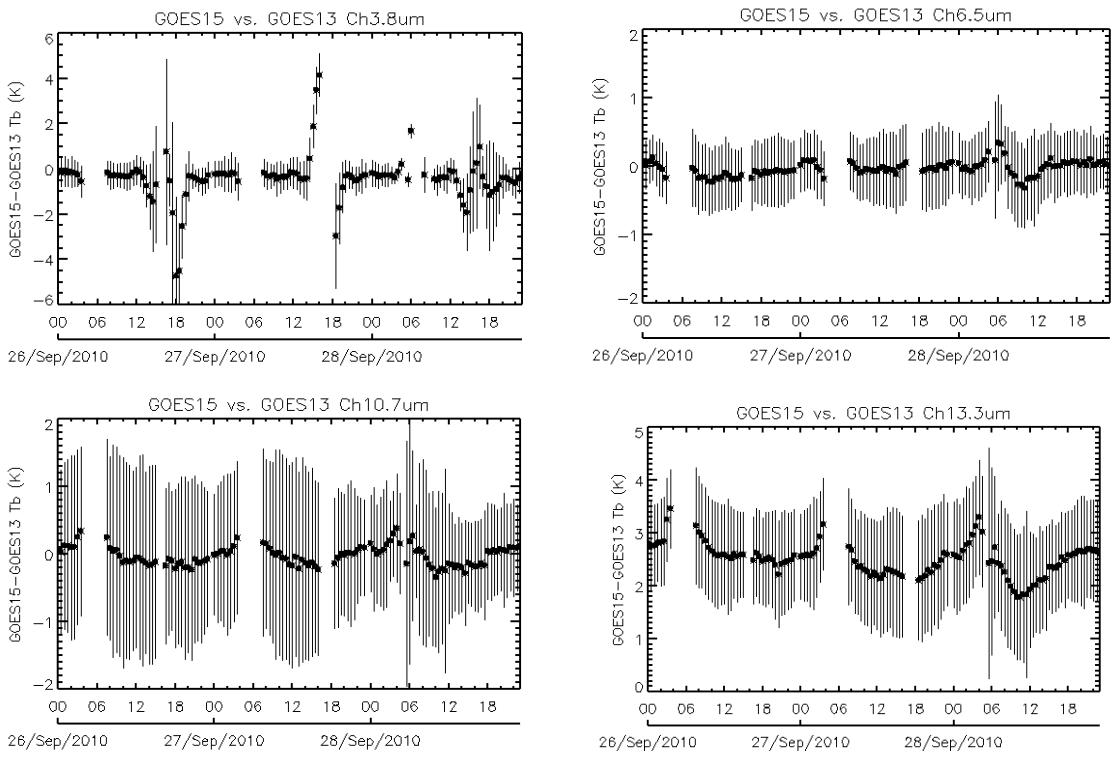

Figure 4.18: Direct inter-comparison of GOES-15 vs. GOES-13 Imager IR bands. No account was made for the differing SRFs.

Figure 4.19 plots the latitudinal distributions of the mean Tb difference (black dots) and the standard deviation (gray segments) between GOES-15 and GOES-13 within 0.5° latitude bins for the four IR bands on 10 August 2010. There is no significant Tb difference trend in bands 3 and 4, yet the Tb difference of band-6 increases significantly as the longitude increases. As the radiometric calibration of band-6 is especially sensitive to the SRF distribution (Wu et al. 2009), the longitudinal-dependent Tb bias is attributed to the increasing optical length which exaggerates the impact of the SRF difference on the radiance of this band.

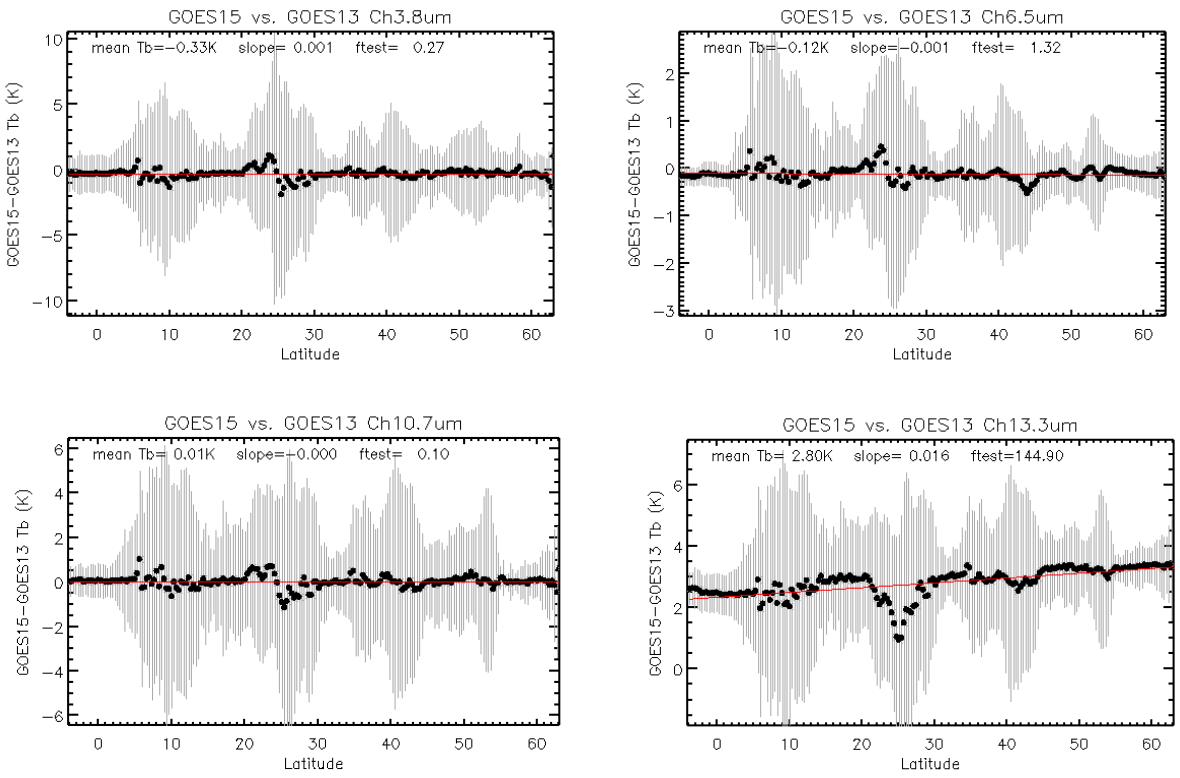

Figure 4.19: Latitudinal distribution of the mean Tb difference (dark dots) and the standard deviation (gray segments) between GOES-15 and GOES-13 for the four Imager IR bands (Tb difference = GOES-15 – GOES-13).

The mean Tb difference and standard deviation values for GOES-15 vs. GOES-13 and GOES-15 vs. GOES-11 are reported in Table 4.10. The mean Tb differences between GOES-15 and GOES-11 are -0.63 K, 2.51 K, and 0.41 K for bands 2, 3, and 4, respectively. The large standard deviation of the band-2 Tb difference (±1.00 K) is due to the strong BRDF effect during the daytime as these two satellites are located about 45^{o} apart. The SRF difference is most likely the main factor causing the large band-3 Tb difference as the GOES-15 band-3 SRF is much wider than that of GOES-11 (Schmit et al. 2002a).

Table 4.10: Mean Tb difference (K) and the standard deviation values for the IR bands between the Imagers on GOES-15 vs. GOES-13 and GOES-15 vs. GOES-11.

Imager Band	Central Wavelength (μm)	GOES-15 – GOES-13	GOES-15 – GOES-11
		K	
2	3.9	-0.30 (±0.19)	-0.63 (±1.00)
3	6.5	-0.05 (±0.06)	2.51 (±0.13)
4	10.7	0.08 (±0.15)	0.41 (±0.35)
6	13.3	2.94 (±0.27)	-

Similar collocation criteria are applied to identify the collocation pixels for the Sounder pairs, except that the maximum temporal difference is set to 15 minutes instead of 5 minutes. The spatial distribution of the collocation pixels are shown in Figure 4.20 for the two pairs of Sounder instruments. Similar to the Imager collocation, GOES-13 and GOES-15 have a much wider collocation distribution than that of GOES-11 and GOES-15, due to the much closer sub-satellite deployment. The mean of the Tb difference and the standard deviation for the 18 IR bands are reported in Table 4.11. Note that no corrections have been done to account for SRF differences.

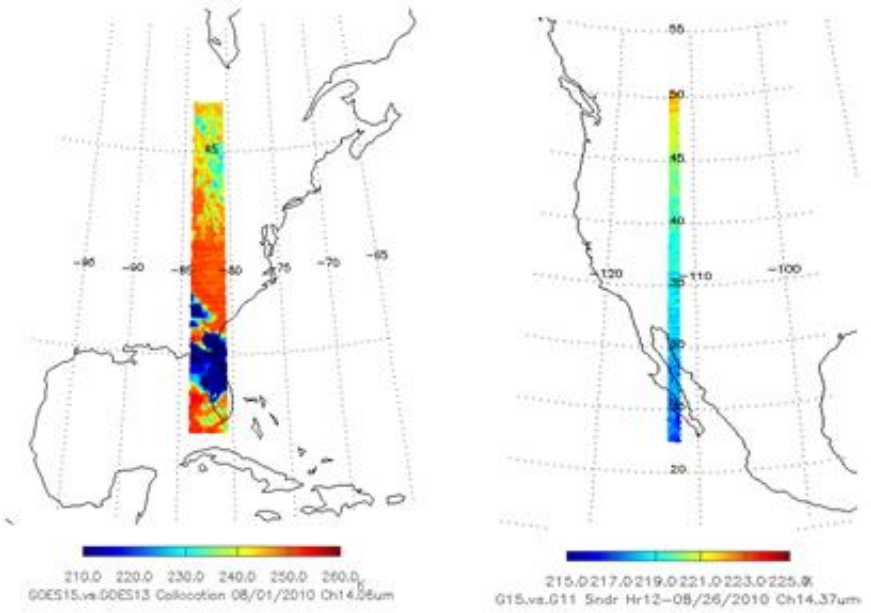

Figure 4.20: Spatial distribution of Sounder collocation pixels for GOES-15 vs. GOES-13 (left) and GOES-15 vs. GOES-11 (right).

Table 4.11: Mean Tb difference (K) and the standard deviation values for the IR bands between the Sounders on GOES-15 vs. GOES-13 and GOES-15 vs. GOES-11.

Sounder Band	Central Wavelength (μm)	GOES-15 – GOES-13	GOES-15 – GOES-11
		K	
1	14.71	0.23 (±0.09)	0.95 (±0.64)
2	14.37	-0.60 (±0.19)	-0.53 (±0.56)
3	14.06	-0.05 (±0.12)	-2.73 (±0.58)
4	13.64	0.18 (±0.12)	0.04 (±0.58)
5	13.37	-0.84 (±0.10)	0.66 (±0.68)
6	12.66	0.07 (±0.09)	0.30 (±1.47)
7	12.02	0.12 (±0.16)	0.26 (±1.25)
8	11.03	0.28 (±0.17)	-0.07 (±0.52)
9	9.71	0.25 (±0.21)	-0.12 (±0.44)
10	7.43	0.27 (±0.14)	-0.37 (±0.26)
11	7.02	0.26 (±0.19)	0.40 (±0.27)
12	6.51	0.05 (±0.30)	0.06 (±0.28)
13	4.57	-0.21 (±0.31)	3.50 (±0.42)
14	4.52	1.72 (±0.29)	1.33 (±0.20)
15	4.46	-1.05 (±0.39)	4.62 (±0.39)
16	4.13	0.87 (±0.27)	-0.51 (±0.27)
17	3.98	0.26 (±0.36)	-0.11 (±0.31)
18	3.74	0.27 (±0.35)	-0.04 (±0.36)

4.7. Imager-to-Polar-Orbiter Comparisons

Data were collected during the Science Test near the GOES-15 sub-satellite point from the high-spectral-resolution IASI on the European Organization for the Exploitation of Meteorological Satellites' (EUMETSAT's) polar-orbiting MetOp-A satellite. GOES-15 Imager data were collected within 30 minutes of the polar-orbiter overpass time. During the Science Test there were 25, 55, 56 and 57 comparisons (respectively) between GOES-15 and IASI. Fewer band-2 comparisons are available as they were only nighttime comparisons. The methodology for the comparisions, the CIMSS method, was nearly identical to that outlined in Gunshor et al. (2009), though applied to IASI data with no spectral gaps. The results are presented in Table 4.12. The mean brightness temperature differences for these comparisons show that GOES-15 was well calibrated for bands 2 and 4, based on the accuracy of IASI measurements. The large Imager band-3 and band-6 bias on GOES-13 was subsequently reduced when the SRF was updated (see section 5.1).

Table 4.12: Comparison of GOES-15 Imager to IASI using the CIMSS method. The bias is the mean of the absolute values of the differences. These comparisons were made with the SRF used during the Science Test, not the shifted SRF.

Imager Band	Mean Temperature Differences (K)	Standard Deviations (K)	Number of cases
2	-0.03	0.31	Shortwave Window band (9 night cases)
3	1.98	0.38	Water Vapor band (20 cases)
4	-0.03	0.66	Longwave IR Window band (22 cases)
6	0.53	0.59	CO_2 Absorption band (23 cases)

The GOES-15 IR radiometric calibration accuracy was evaluated by inter-calibrating to two well-calibrated hyperspectral radiometers on LEO satellites: the Atmospheric Infrared Sounder (AIRS) on the EOS-Aqua satellite, and the Infrared Atmospheric Sounding Interferometer (IASI) on the MetOp-A satellite (Wu et al. 2009). The collocation data were identified when both the GEO and LEO instruments viewed the same scene at similar times and viewing zenith angles. The detailed description of the collocation selection is also documented in the Global Satellite Inter-Calibration System (GSICS) GEO-LEO baseline inter-calibration Algorithm Theoretical Basis Document (ATBD). At each collocated scene, the hyperspectral measurements are transferred to the broadband radiance using the spectral convolution equation as follows:

$$R_{LEO} = \frac{\int_{\nu} R_{\nu} \Phi_{\nu} d\nu}{\int_{\nu} \Phi_{\nu} d\nu}$$

where R_{LEO} is the simulated GOES measurement from AIRS/IASI radiances, R_{ν} is the AIRS/IASI radiance at wavenumber ν, and Φ_{ν} is GOES spectral response at wavenumber ν. As shown in Figure 4.21, AIRS has a problem with spectral gaps and unstable or dead detectors. The Japanese Meteorological Agency (JMA)'s gap-filling method is applied to compensate for the discontinuities before the spectral convolution method is applied (Tahara and Kato 2009).

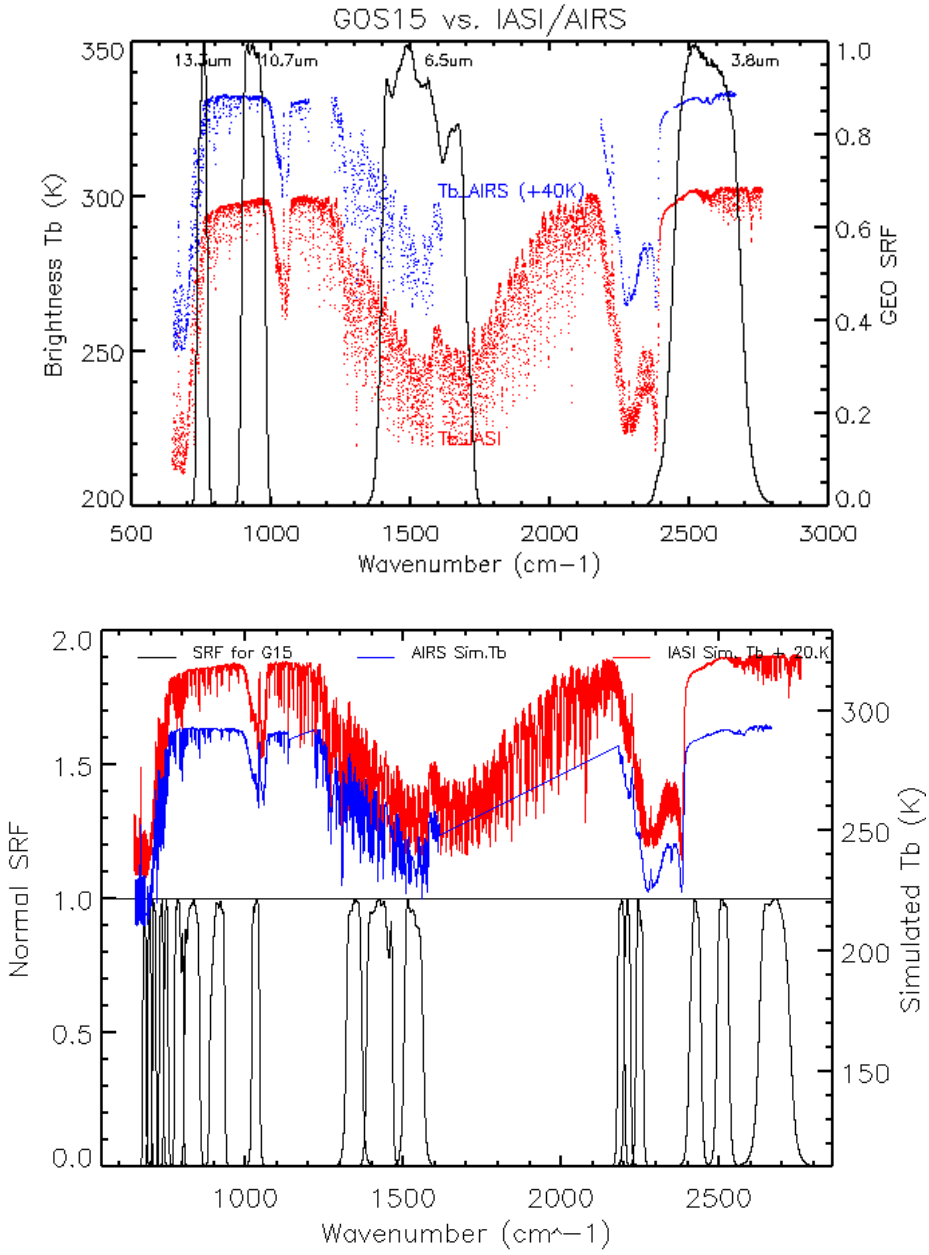

Figure 4.21: SRF of GOES-15 Imager (top) and Sounder (bottom), together with the AIRS/IASI spectra.

Two sets of GEO-LEO inter-calibration data, based on the daytime and nighttime collocation pixels, are used to evaluate the Imager IR radiometric calibration accuracy. Both inter-calibrations with AIRS and IASI yielded very similar results in Table 4.13. Note that during the GOES-15 PLT, the Imager SRFs that were used were the latest available, and hence not the Rev. H (shifted) that came out in August 2011 to correct the noted shift in the two absorptive bands. The Rev. H values have been employed, in the creation of GVAR, in the Satellite Operations Control Center (SOCC) data since 5 August 2011. The mean brightness temperature (Tb) differences listed in Table 4.13 are calculated with the homogeneous collocation pixels. Unlike GOES-12 which has very small GEO-LEO Tb differences in the water vapor band (6.5 μm),

both the GOES-AIRS and GOES-IASI inter-calibration results indicated large and consistent bias for the GOES-15 water vapor band and CO_2 sensitive band. The two-IR window bands (bands 2 and 4) are well-calibrated with a Tb bias less than 0.2 K. The two absorptive bands, however, have relatively large Tb biases to both AIRS and IASI measurements. The Tb bias compared to AIRS/IASI for band-6 ranges from 0.66 K to 0.77 K, depending on the collocation time and LEO instrument. Compared to both LEO instruments, the water vapor band (band-3) consistently has the largest Tb bias (~2 K), which exceeds specification. Note that the implemented SRF during the Science Test is that of version Rev. F, which is the same as the Rev. E version for the Imager IR bands (ITT technical memo, 2010). Per this analysis, ITT, the instrument vendor, re-visited the pre-launch sample data and came up with a new version of SRF (Rev. G). These data were then empirically shifted to reduce the systemic bias (Rev. H). The shortwave band (3.9 μm) had a large Tb difference during the daytime (not shown) due to reflected solar radiation. As shown in Figure 4.22 and 4.23, the Tb difference is consistent over the study period.

Table 4.13: Brightness temperature (Tb) biases between GOES-15 Imager and AIRS/IASI for the daytime and nighttime collocated pixels between AIRS and IASI through GOES-15 Imager daytime collocation data using the GSICS method. The Tb biases were based on the collocated pixels acquired from 3 June 2010 and 25 October 2010. Standard deviations are given in parentheses. Again, these values were obtained before the final, shifted SRF were employed.

Imager Band	Central Wavelength (μm)	daytime (K)		nighttime (K)
		GOES-AIRS	GOES-IASI	GOES-IASI (9:30 pm)
2	3.9	-	-	0.09 (±0.08)
3	6.5	2.04 (±0.13)	2.12 (±0.11)	1.98 (±0.14)
4	10.7	0.18 (±0.18)	0.10 (±0.20)	0.03 (±0.10)
6	13.3	0.77 (±0.14)	0.74 (±0.14)	0.66 (±0.12)

These GSICS-method results are consistent with the CIMSS-method results in Table 4.13.

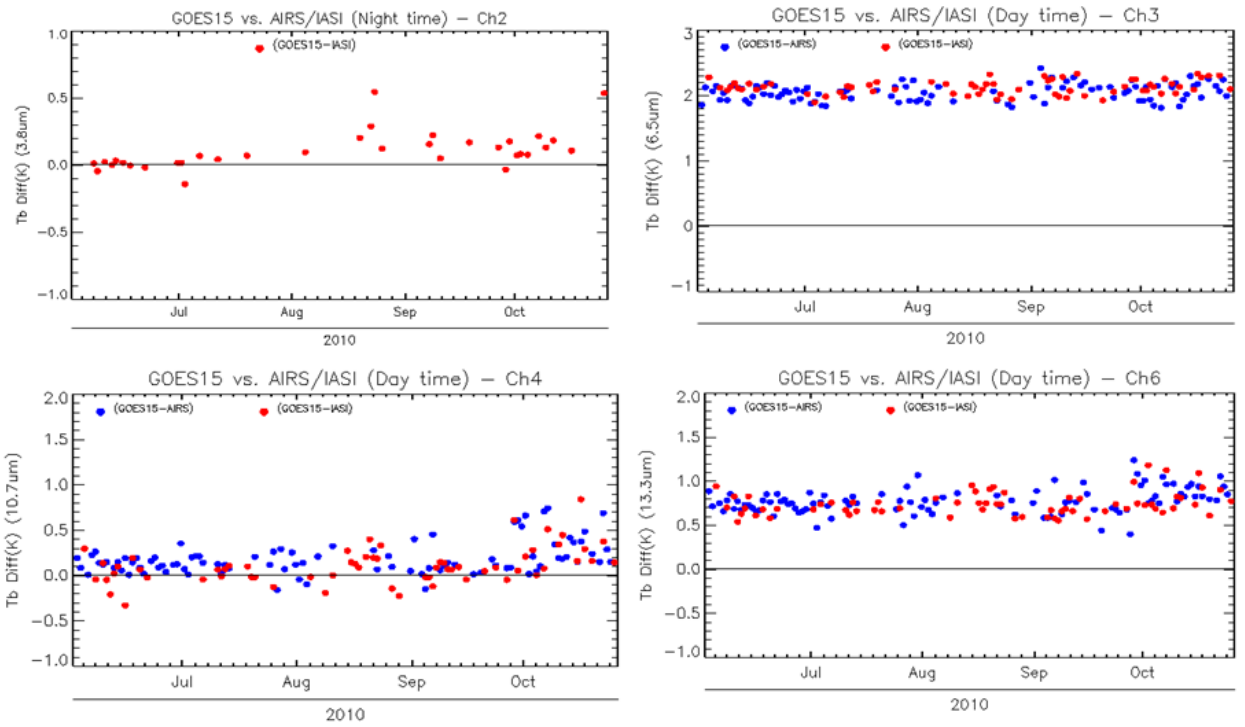

Figure 4.22: GOES-15 Imager IR bands time series of the brightness temperature bias with AIRS and IASI inter-calibration. Band-2 values are only during the night, while the other bands are during the day. Note that these are from the Science Test and hence before the SRF shift of bands 3 and 6.

Like the other 3-axis stabilized GOES satellites, the GOES-15 Imager and Sounder experience an abnormal heating process resulting in erroneous calibration slopes around the satellite midnight (Johnson and Weinreb 1996). An empirical MBCC method was developed and implemented to mitigate this midnight calibration anomaly. Figure 4.23 shows the mean Tb bias compared to AIRS and IASI (open and solid dots at primary y-axis) and the frequency of MBCC onset (solid line at second y-axis) at every half hour during the PLT period. Apparent diurnal calibration variation can be observed in bands 3, 4, and 6. The onset of MBCC varies at different bands. It should have the most effect two to three hours before "satellite" midnight and the next three to six hours after, depending on the IR band. Since MBCC is the major factor in determining the diurnal calibration variation, it was evaluated using the method described by Yu et al. (2011). The MBCC correction residual (ΔTb_{MBCC}) can be calculated as:

$$\Delta Tb_{MBCC} = Tb_{GEO-AIRS,noon} - Tb_{GEO-AIRS,midnight}$$

where $Tb_{GEO\text{-}AIRS,\ noon}$ is the mean Tb difference between GOES and AIRS between 12:00 pm and 2:00 pm, and $Tb_{GEO\text{-}AIRS,\ midnight}$ is the mean Tb difference between GOES and AIRS between 12:00 am and 2:00 am.

As shown in the last column of Table 4.14, the MBCC works very efficiently for band-6, and seems ineffective for bands 3 and 4. Although the MBCC has been intensively turned on around satellite midnight, approximately 0.35 K and 0.41 K in calibration residuals remained for bands 3 and 4, respectively. Our previous analysis on the MBCC indicates that it works well for GOES-

11/12/13 band-3 with less than 0.1 K to 0.2 K residual but is less effective for band-4. More research may be needed to investigate the discrepancy on the band-3 MBCC correction for GOES-15. For band-2 (not shown), the small and consistent Tb bias compared to IASI before and after the MBCC onset implies that MBCC works well for this band.

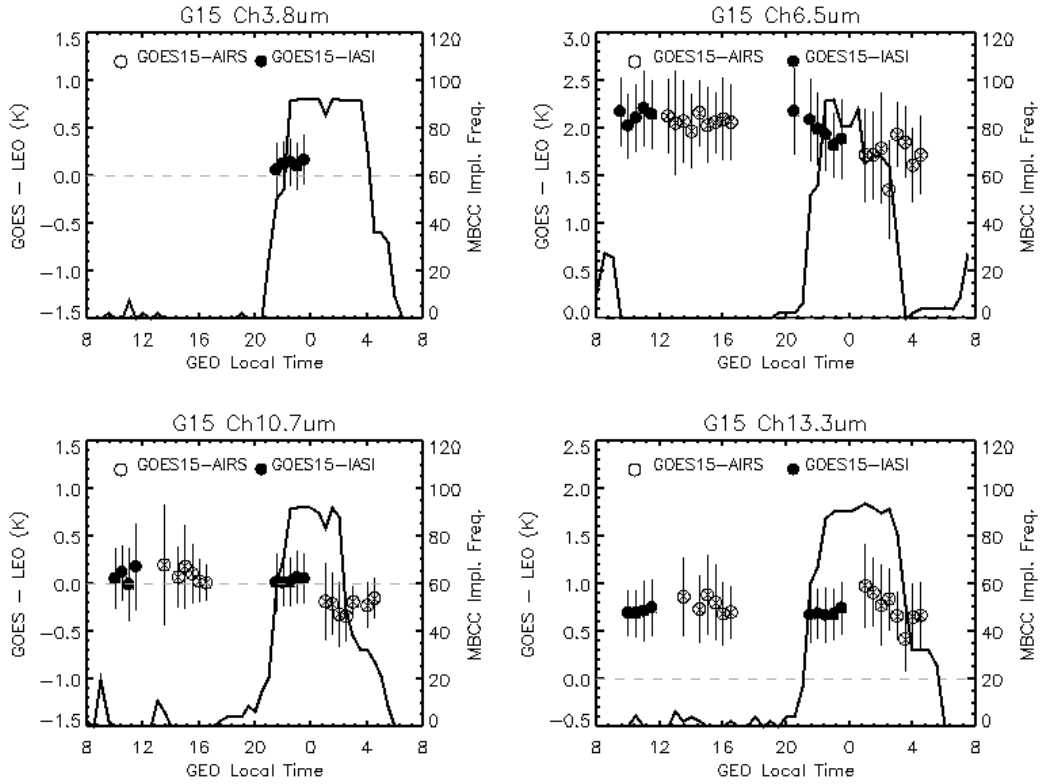

Figure 4.23: The Mean Tb bias compared to AIRS/IASI for GOES-15 Imager IR bands.

Table 4.14: GOES-15 Imager diurnal calibration variation.

Imager Band	Central Wavelength (μm)	Mean GOES-AIRS (12:00 pm-2:00 pm)	Mean GOES-AIRS (12:00 am-2:00 am)	MBCC residual (K)
3	6.5	2.07	1.72	0.35
4	10.7	0.20	-0.21	0.41
6	13.3	0.87	0.91	-0.04

A similar GEO-LEO inter-calibration (GSICS) method was applied to the GOES-15 Sounder IR bands to evaluate the radiometric calibration accuracy. Unlike the GEO-LEO inter-calibration for the GOES Imager data, the GOES vs. IASI collocation for the Sounder only occurs in the evening time. Figure 4.24 and Table 4.15 show the mean and standard deviation of the Tb bias compared to the IASI homogeneous scenes from 3 June 2010 to 3 August 2010 and compared with those of the other GOES satellites. The results indicate that GOES-15 Sounder IR bands are well-calibrated and comparable with the other two GOES-N/O/P instruments during this

period. The Tb bias of most bands is less than 0.2 K, except for band-5 (0.48 K) and band-13 (0.40 K). GOES Sounder band-18 is not included due to its spectral coverage.

Table 4.15: GOES-15 Sounder IR vs. IASI brightness temperature difference at nighttime, compared to other GOES Sounders using the GSICS method. The data in the parentheses are the standard deviation of the Tb difference at the collocation pixels.

Sounder Band	Central Wavelength (μm)	GOES-15 Mean (±stdv) (K)	GOES-14 Mean (±stdv) (K)	GOES-13 Mean (±stdv) (K)	GOES-12 Mean (±stdv) (K)
1	14.71	0.23 (±0.15)	0.274 (±0.195)	0.19 (±0.17)	-0.006 (±0.233)
2	14.37	0.04 (±0.54)	0.127 (±0.245)	0.18 (±0.15)	0.078 (±0.197)
3	14.06	-0.10 (±0.98)	0.103 (±0.610)	-0.02 (±0.48)	0.180 (±0.739)
4	13.64	0.07 (±1.28)	0.208 (±0.917)	0.08 (±0.77)	-0.258 (±1.373)
5	13.37	-0.48 (±1.42)	0.041 (±1.159)	-0.10 (±1.05)	0.313 (±1.837)
6	12.66	-0.01 (±1.29)	0.106 (±1.601)	0.08 (±1.37)	-0.160 (±2.094)
7	12.02	0.01 (±1.15)	-0.041 (±1.575)	-0.01 (±1.46)	-0.086 (±2.068)
8	11.03	0.02 (±1.10)	-0.067 (±1.363)	0.00 (±1.37)	-0.109 (±1.906)
9	9.71	-0.15 (±0.94)	0.076 (±0.838)	-0.04 (±1.01)	-0.055 (±1.366)
10	7.43	-0.04 (±0.62)	-0.040 (±0.747)	-0.02 (±0.70)	-0.328 (±1.088)
11	7.02	-0.05 (±0.62)	-0.121 (±0.574)	-0.28 (±0.60)	-0.119 (±0.994)
12	6.51	-0.03 (±0.60)	-0.178 (±0.438)	-0.19 (±0.45)	-0.236 (±0.680)
13	4.57	0.40 (±0.51)	0.263 (±0.506)	-0.12 (±0.62)	-0.883 (±1.052)
14	4.52	-0.07 (±0.41)	-0.049 (±0.341)	-0.34 (±0.51)	-0.499 (±0.936)
15	4.45	0.06 (±0.44)	0.144 (±0.506)	-0.55 (±0.42)	-5.076 (±2.766)
16	4.13	0.03 (±0.57)	0.076 (±0.517)	-0.06 (±0.57)	0.304 (±1.283)
17	3.98	-0.01 (±0.66)	-0.116 (±0.648)	-0.13 (±0.65)	0.106 (±1.529)

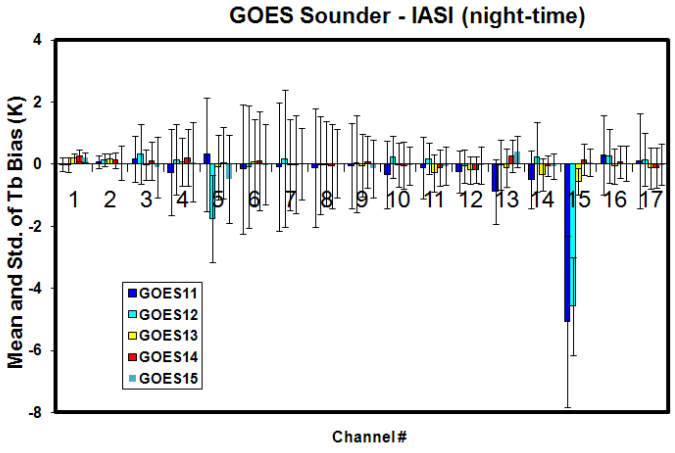

Figure 4.24: Mean and standard deviation of GOES-11 through GOES-15 Sounder brightness temperature difference from nighttime IASI data using the GSICS method.

4.8. Stray-Light Analysis

By supplying data through the eclipse periods, the GOES-13/14/15 system addresses one of the major limitations which are eclipse and related outages. This change is possible due to larger spacecraft batteries. Outages due to KOZ will be minimized. Outages due to KOZ will be replaced by Stray-Light Zone outages and reduced by utilizing partial-image frames away from the sun and possibly stray-light correction via a Sensor Processing System (SPS) algorithm under development. Figure 4.25 shows why this correction is needed.

With the new capability of data comes the risk of producing images contaminated by the energy of the sun. An image with artificial brightness temperature excursions up to 75 K (e.g. Imager band-2) may affect products. To determine how much good data can be acquired, at the same time minimizing the amount of bad data, many scans were conducted during the eclipse period in 2010.

While all Imager bands can be affected, the visible and shortwave (band-2) are affected the most. There are investigations into the possibility of correcting these stray-light affected images before distribution via GVAR.

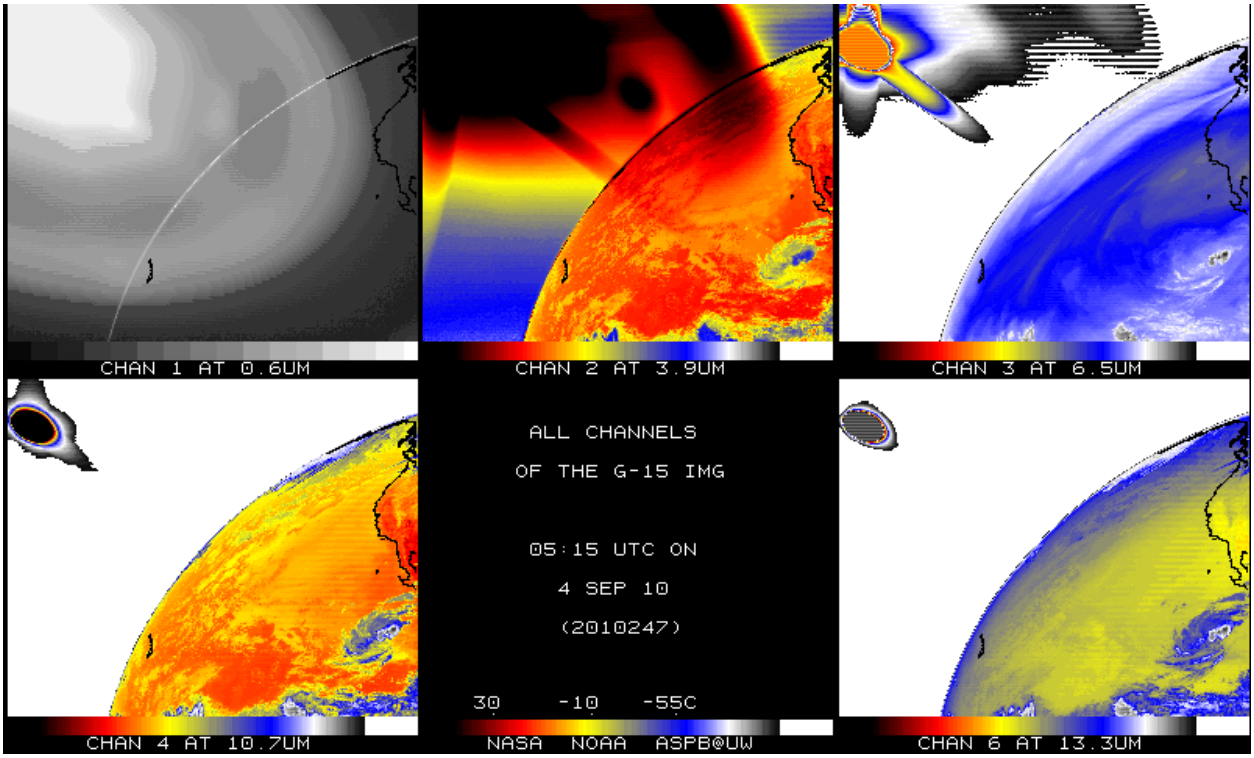

Figure 4.25: GOES-15 Imager multi-panel. Note the "stray light" associated with the sun.

In general, the GOES Sounder can be affected even more during the KOZ periods due to the relatively slow Sounder scanning (not shown).

4.9. Instrument Performance Monitoring

The GOES IPM system uses the near real-time GVAR Block 11 (B11) data routinely downloaded from the NOAA Comprehensive Large Array-data Stewardship System (CLASS) data source. Four types of calibrated related parameters are ingested from the GVAR B11 data, including the instrument telemetry data, IR calibration coefficients, statistics of space-look and blackbody scan data. Instrument noise, such as NEdR and NEdT, is also monitored for each detector. To detect any potential calibration anomaly, all these monitored parameters are displayed at various temporal scales for diurnal to long-term variations.

4.9.1. Telemetry Monitoring

The GOES-15 Imager and Sounder instrument performance was intensively monitored using the GVAR B11 data from 11 August 2010 through 25 October 2010. Approximately 14 Imager and 16 Sounder telemetry parameters were monitored with the GOES IPM system (Yu and Wu 2010). The monitored GOES-15 IPM parameters are listed in Table 4.16. Most of these parameters were functioning well and comparable with the other GOES instruments. In this report, the behaviors of the Imager and Sounder blackbody (BB), scan mirror, and patch temperatures are summarized.

Table 4.16: GOES-15 Imager and Sounder telemetry parameters monitored with the GOES-IPM system during the PLT Science Test.

	Telemetry variables	Detector Number (Imager)	Detector Number (Sounder)
1	Electronics Temperature	2	2
2	Sensor Assembly Baseplate Temperature	6	6
3	BB Target Temperature	8	8
4	Scan Mirror Temperature	1	1
5	Telescope Primary Temperature	1	1
6	Telescope Secondary Temperature	2	2
7	Telescope Baffle Temperature	2	2
8	Aft Optics Temperature	1	1
9	Cooler Radiator Temperature	1	1
10	Wide Range IR Detector Temperature	1	1
11	Narrow Range IR Detector Temperature	1	1
12	Filter Wheel Housing Temperature	X	1
13	Filter Wheel Control Heater Voltage	X	1
14	Patch Control Voltage	1	1
15	Instrument Current	1	1
16	Cooler-Housing Temperature	1	1

Similar to the other GOES Imagers (of the 3-axis design), the GOES-15 Imager experienced about +15 K diurnal variation in the blackbody (BB) temperature and +40 K variation in the scan mirror temperature with the highest temperature peak around satellite midnight (Figure 4.26).

During the eclipse period between 31 August 2010 and 13 October 2010, the diurnal variations of the telemetry temperature were reduced because of the reduced peak temperature. The reduced peak telemetry temperature during the eclipse season is also observed by the other GOES instruments.

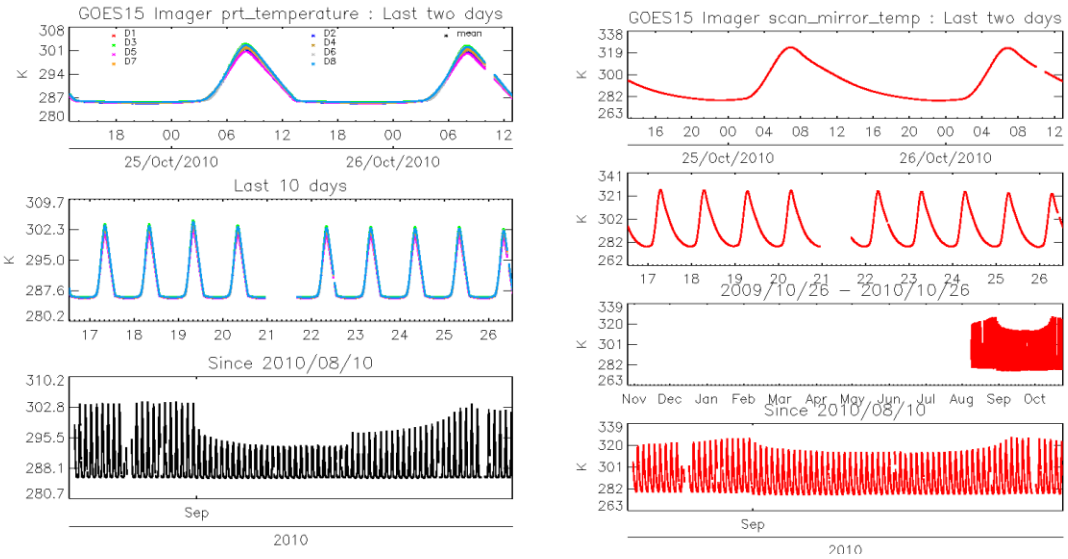

Figure 4.26: The GOES-15 Imager Platinum Resistance Thermometer (PRT, left) and scan mirror (right) temperature shown with various temporal scales.

The Imager patch temperature was controlled consistently at the low-level (~81 K) with a slight variation in the narrow patch temperature in the beginning of the PLT period. The wide-range patch temperature was slightly higher (~0.23 K) than the narrow-range one. Meanwhile, the two operational GOES, GOES-11 (GOES-West) and GOES-13 (GOES-East) Imagers, experienced the annual patch temperature switch from mid- to low-level in September 2010.

Similar to the other GOES instruments, the GOES-15 Sounder BB and scan mirror also experienced significant diurnal variations with the highest temperature occurring around the satellite midnight (Figure 4.27). The magnitude of diurnal variation due to the reduced peak values can also be observed between 31 August 2010 and 13 October 2010.

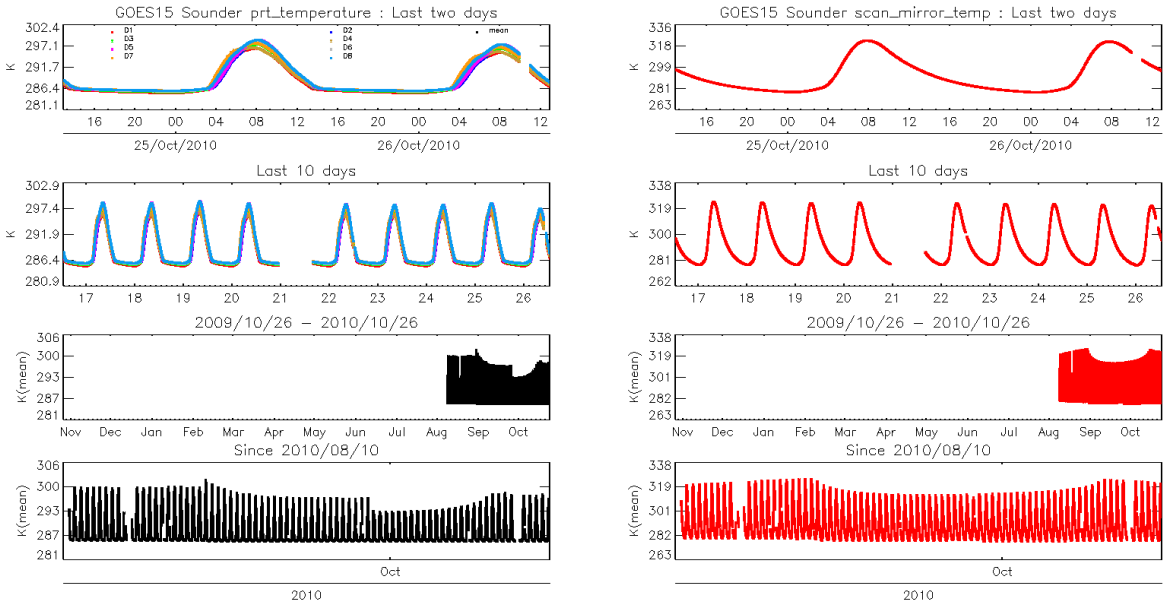

Figure 4.27: GOES-15 Sounder BB temperature (left) and scan mirror temperature (right) at different temporal scales.

4.9.2. Monitoring the GOES Sounder Patch Temperatures

The GOES-15 Sounder patch experienced floating temperatures resulting from the "blanket-heating" effect in two periods: 11 August 2010 to 31 August 2010, and 17 September 2010 to 27 September 2010 (Figure 4.28). During these two periods, the spacecraft was flipped from an inverted to an upright orientation. Due to the "dislodged thermal blanket issue", the Sounder patch temperature could not be controlled in the upright orientation during the summer. NOAA/NASA decided to invert the spacecraft (SC) to establish patch control so that the Science Test could be performed. The SC was inverted on 31 August 2010, and the patch control "low" setting was reached soon after. The Sounder patch began floating again on 17 September 2010 in the inverted orientation as the Sun declination was approaching equinox. First, the patch was raised to the "mid" setting (~85 K) to reduce the daily range on 22 September 2010. Then, on September 27, the SC was yaw-flipped to an "upright" orientation (preferred orientation for winter) to achieve control at a "low" patch setting (~81.6 K) (Figure 4.28). A slight diurnal variation (~0.02 K) can also be observed at the "low" patch setting (Figure 4.29). Meanwhile the patch temperature of the two operational Sounders at GOES-11/13 switched from mid- to low-level in September 2010.

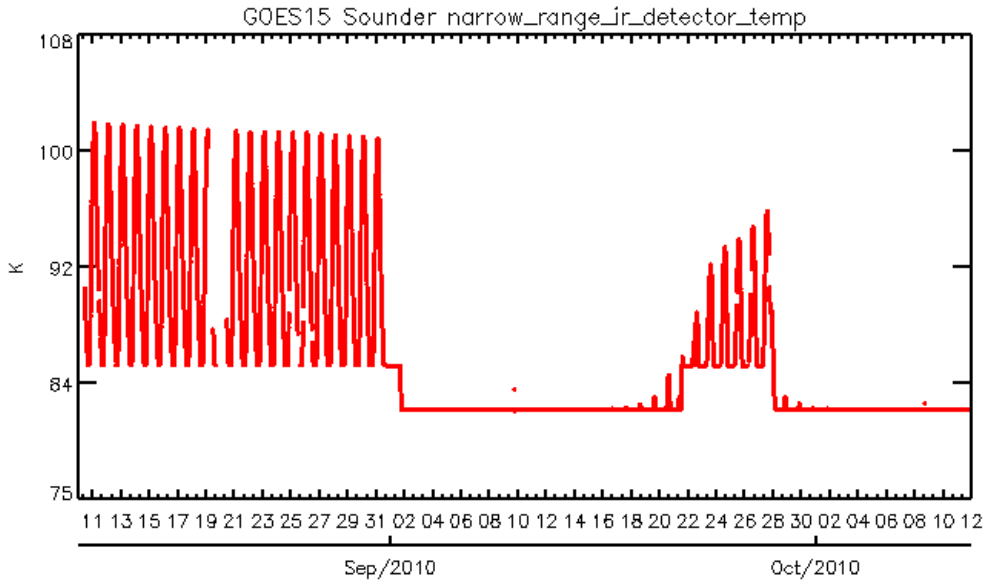

Figure 4.28: Time-series of GOES-15 Sounder narrow-range patch temperatures from 10 to 12 August 2010.

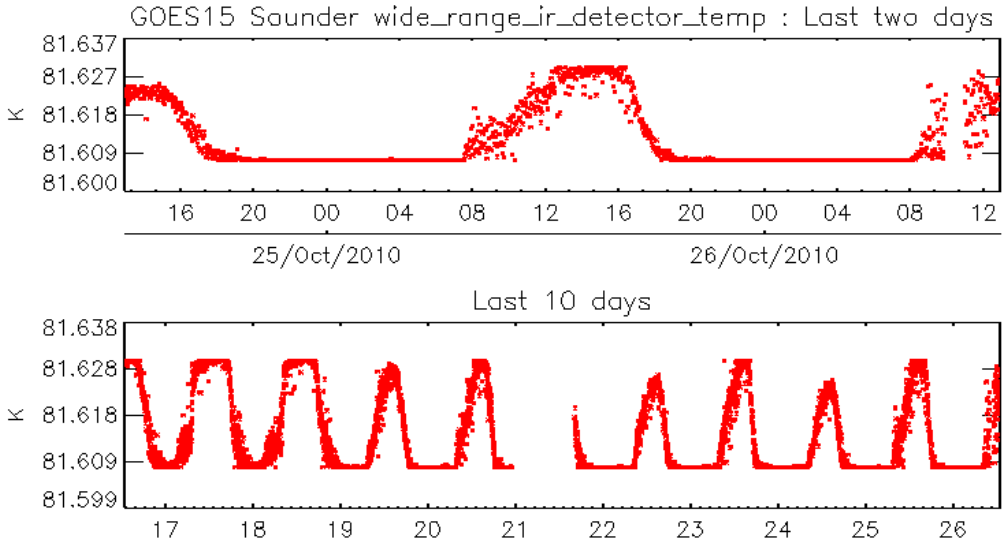

Figure 4.29: Diurnal variations of the GOES-15 Sounder patch temperature from 25 to 26 October 2010 (upper panel) and from 16 to 26 October 2010 (lower panel).

4.10. Finer Spatial Resolution GOES-15 Imager

The water vapor band on the GOES-15 Imager is improved compared to that on the GOES-11 Imager. The detector sizes improved from 8 to 4 km. While each image is shown in its native position, the finer scale features on GOES-15 are clearly seen (Figure 4.30). The improved (4 km FOV at the sub-point) spatial resolution of the 13.3 µm band (band-6) required changes to the GVAR format. Several issues with implementing the new GVAR format were discovered, communicated, rectified, and verified. For example, the paired detectors on the higher-resolution

13.3 µm band (band-6) were inadvertently swapped when the satellite was in an inverted mode. This situation was quickly resolved. The image in Figure 4.31 demonstrates the improved spatial resolution of this band on the GOES-15 Imager.

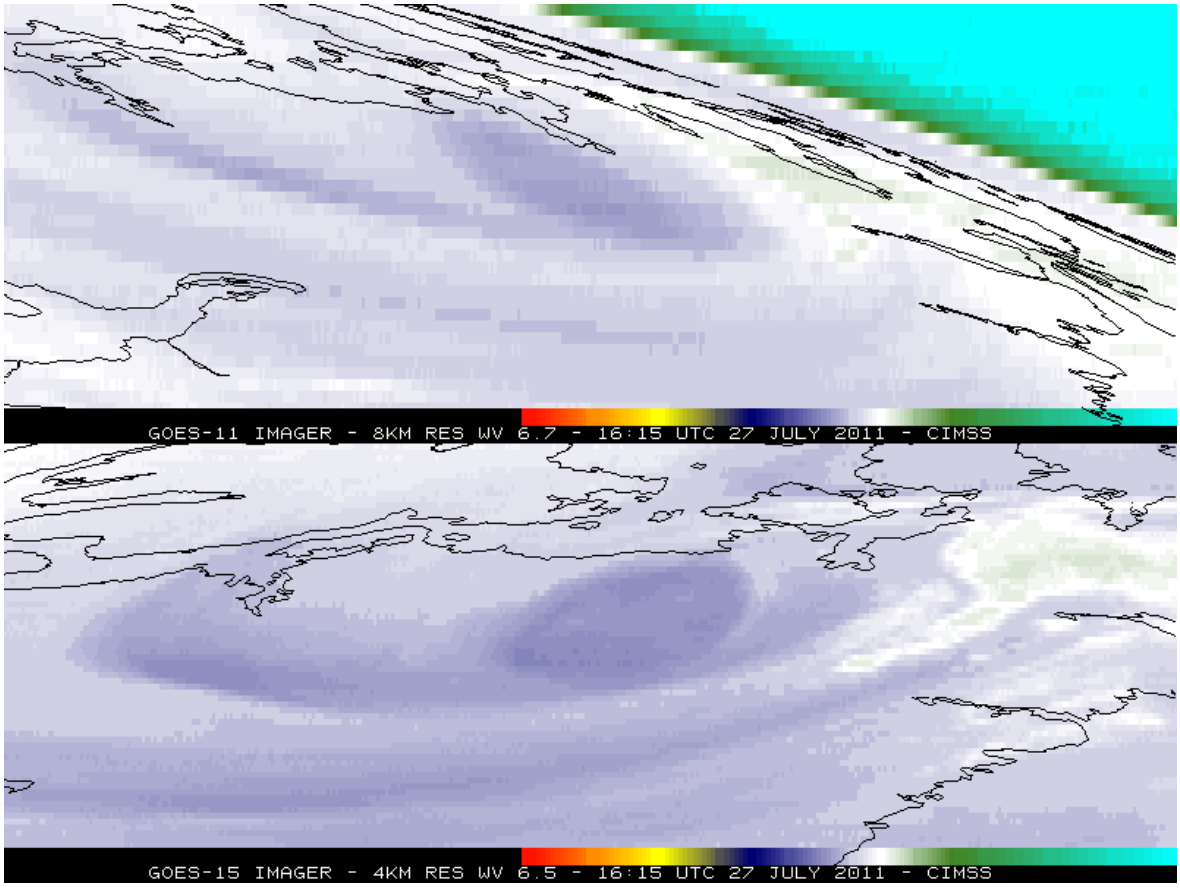

Figure 4.30: Improved Imager spatial resolution of the water vapor band for GOES-15 (lower panel) compared to GOES-11 (top panel) from 27 July 2011.

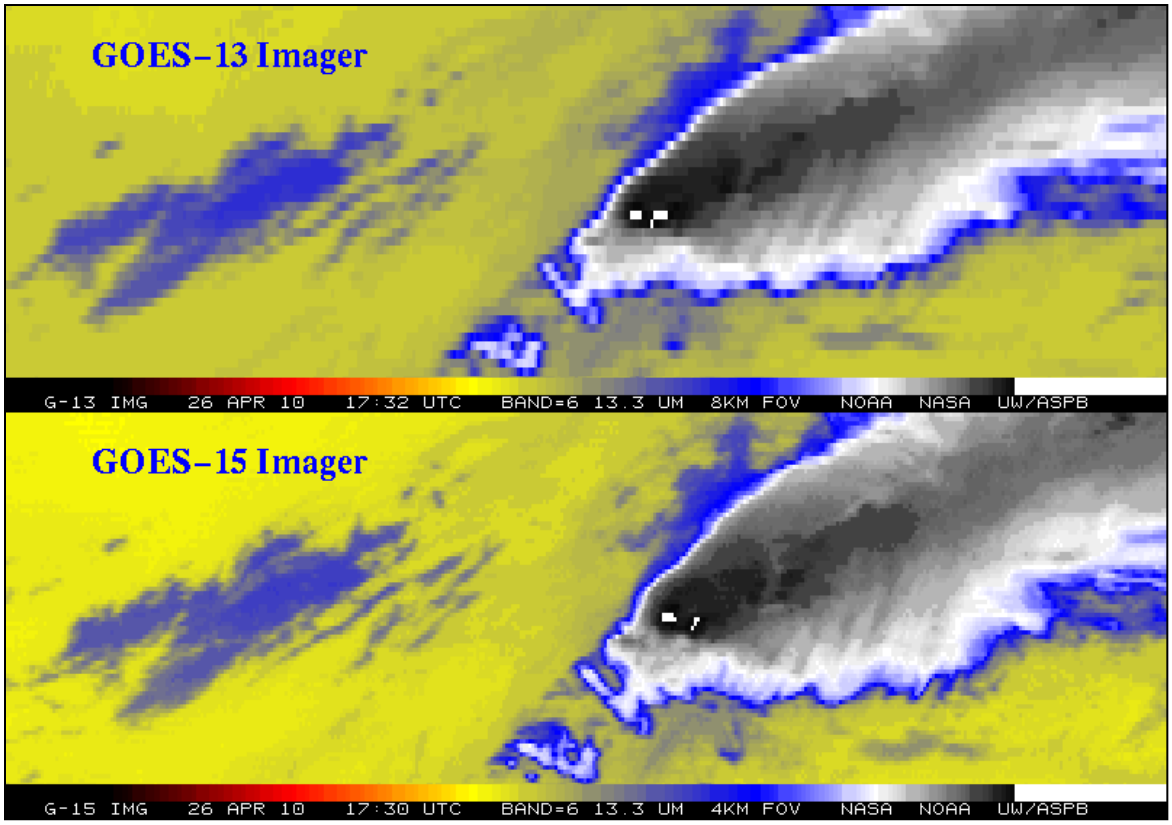

Figure 4.31: Improved Imager spatial resolution at 13.3 μm for GOES-15 (lower panel) compared to GOES-13 (top panel) from 26 April 2010.

4.11. Corrections of SRF for GOES-14/15 Imagers

During the Post-Launch Science Tests (PLT) of GOES-14 and GOES-15, NOAA reported biases for Imager band-3 (6.5 μm), based on the GSICS GEO-LEO inter-calibration analysis. The bias, in terms of brightness temperature (T_b), was +0.99 K for GOES-14 and +2.12 K for GOES-15 (Table 4.17, column 3). Biases of −0.50 K and +0.76 K were also found for Imager band-6 (13.3 μm) of GOES-14/15, respectively, which are within the specified accuracy requirement of 1 K.

In response, ITT Industries, the instrument vendor, re-analyzed the pre-flight instrument calibration data and revised the SRF, which was released as Rev. H. The radiometric calibration accuracy with the Rev. H SRF was then evaluated using the simulated earth radiance as described in Wu and Yu (2011). Re-evaluation confirmed that Rev. H substantially reduced the bias, yet a residual bias of up to 1 K remained. While meeting (marginally for some bands) the instrument specification of 1 K, the bias can be attributed to uncertainty in the SRF (Wu et al. 2009). Therefore it was recommended to further correct the ITT Rev. H SRF by shifting the SRF (Wu and Yu 2011). The SRF of the shifted Rev. H SRF, together with the original Rev. G SRF for GOES-14/15 band-3 and band-6 are plotted in Figure 4.32. These shifted SRFs were implemented on 5 August 2011 for both GOES-14 and GOES-15.

Table 4.17: Biases for selected GOES-14/15 Imager bands using the SRF as originally supplied by ITT (Rev. E), revised by ITT (Rev. H), further corrected by NOAA, and the recommended correction.

GOES and Band number	Central Wavelength (μm)	Bias with ITT Rev. E (K)	Bias with ITT Rev. H (K)	Recommended Shift (cm^{-1})	Bias with Shifted SRF (K)
GOES-14 band-3	3.9	0.99	0.97	−8.75	+0.07
GOES-14 band-6	6.5	-0.53	-0.27	-0.50	+0.08
GOES-15 band-3	10.7	2.12	0.73	-6.75	+0.07
GOES-15 band-6	13.3	0.76	0.42	+0.50	+0.19

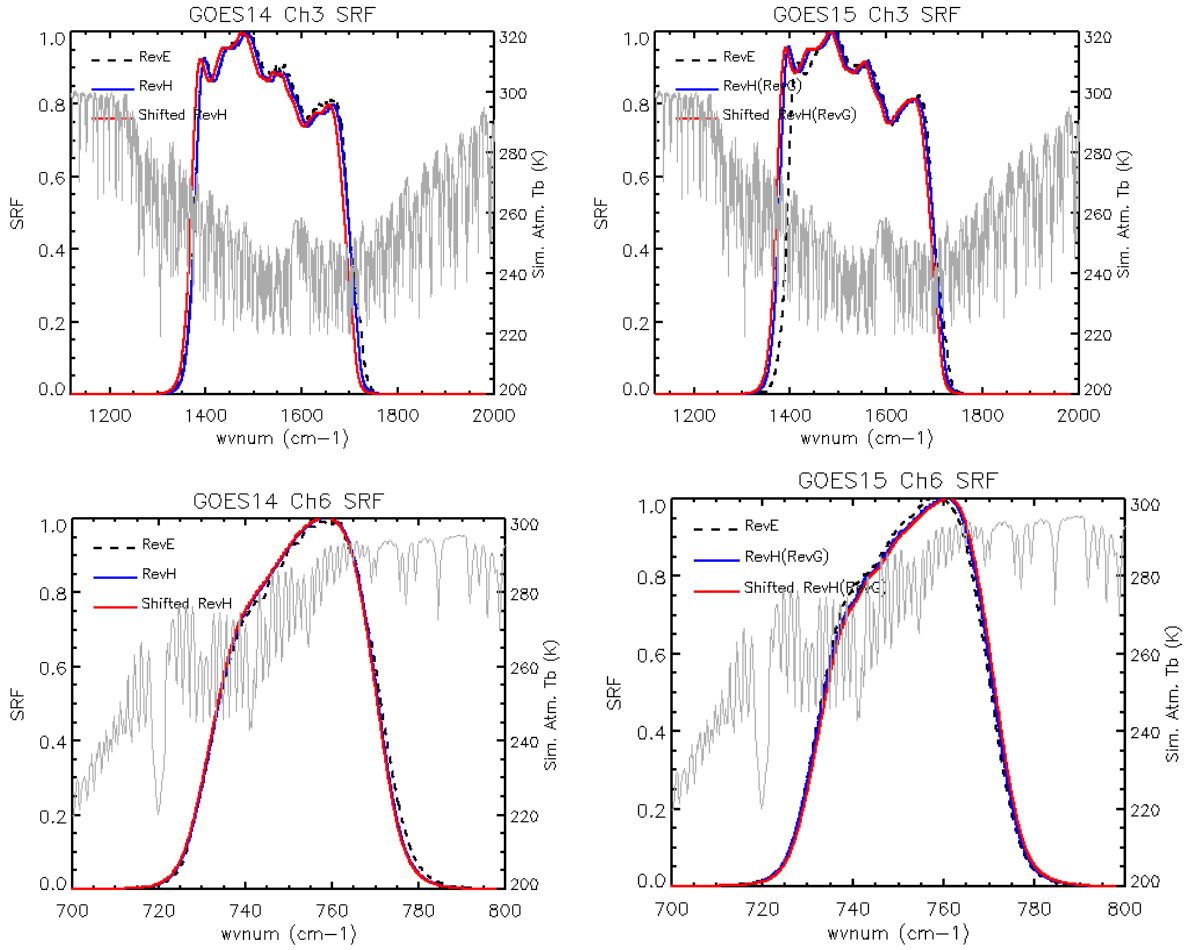

Figure 4.32: Rev. E, Rev. H, and shifted Rev. H SRFs for GOES-14/15 Imager band-3 and band-6 (dash black, blue solid and red solid lines), together with the IASI simulated TOA Tb for a clear tropical atmospheric profile (gray lines at second y-axis). Note that Rev. G and Rev. H SRFs are identical for GOES-15 Imager IR bands.

The quality of the GOES-15 Imager band-3 and 6 spectral shifts were also validated once GOES-15 began resending data in the fall of 2011. Note the greatly reduced bias on the few points on the right-hand-side of Figure 4.33. The band-3 bias was reduced from over 2 K to approximately 0 K, when compared to high spectral resolution observations.

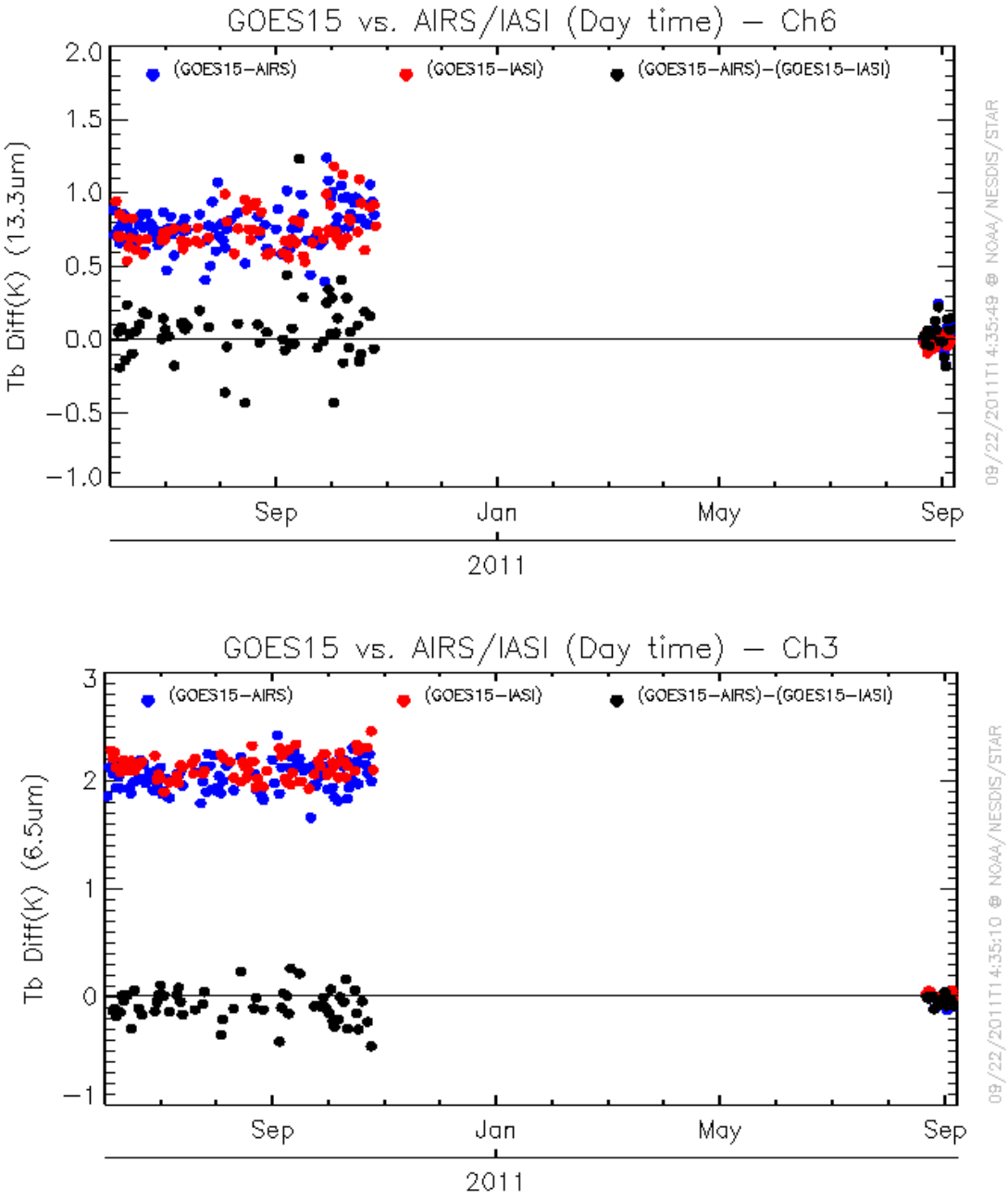

Figure 4.33: Comparisons of GOES-15 band-6 (top panel) and band-3 (lower panel) before (left-hand-side) and after (right-hand-side) the spectral response shift was implemented.

5. Product Validation

A number of products were generated with data from the GOES-15 instruments (Imager and Sounder) and then compared to the same products generated from other satellites or ground-based measurements. Products derived from the Sounder include: Total Precipitable Water (TPW), Lifted Index (LI), Cloud products, and Atmospheric Motion Vectors (AMVs). The products derived from the Imager include: Clouds, AMVs, CSBT, SST, and Fire Detection. It should be noted that most of these product comparisons were completed with the SRF available during the PLT.

5.1. Total Precipitable Water (TPW) from the Sounder

5.1.1. Validation of Precipitable Water (PW) Retrievals from the GOES-15 Sounder

GOES-15 retrievals of Precipitable Water (PW) were validated against Radiosonde Observation (RAOB) PW for 2 September 2010 to 21 September 2010. For the validation, GOES-15 retrievals were collocated in space (within 11 km) and time (within 30 minutes) to daily RAOBs at 0 UTC and 1200 UTC. At the same time, these GOES-15 retrievals were collocated in space (within 11 km) and time (within 60 minutes) to GOES-13 retrievals. The relative performance of the GOES-15 PW retrievals, GOES-13 PW retrievals, and first guess PW supplied to the retrieval algorithm could then be compared since all of these PW values were collocated to the same RAOBs. Table 5.1 provides a summary of these statistics for the TPW and the PW at three layers (Sfc-900 hPa, 900-700 hPa, and 700-300 hPa). The short time period reflects instrument problems which were not resolved until 1 September 2010. Despite the short observational time period, the statistics indicate that the quality of the GOES-15 Sounder PW retrievals compare very well to the quality of the operational GOES-13 PW retrievals. The relatively large sample size is indicative of the low amount of cloudiness during this period.

Table 5.1: Verification statistics for GOES-13 and GOES-15 retrieved PW, first guess (GFS) PW, and RAOB PW for 2 September 2010 to 21 September 2010.

Statistic	GOES-13/RAOB	GOES-15/RAOB	Guess/RAOB	RAOB
Total Precipitable Water (TPW)				
RMS (mm)	3.99	4.11	4.70	
Bias (mm)	-0.55	-0.41	-0.96	
Correlation	0.96	0.95	0.94	
Mean (mm)	28.46	28.60	28.05	29.01
Sample	3907	3907	3907	3907
Layer Precipitable Water (surface to 900 hPa)				
RMS (mm)	2.08	2.07	2.27	
Bias (mm)	-1.25	-1.16	-1.48	
Correlation	0.94	0.93	0.93	
Mean (mm)	9.65	9.74	9.42	10.90
Layer Precipitable Water (900 hPa to 700 hPa)				
RMS (mm)	2.40	2.44	2.55	
Bias (mm)	-0.15	-0.07	-0.33	
Correlation	0.92	0.92	0.91	
Mean (mm)	12.89	12.97	12.71	13.04
Layer Precipitable Water (700 hPa to 300 hPa)				
RMS (mm)	1.75	1.75	2.04	
Bias (mm)	0.79	0.74	0.77	
Correlation	0.91	0.90	0.87	
Mean (mm)	5.79	5.74	5.77	5.00

Figures 5.1 through 5.4 present time series of various comparison statistics (GOES retrieved TPW vs. RAOB-observed TPW) for GOES-15 (in green open circles) and GOES-13 (in red filled circles) for the same time as in Table 5.1. Each tick mark represents a data point (2 points per day) with the calendar day label centered at 0 UTC of that day. A majority of the GOES-15 data points are very close to, if not on top of, the GOES-13 data points.

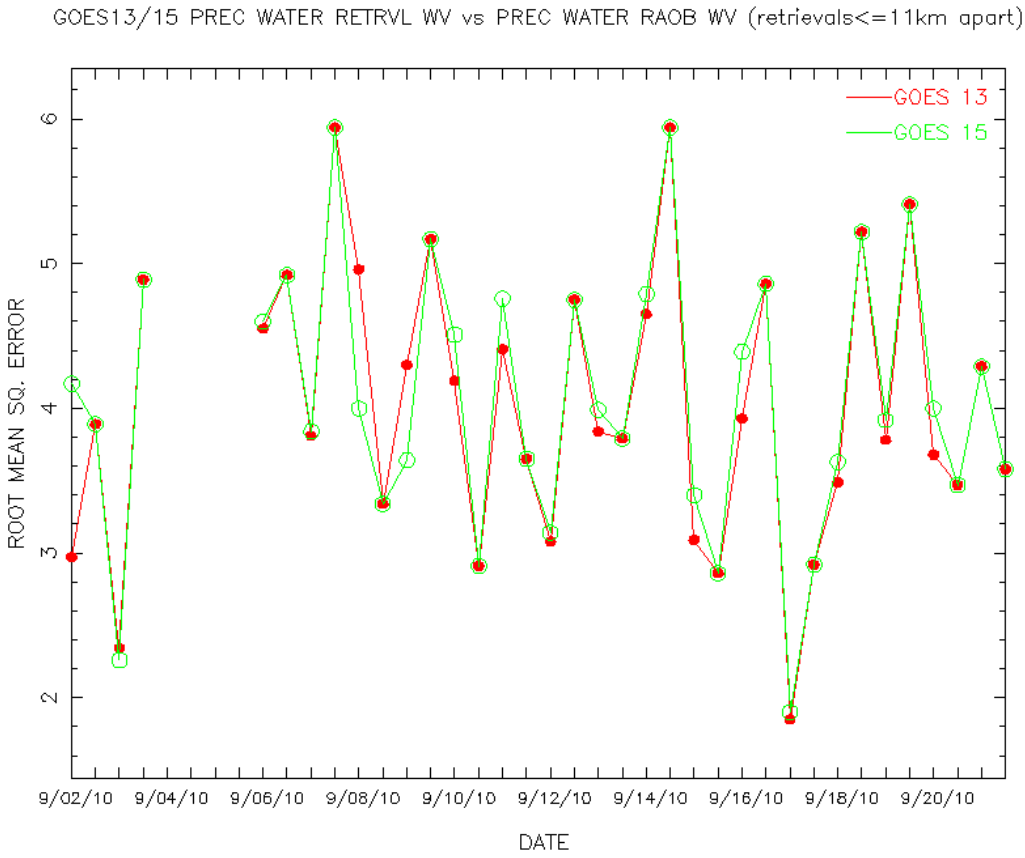

Figure 5.1: Time series of Root Mean Square Error (RMSE) between GOES-13 and GOES-15 retrieved PW and RAOB PW for 2 September 2010 to 21 September 2010.

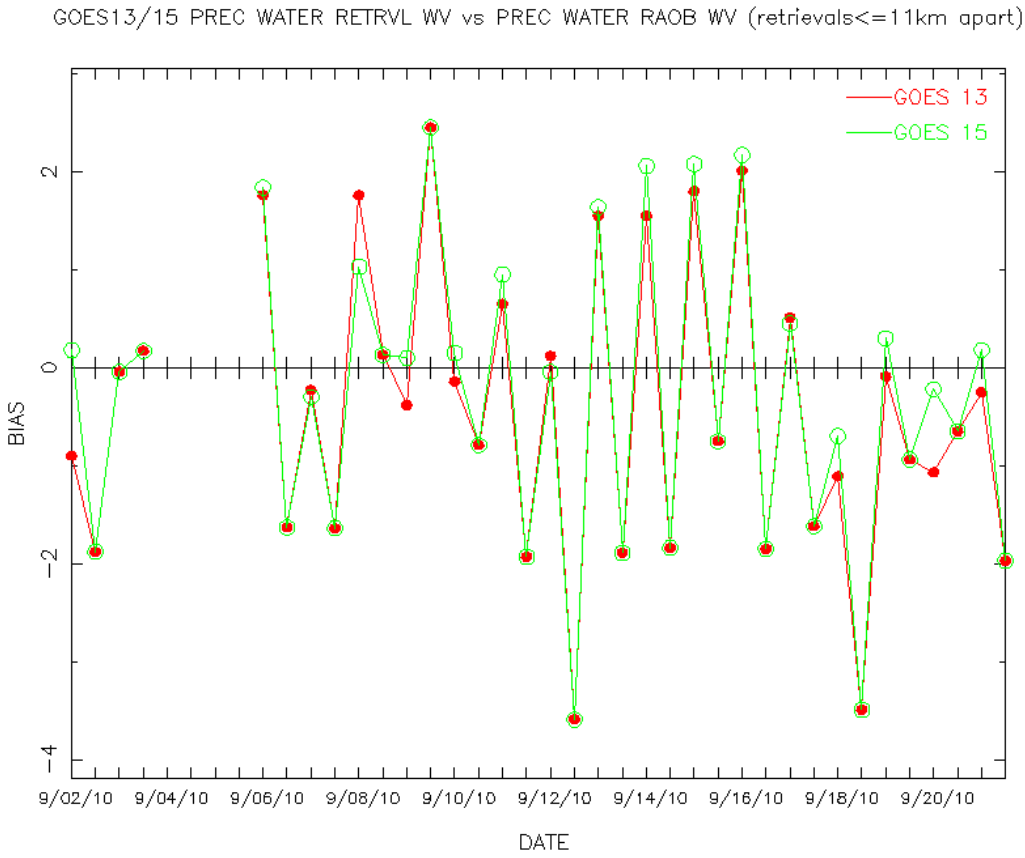

Figure 5.2: Time series of bias (GOES-RAOB) between GOES-13 and GOES-15 retrieved PW and RAOB PW for 2 September 2010 to 21 September 2010.

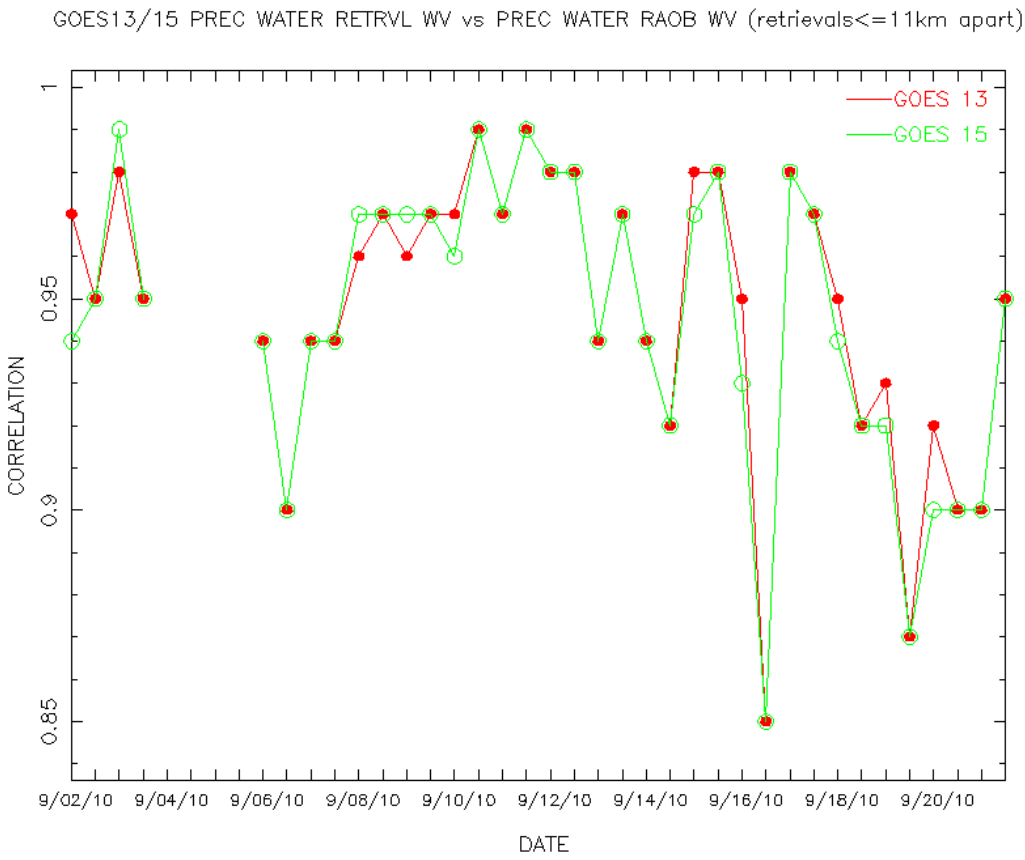

Figure 5.3: Time series of correlation between GOES-13 and GOES-15 retrieved PW and RAOB PW for 2 September 2010 to 21 September 2010.

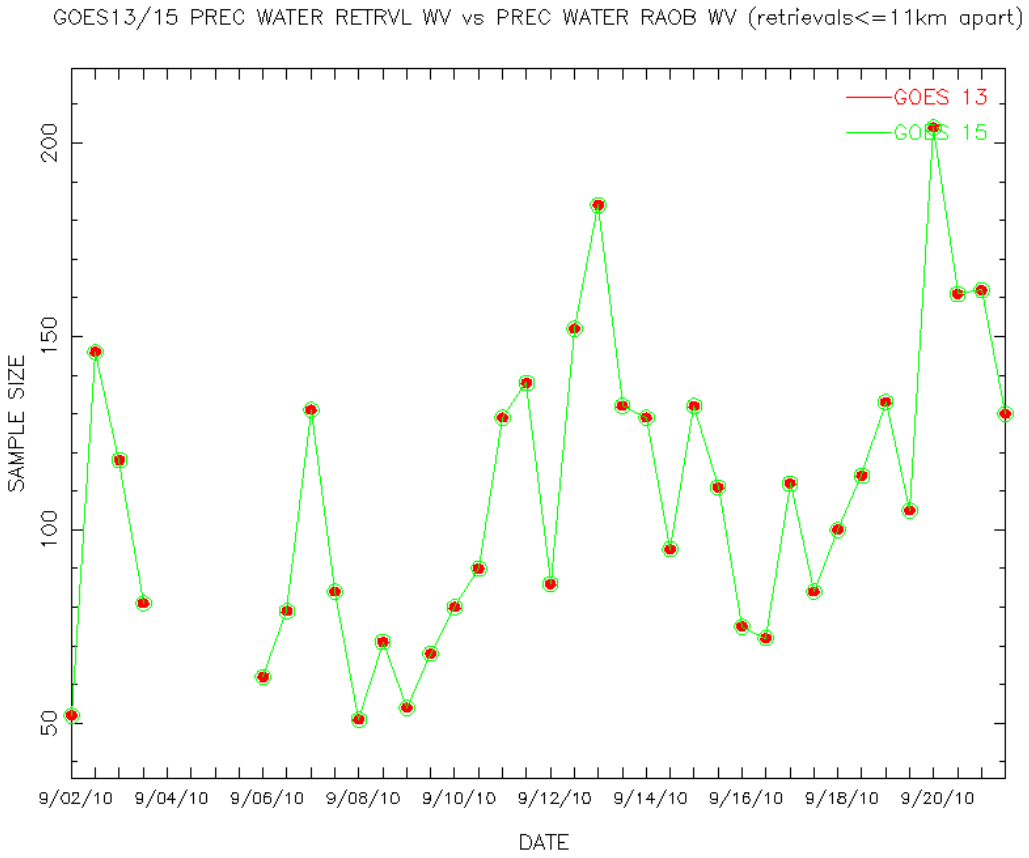

Figure 5.4: Time series of the number of collocations between GOES-13 and GOES-15 retrieved PW and RAOB PW for 2 September 2010 to 21 September 2010.

TPW retrievals (displayed in the form of an image) for GOES-13 and GOES-15 are presented in Figure 5.5 over the same area at approximately the same time. These retrievals are generated for each clear radiance FOV. Radiosonde measurements of TPW are plotted on top of the images. Qualitatively, there is good agreement between the GOES-13 and GOES-15 TPW retrievals that, in turn, compare reasonably well with the reported radiosonde measurements of TPW. Although the GOES-15 shows more striping, it should be noted that the calibration mode was not yet in full operational configuration at that time. When comparing measurements from two satellites, one must consider the different satellite orbital locations; even precisely co-located fields-of-view are seen through different atmospheric paths. Both sets of satellite retrievals are based on the "Li" method (Li et al. 2008). The striping in the GOES-15 Derived Product Image (DPI) may be due to striping in Sounder band-15 (and other bands).

Figure 5.6 shows one time period with two retrieval methods (the "Li" and "Ma" (Ma et al. 1999) methods); note that the GPS/Met data (Wolfe and Gutman 2000) are over-plotted on each image.

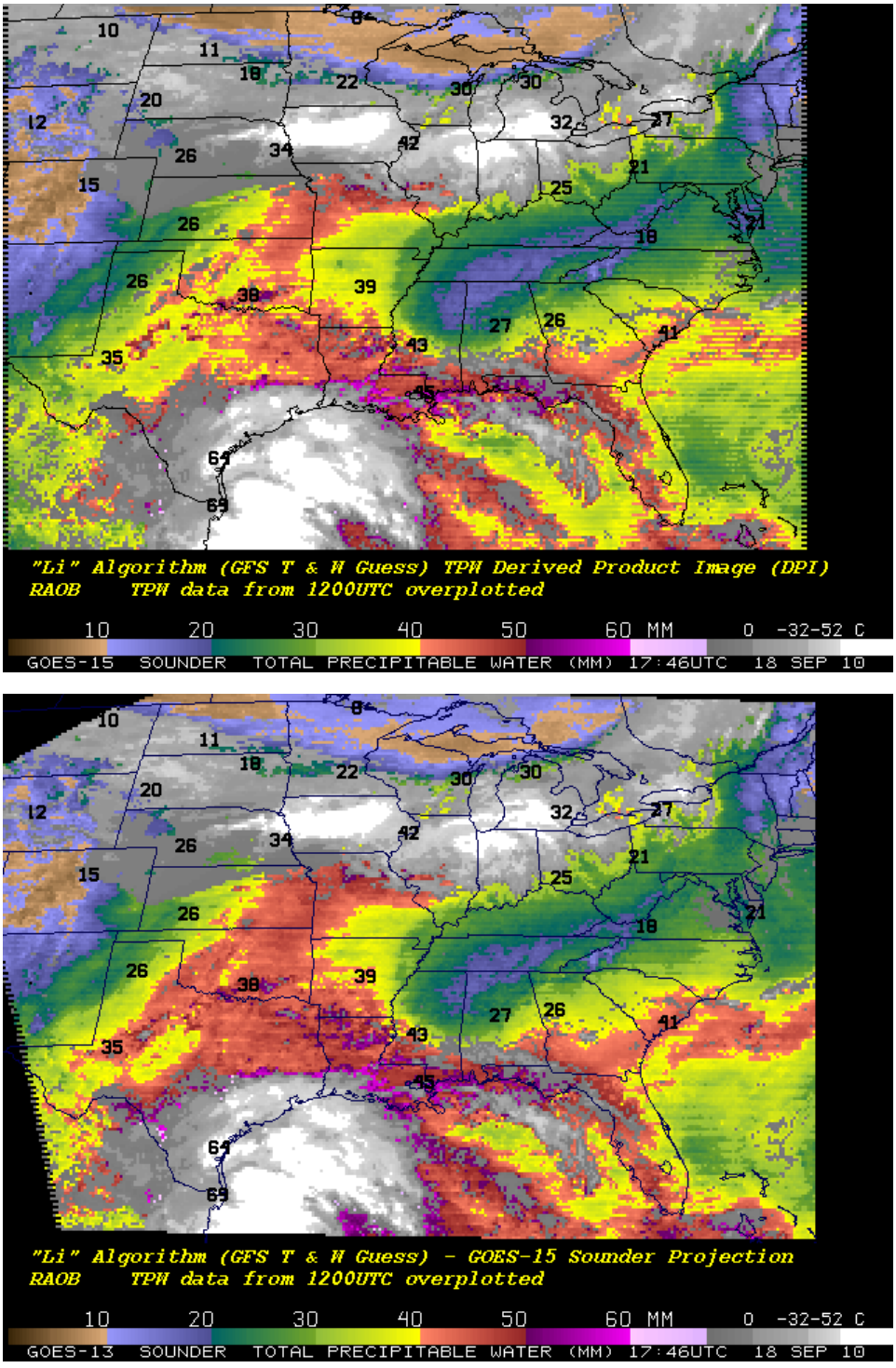

Figure 5.5: GOES-15 (top panel) and GOES-13 (lower panel) retrieved TPW (mm) from the Sounder displayed as an image. Cloudy FOVs are denoted as shades of gray. The data are from 1800 UTC on 18 September 2010. Measurements from RAOBs are overlaid as text.

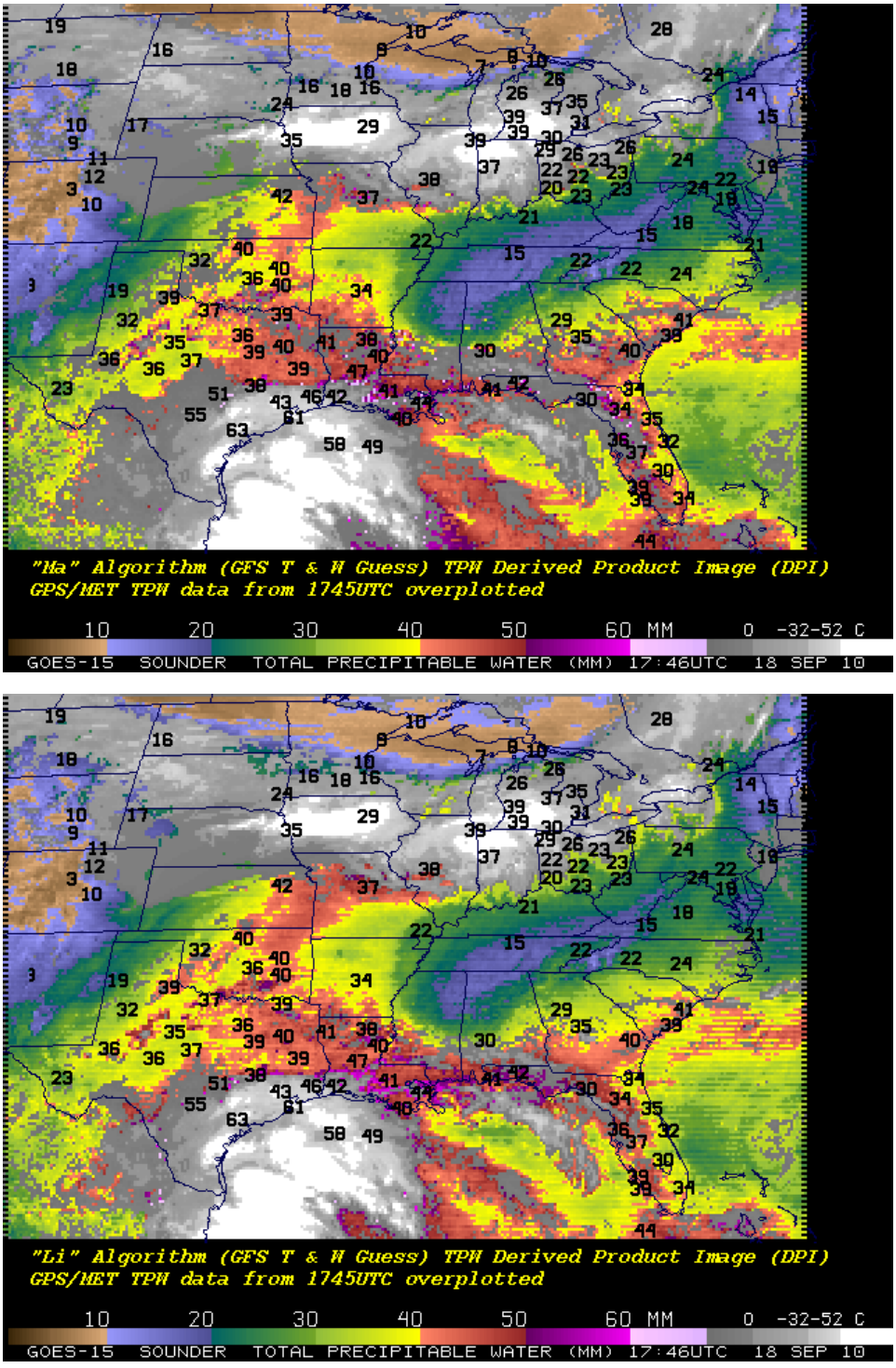

Figure 5.6: GOES-15 Sounder TPW from two retrieval algorithms ("Ma" (upper-panel) and "Li" (lower-panel)). Both images are from 18 September 2010.

5.2. Lifted Index (LI) from the Sounder

The lifted index (LI) product is generated from the retrieved temperature and water vapor profiles that are generated from clear radiances for each FOV. Figure 5.7 shows LI retrievals

(displayed in the form of an image) for GOES-13 and GOES-15 over the same area at approximately the same time, showing no discernible bias in the LI values. Both images are shown in the same projection.

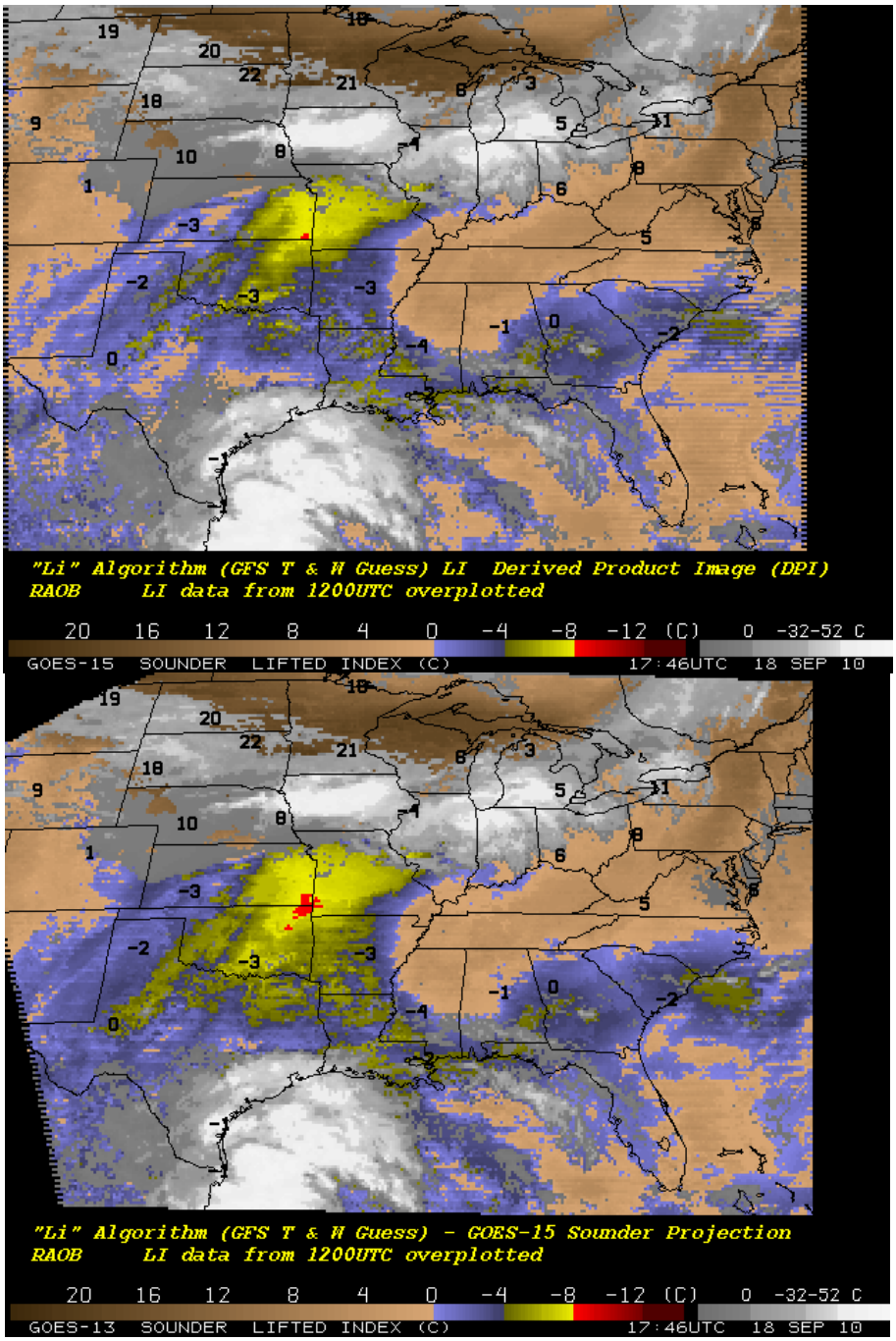

Figure 5.7: GOES-15 (top) and GOES-13 (lower) retrieved LI from the Sounder displayed as an image. The data are from 1746 UTC on 18 September 2010.

5.3. Cloud Parameters from the Sounder and Imager

The presence of band-6 (13.3 μm) on the GOES-15 Imager, similar to the GOES-12 Imager, makes near full-disk cloud products possible. This cloud product complements that from the GOES Sounders.

Figures 5.8 and 5.9 show a comparison of GOES-15 Imager (and Sounder) cloud-top pressure derived product images from the fall of 2010. Not shown is the larger coverage possible from the Imager-based product. Another comparison between the GOES-13 Sounder and MODIS on EOS-Aqua showed generally good correlations, as seen in Figures 5.10 through 5.12.

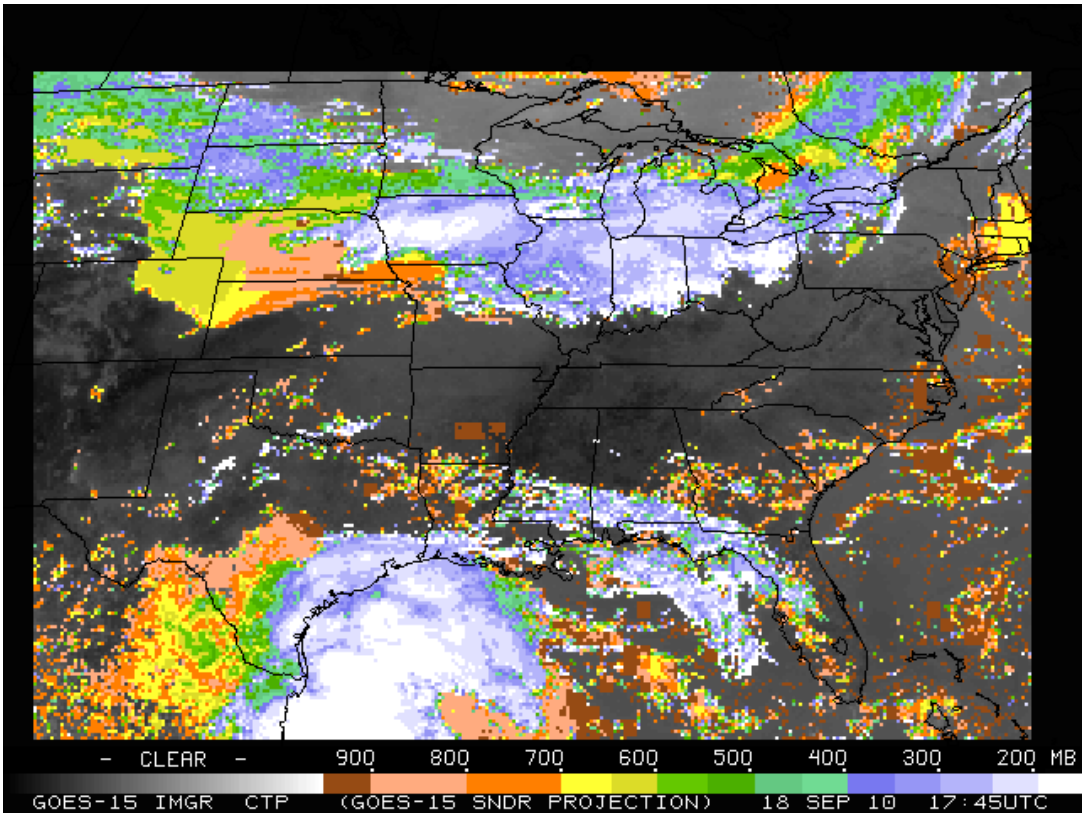

Figure 5.8: GOES-15 Imager cloud-top pressure from 18 September 2010 starting at 1745 UTC. The Imager data have been remapped into the GOES-15 Sounder projection.

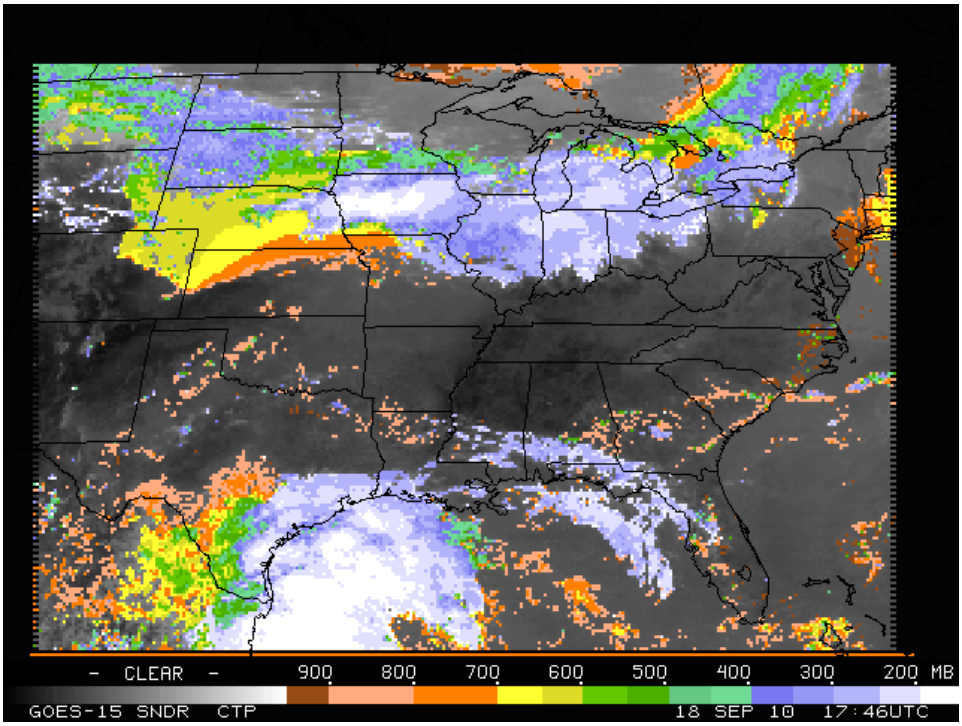

Figure 5.9: GOES-15 Sounder cloud-top pressure from 18 September 2010 starting at 1746 UTC.

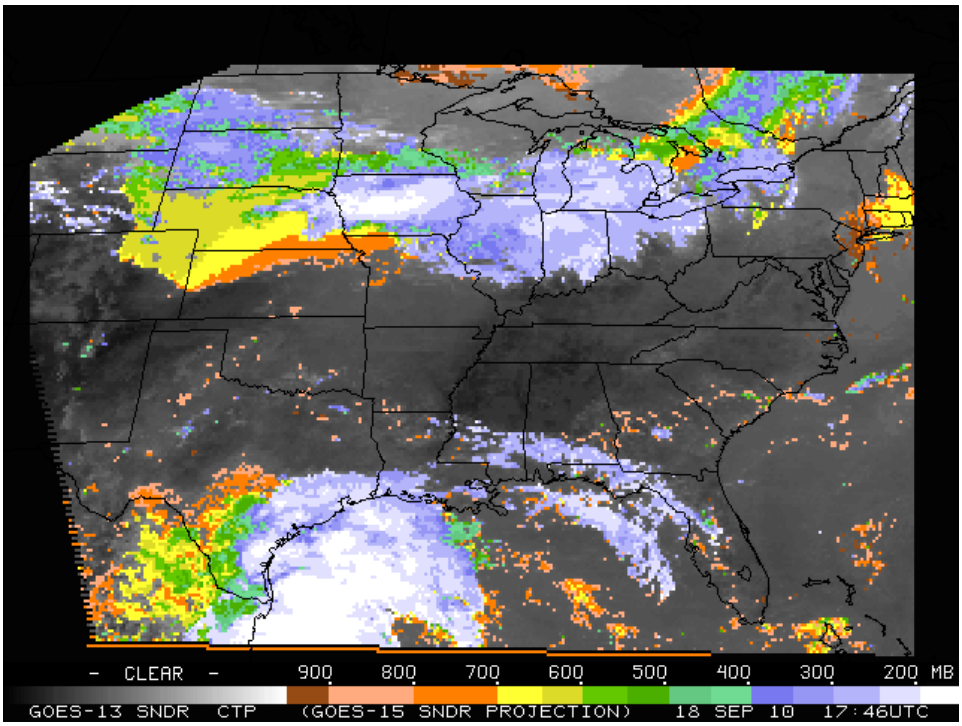

Figure 5.10: GOES-13 Sounder cloud-top pressure from 18 September 2010 starting at 1746 UTC.

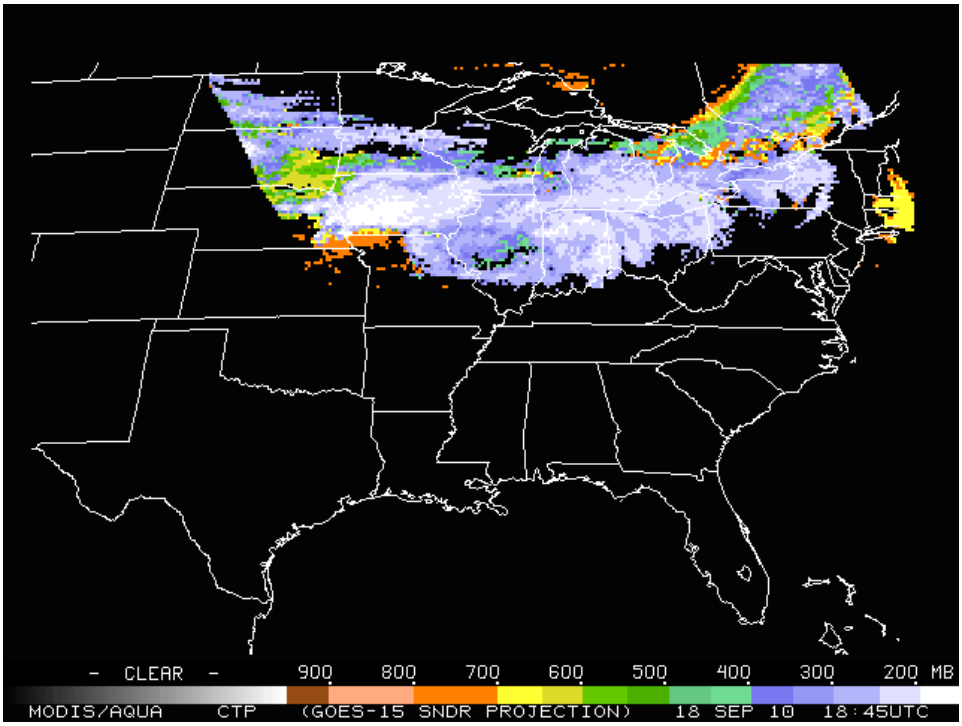

Figure 5.11: EOS-Aqua MODIS cloud-top pressure at 1800 UTC on 18 September 2010.

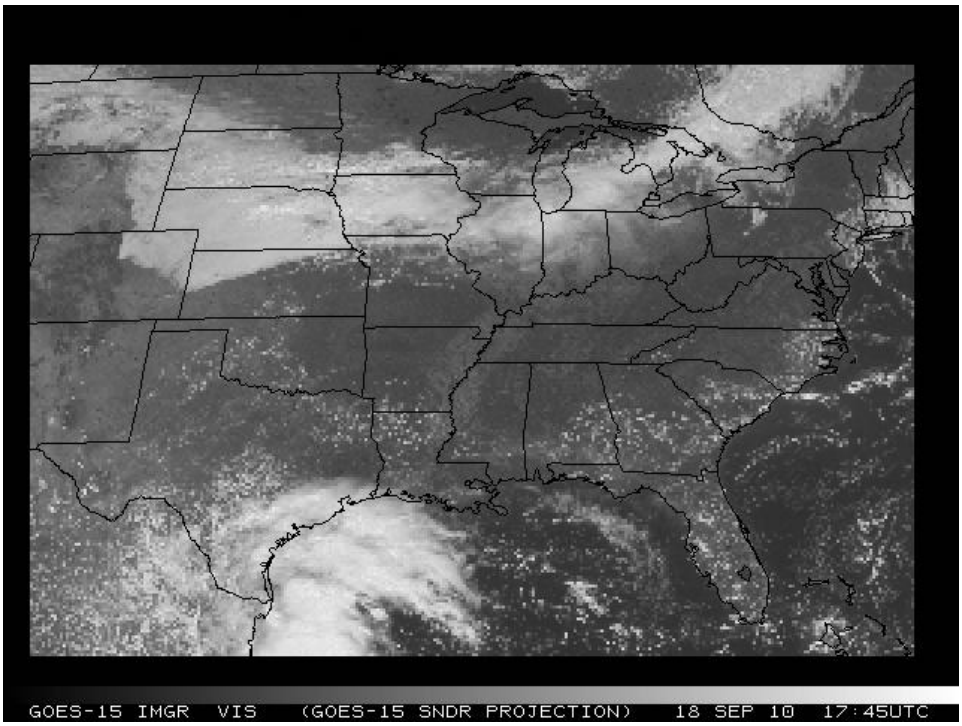

Figure 5.12: GOES-15 Sounder visible image from the nominal 1746 UTC on 18 September 2010.

5.4. Atmospheric Motion Vectors (AMVs) from the Imager

Atmospheric Motion Vectors (AMVs) from GOES are derived using a sequence of three images. Features targeted in the middle image (cirrus cloud edges, gradients in water vapor, small cumulus clouds, etc.) are tracked from the middle image back to the first image, and forward to the third image, thereby yielding two displacement vectors. These vectors are averaged to give the final wind vector, or AMV. This section summarizes the quality of AMVs from GOES-15 as part of the NOAA Science Test in 2010.

The varied imaging schedules activated during the GOES-15 Science Test provided an opportunity to run AMV assessments for what are currently considered operational as well as special case scenarios. A thinned sample (for display clarity) of AMVs from GOES-15 on 10 August 2010 at 1145 UTC is shown for Cloud-Drift (Figure 5.13) and Water Vapor (Figure 5.14) AMVs.

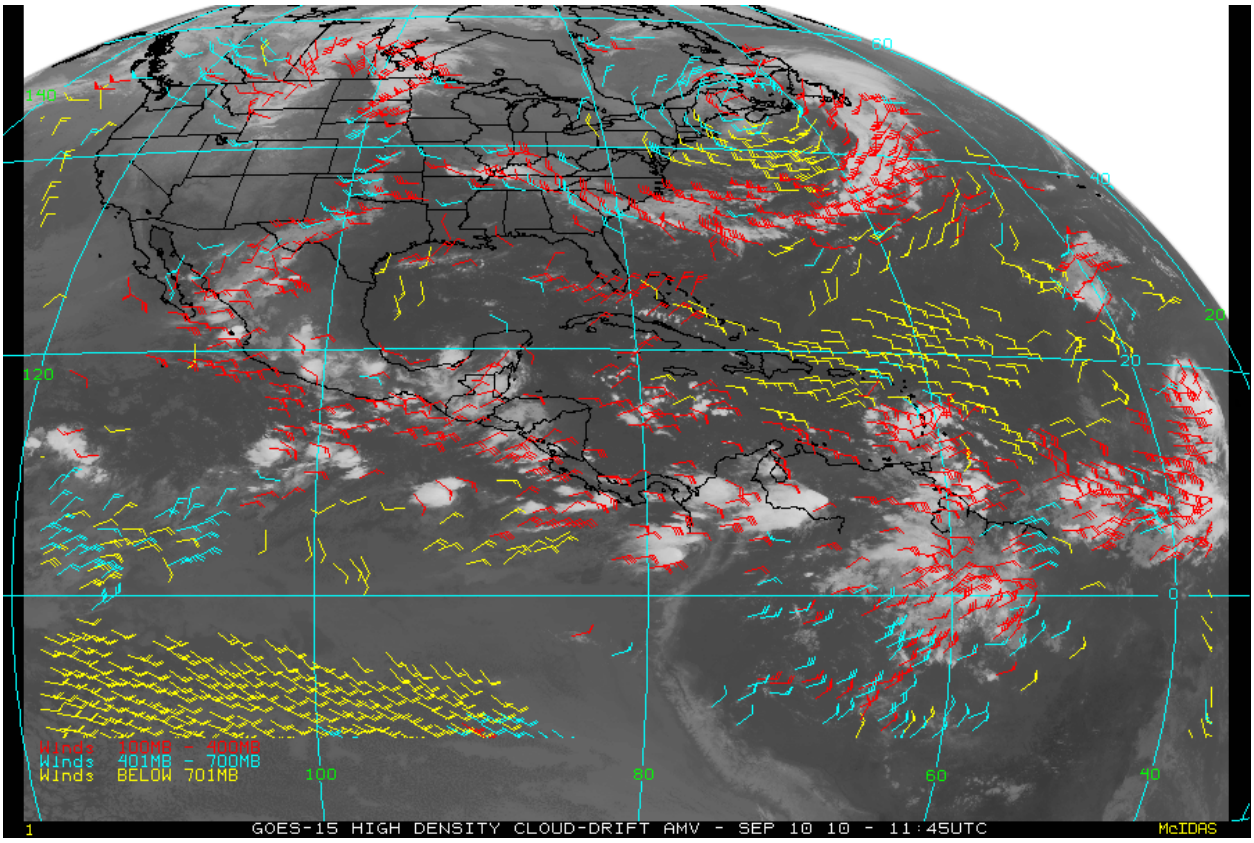

Figure 5.13: GOES-15 Northern Hemisphere (NHEM) cloud-drift AMVs at 1145 UTC on 10 September 2010.

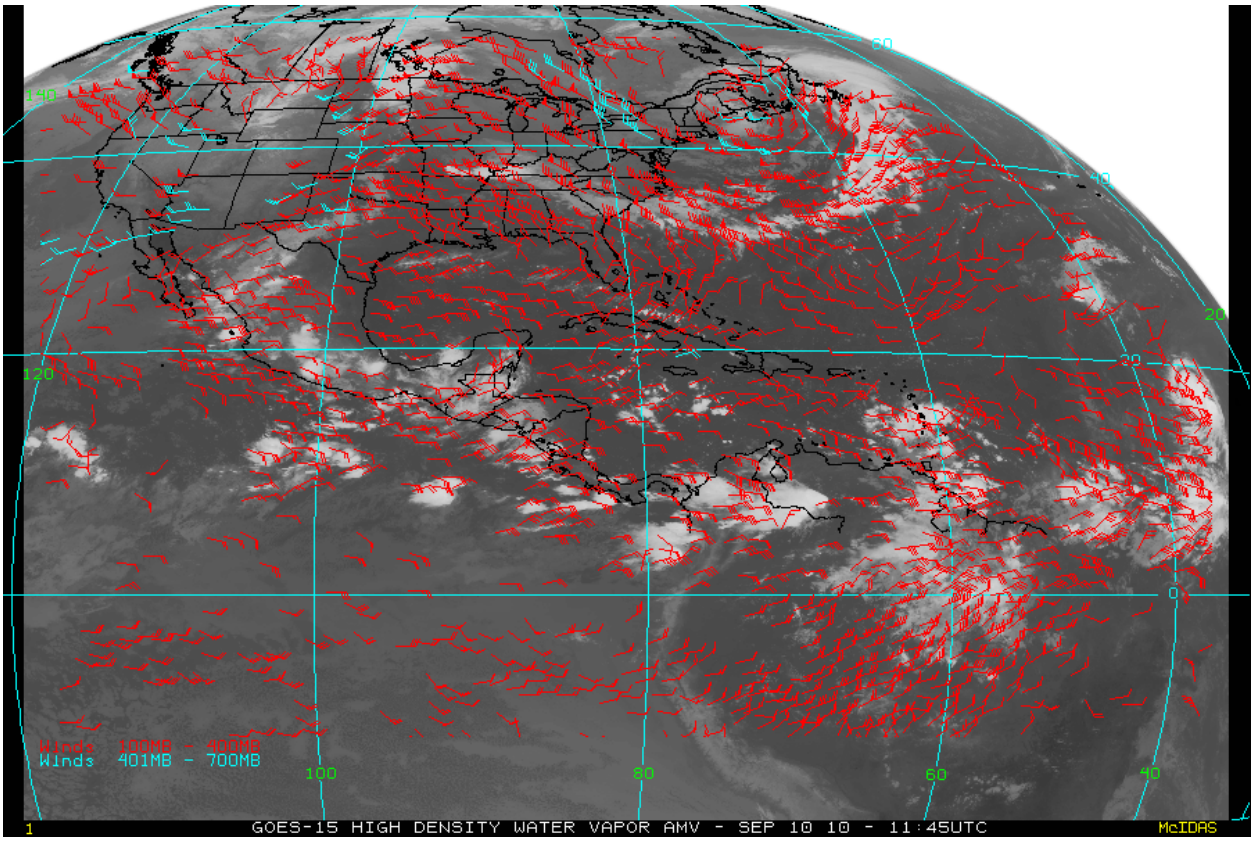

Figure 5.14: GOES-15 Northern Hemisphere (NHEM) water vapor AMV at 1145 UTC on 10 September 2010.

During the Science Test, objective statistical comparisons were made using collocated radiosonde (RAOB) data matched to the various GOES-15 AMVs. Table 5.2 shows the results of these GOES vs. RAOB match statistics for cloud-drift and water vapor AMVs.

Table 5.2: Verification statistics for GOES-15 vs. RAOB match verification statistics NHEM winds (m/s): 11 September 2010 – 25 October 2010. MVD is the mean vector difference.

NHEM	RMS	MVD	Std Dev	Speed Bias	Mean Speed (Sat)	Mean Speed (RAOB)	Sample Size
Cloud-Drift	6.23	5.14	3.52	-0.63	15.21	15.85	25330
Water Vapor	6.37	5.29	3.55	-0.27	16.35	16.62	51413

Comparison statistics were also generated for collocated GOES-13 and GOES-15 AMV datasets with RAOBs. To be considered in the statistical evaluation, the respective GOES AMVs had to be within 0.1° horizontally and 25 hPa vertically. Table 5.3 shows the results of this comparison. The small differences confirm that the AMV products from GOES-15 are at least comparable in quality with the existing GOES-13 operational AMVs.

Table 5.3: RAOB verification statistics for GOES-13 and GOES-15 collocated (0.1 deg, 25 hPa) for NHEM winds (m/s): 11 September 2010 – 25 October 2010.

NHEM	RMS	MVD	Std Dev	Speed Bias	Mean Speed (Sat)	Mean Speed (RAOB)	Sample Size
GOES-13 Cloud-Drift	6.14	5.03	3.53	-0.68	14.54	15.23	1358
GOES-15 Cloud- Drift	6.12	4.98	3.56	-0.61	14.55	15.16	1358
GOES-13 Water Vapor	6.19	5.13	3.46	-0.26	15.18	15.44	4051
GOES-15 Water Vapor	6.02	5.02	3.32	-0.31	15.11	15.42	4051

5.5. Clear Sky Brightness Temperature (CSBT) from the Imager

A satellite-derived product, called the Clear-Sky Brightness Temperature (CSBT), based on Geostationary Operational Environmental Satellite (GOES) Imager radiance data, was originally requested by the National Centers for Environmental Prediction (NCEP) / Environmental Modeling Center (EMC) and the European Centre for Medium-range Weather Forecasts (ECMWF) for assimilation into global weather prediction models to better analyze the initial atmospheric state.

Current coverage for the operational CSBT extends from roughly 67°S to 67°N and 30°W to 165°E for GOES-11 and GOES-13. The data are averaged over boxes measuring approximately 50 km per side. Each box consists of 187 FOVs (11 rows by 17 columns). For a given box, a cloud detection algorithm is used. For each 50 km box the average brightness temperature for each IR band and the albedo in percent for the visible band are calculated along with the average clear and cloudy brightness temperatures. Additional parameters determined are the number of clear and cloudy FOVs, center latitude and longitude of the box, center local zenith and solar zenith angles of the box, land/sea flag, standard deviation of the average clear and cloudy brightness temperatures, and two quality indicator flags. The quality indicator flags provide information on the likelihood of a particular observation being affected by sun glint and the relative quality of the SST observation.

A derived product image, Figure 5.15 (top left), below, is also generated. This CSBT product is a single FOV result. It is compared to a "merged" version of the current GOES-11 and GOES-13 derived image reformatted to the GOES-15 projection (Figure 5.15, top panels). In general, there is fair agreement between the GOES-15 image and the GOES-11/GOES-13 combined image. In addition the GOES-15 Imager visible and long wave window images are depicted (left and right, lower panels) and further demonstrate consistency between the two derived products.

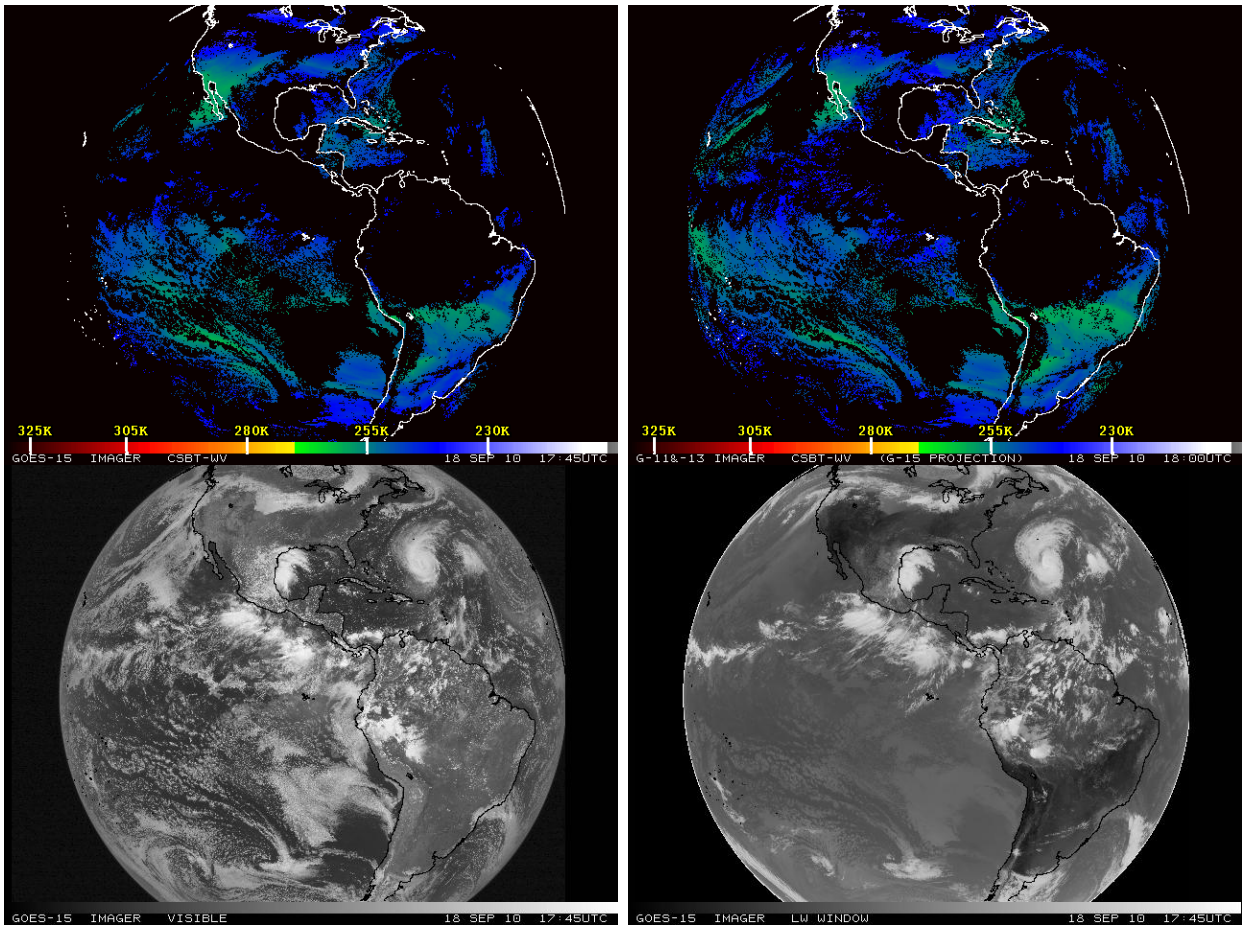

Figure 5.15: GOES-15 Imager CSBT cloud mask image from 18 September 2010 for the nominal 1800 UTC time (upper-left). In the upper-right is the GOES-13 Imager CSBT cloud mask image for the same date and nominal time as shown in the GOES-15 Imager satellite projection. Clear regions display the band-3 water vapor (6.5 µm) Brightness Temperature. GOES-15 Imager visible (lower-left) and Long Wave Window (lower-right) from 18 September 2010 for the nominal 1800 UTC time period.

5.6. Sea Surface Temperature (SST) from the Imager

GOES-15 Imager data were collected, archived locally, and used as input for Sea Surface Temperature (SST) retrievals. These were collected for the entire Science Test from 11 August 2010 to 25 October 2010. The sector for GOES-East is approximately 30°E to 110°W and 60°N to 45°S. Examples of GOES-15 SSTs for day and night with their associated Probability of Clear Skies are shown in the following figures.

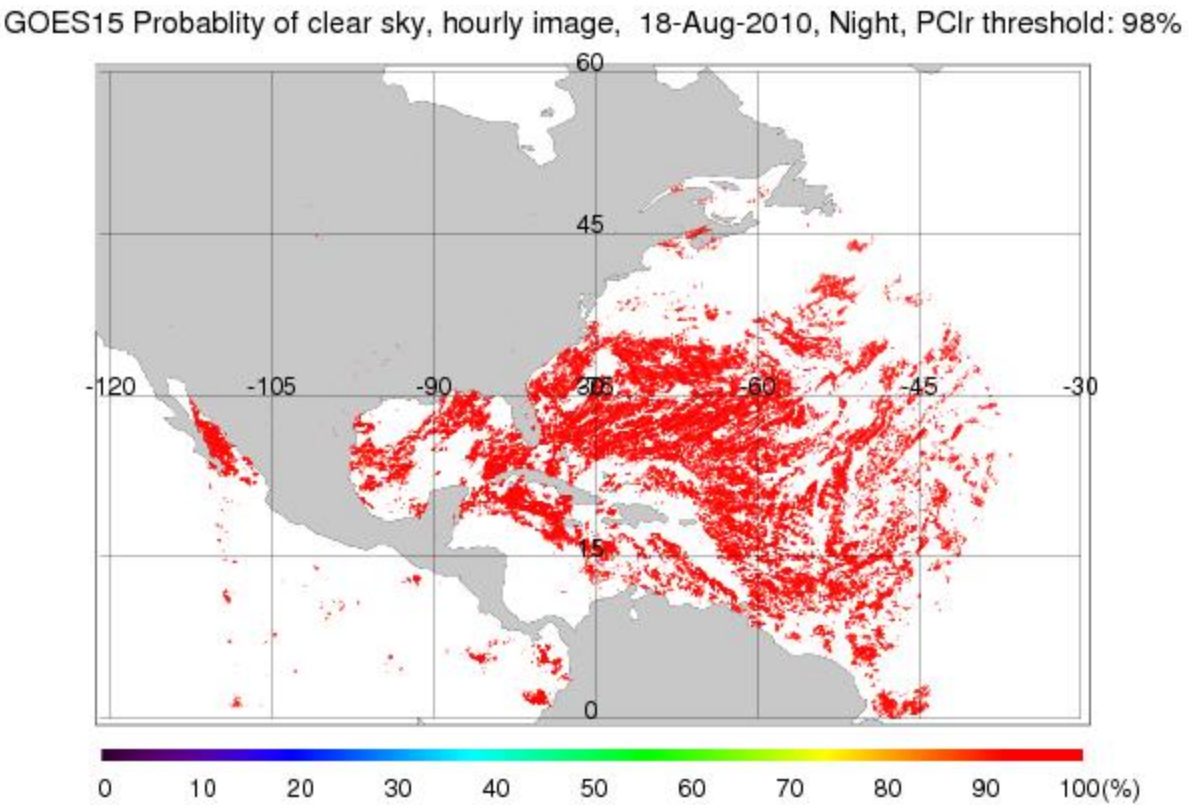

Figure 5.16: The nighttime areas that are considered clear pixels based on Bayesian estimate of ≥98% clear sky probability. The mask is based on the highest clear sky probability for the three nighttime images that went into generating this GOES-15 product.

The GEO-SST software is comprised of two steps – SST retrievals generation, and estimation of cloud contamination probability. The cloud estimation is performed using a Bayesian estimation technique.

The GOES-15 coefficients for 75°W were used to generate SST retrievals. Then a Bayesian Cloud Mask was applied to obtain clear sky pixels. Bayes' theorem is applied to estimate the probability of a particular pixel being clear of cloud. The inputs are the satellite-observed brightness temperatures, a measure of local texture and band brightness temperatures calculated for the given location and view angle. NCEP Global Forecast System (GFS) surface and upper air data and the Community Radiative Transfer Model (CRTM v2.0) fast radiative transfer model inputs are used. This method is described in detail in Merchant et al. (2005). Using the current form of the SST equation below, retrievals were generated for dual window bands (3.9 μm and 11 μm).

$$SST = a_0 + a_0 S + \sum_i (a_i + a_i S) T_i$$

where *i* is the GOES-Imager band number (2, 4), S is the satellite zenith angle – 1, and T_i is the band brightness temperature (K). Due to a lack of a 12 μm band (band-5) on GOES-15, a single dual window form was used for both day and night with a correction for scattered solar radiation

in the 3.9 µm band (band-2) being applied for the daytime case (for details see Merchant et al. 2009).

The GEO-SST software for GOES-15 includes major capability upgrades from GOES-14 to enable the use of Physical Retrieval methodology, multi-dimensional lookup tables for Bayesian cloud estimates and other science upgrades.

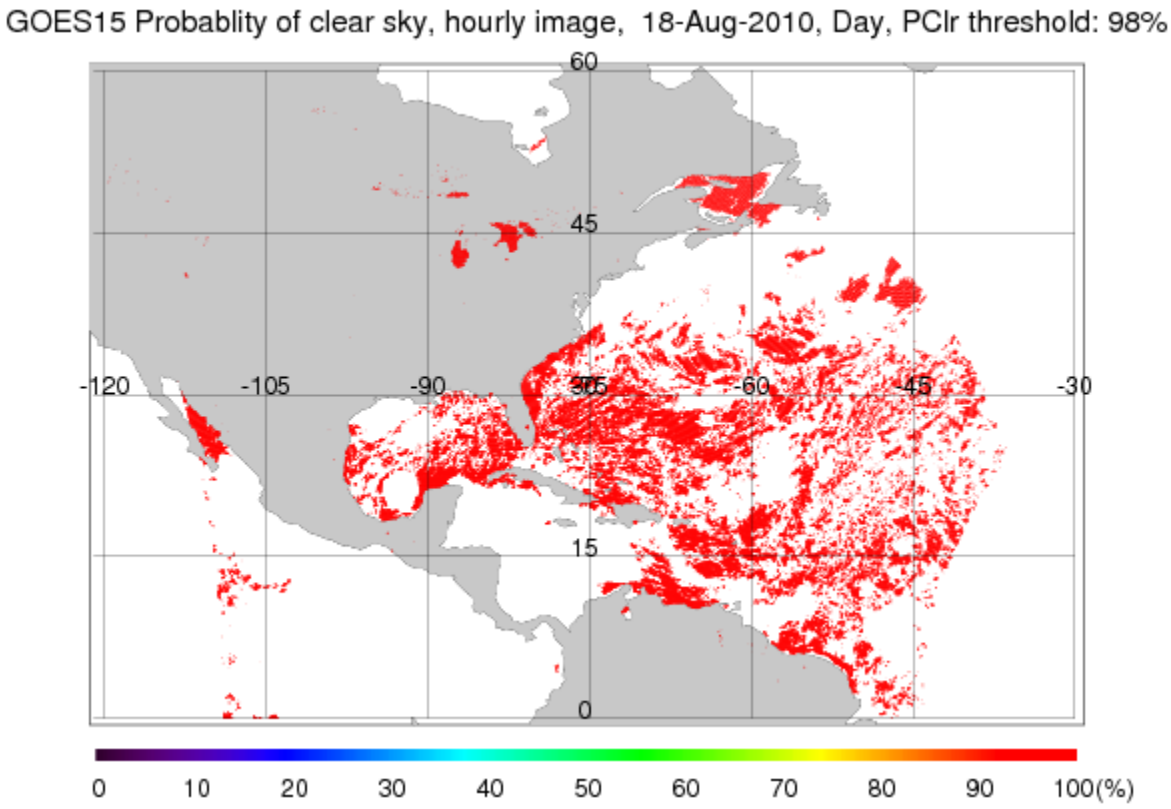

Figure 5.17: The daytime areas that are considered clear pixels based on Bayesian estimate of ≥98% clear sky probability. The mask is based on the highest clear sky probability for the three daytime images that went into generating this GOES-15 product.

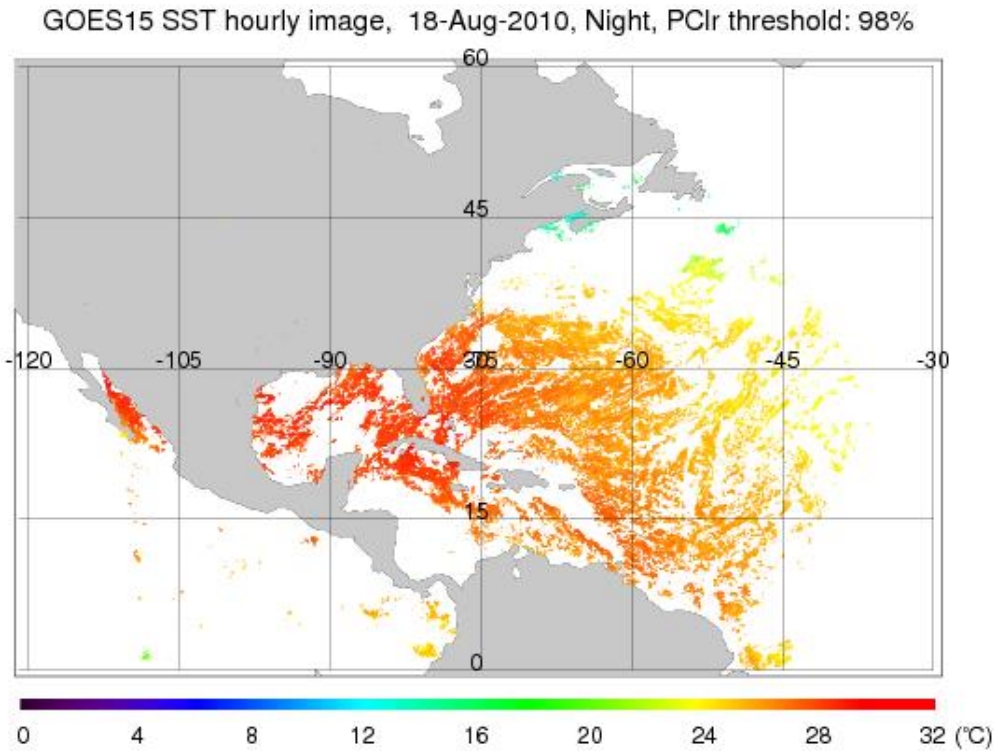

Figure 5.18: The SST from GOES-15 created by compositing three half-hour nighttime SST McIDAS Area files with an applied threshold of ≥98% clear sky probability.

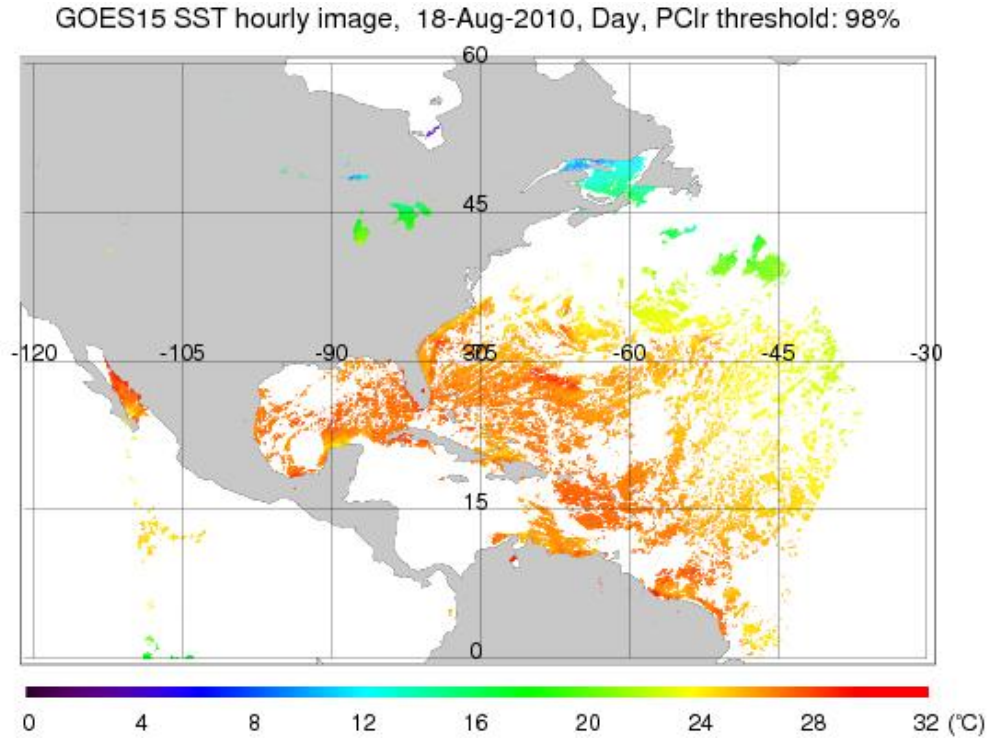

Figure 5.19: The SST from GOES-15 created by compositing three half hour daytime SST McIDAS Area files with an applied threshold of ≥98% clear sky probability.

5.7. Fire Detection and Characterization

Basic fire detection and characterization relies primarily on the short and longwave IR window (3.9 µm, band-2; and 11 µm, band-4) data from the GOES Imager. These two IR windows and ancillary information are used to determine instantaneous estimates of sub-pixel fire size and temperature. The number of fires that can be successfully detected and characterized is related to the saturation temperature, or upper limit of the observed brightness temperatures, in the 3.9 µm band (band-2). A higher saturation temperature is preferable as it affords a greater opportunity to identify and estimate sub-pixel fire size and temperature. That said, the maximum saturation temperature should still be low enough to be transmitted via the GVAR data stream. Low saturation temperatures can result in the inability to distinguish fires from a hot background in places where the observed brightness temperature meets or exceeds the saturation temperature. Furthermore, sub-pixel fire characterization is not possible for saturated pixels.

Most comparisons were made using the band-2 IR imagery. Comparisons done when solar reflectivity was near its minimal, during sunset, resulted in very small, if any, differences in fire or landmass temperature. Afternoon comparisons showed an apparent cool bias of 1 K to 3 K in non-hotspot areas (where a fire was not located). For hotspot (fire) detection, GOES-13 was often hotter than GOES-15 by as much as 7 K. This result seems counter-intuitive since all of the hotspots in the comparison were closer to the GOES-15 subpoint (all locations were west of 91°W) and solar reflection during daylight hours makes fires very sensitive to viewing angles, making direct comparison between different satellites tricky. Furthermore, a given fire may be observed and characterized very differently depending on its location in the respective GOES-13/GOES-15 pixels and the application of the Point Spread Function (PSF). More extensive band-2 IR comparisons would need to be done due to the highly sensitive nature of the 4 µm sensor to solar reflectivity, the rapidly changing radiative power of fires, and the GOES-13/GOES-15 observed differences due to the location of the fire in the pixels. Visible imagery comparisons for smoke analysis and blowing sand/dust plumes revealed no appreciative differences between GOES-15 and GOES-13 imagery.

A comparison of GOES-11 (GOES-West), GOES-15, and GOES-13 (GOES-East) 3.9 µm shortwave IR images in Figure 5.20 indicated that there was a hot spot on 9 September 2010. This hot spot was due to a large natural gas explosion that occurred in San Bruno, CA. The 3 sets of images are displayed in the native projection of their respective satellites. The fire "hotspots" showed up as warmer (darker black or yellow enhancement) pixels.

The plot in Figure 5.21 shows that the warmest 3.9 µm IR brightness temperature on the GOES-15 imagery for this case was approximately 318 K. More information on this case can be found at http://cimss.ssec.wisc.edu/goes/blog/archives/6752.

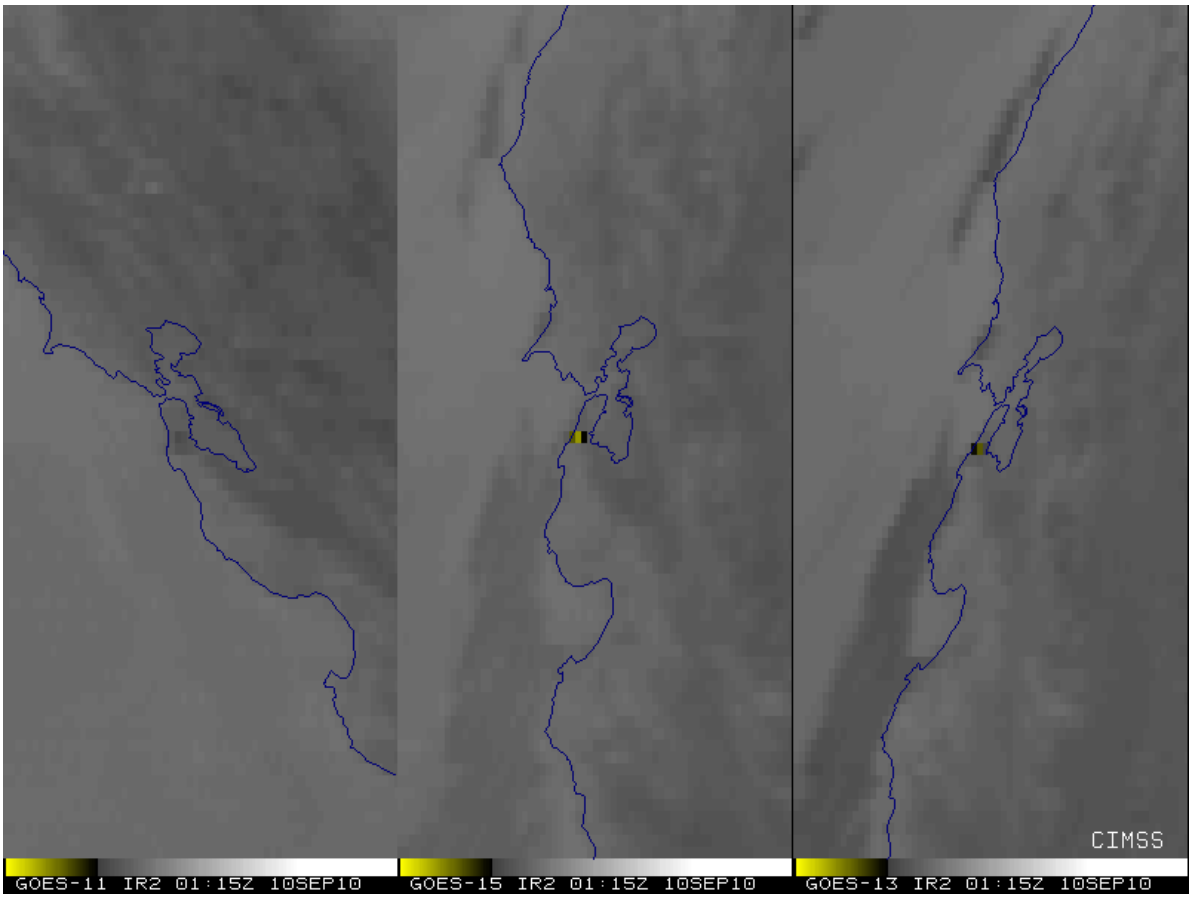

Figure 5.20: GOES Imager 3.9 µm images from GOES-11 (left), GOES-15 (center) and GOES-13 (right). Each satellite is shown in its native perspective.

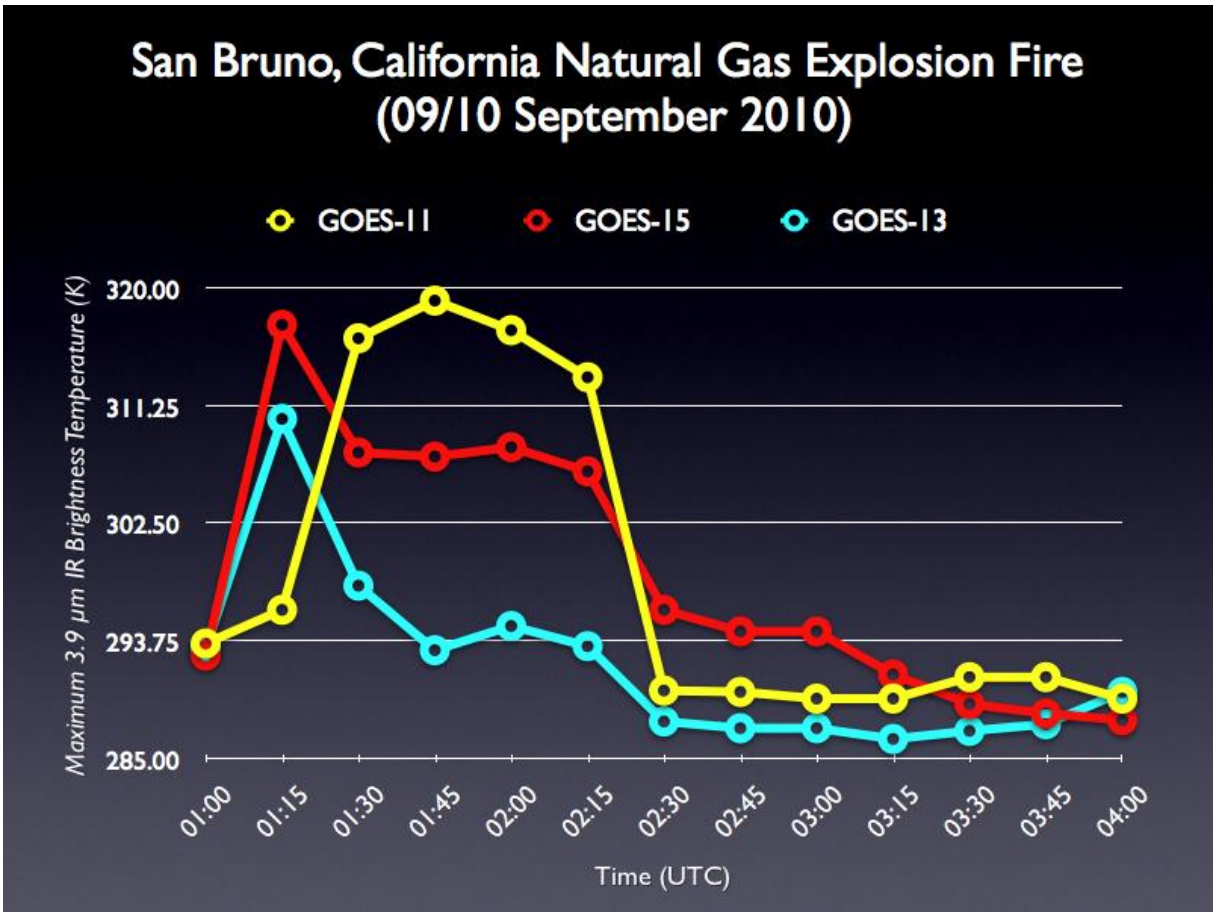

Figure 5.21: GOES Imager 3.9 µm time series from GOES-11, GOES-15, and GOES-13.

The GOES-15 Imager band-6 (3.9 µm) has a saturation temperature of approximately 337.4 K. For reference, the GOES-12 Imager 3.9 µm band (band-2) has a saturation temperature of approximately 339 K, although this value has changed over time, peaking at approximately 342 K.

Preliminary indications are that GOES-15 is performing comparably to GOES-11 and GOES-13.

The Biomass Burning team at CIMSS currently produces fire products for GOES-11/GOES-12/GOES-13 covering North and South America. GOES-11/GOES-13 Wildfire Automated Biomass Burning Algorithm (WF_ABBA) fire products can be viewed at http://cimss.ssec.wisc.edu/goes/burn/wfabba.html in near real time.

5.8. Volcanic Ash Detection

Volcanic ash was only detected by both GOES-13 and GOES-15 one time during the GOES-15 PLT. Ash detection is very event driven, and there was little volcanic activity in the SAB Volcano team's areas of interest in August-September 2010. The ash signature was seen in visible imagery and showed up identically in the GOES-15 and GOES-13 imagery. A few cases where volcanic hotspots could be seen in multi-spectral imagery were noted with any differences being negligible. The multi-spectral imagery used for volcanic ash/hotspot detection is sensitive

to the solar angle and thus the minor differences seen were attributed to the different positions of the satellites being compared. Thus, there were no differences with GOES-15 imagery that would result in degradation in performance for volcanic ash analysis.

5.9. Total Column Ozone

Total Column Ozone (TCO) is an experimental product from the GOES Sounder. The GOES-15 Sounder TCO is expected to be of similar, or higher, quality as derived from earlier GOES Sounders. Note the similar overall patterns between GOES-13 and GOES-15 shown in Figure 5.22 and 5.23.

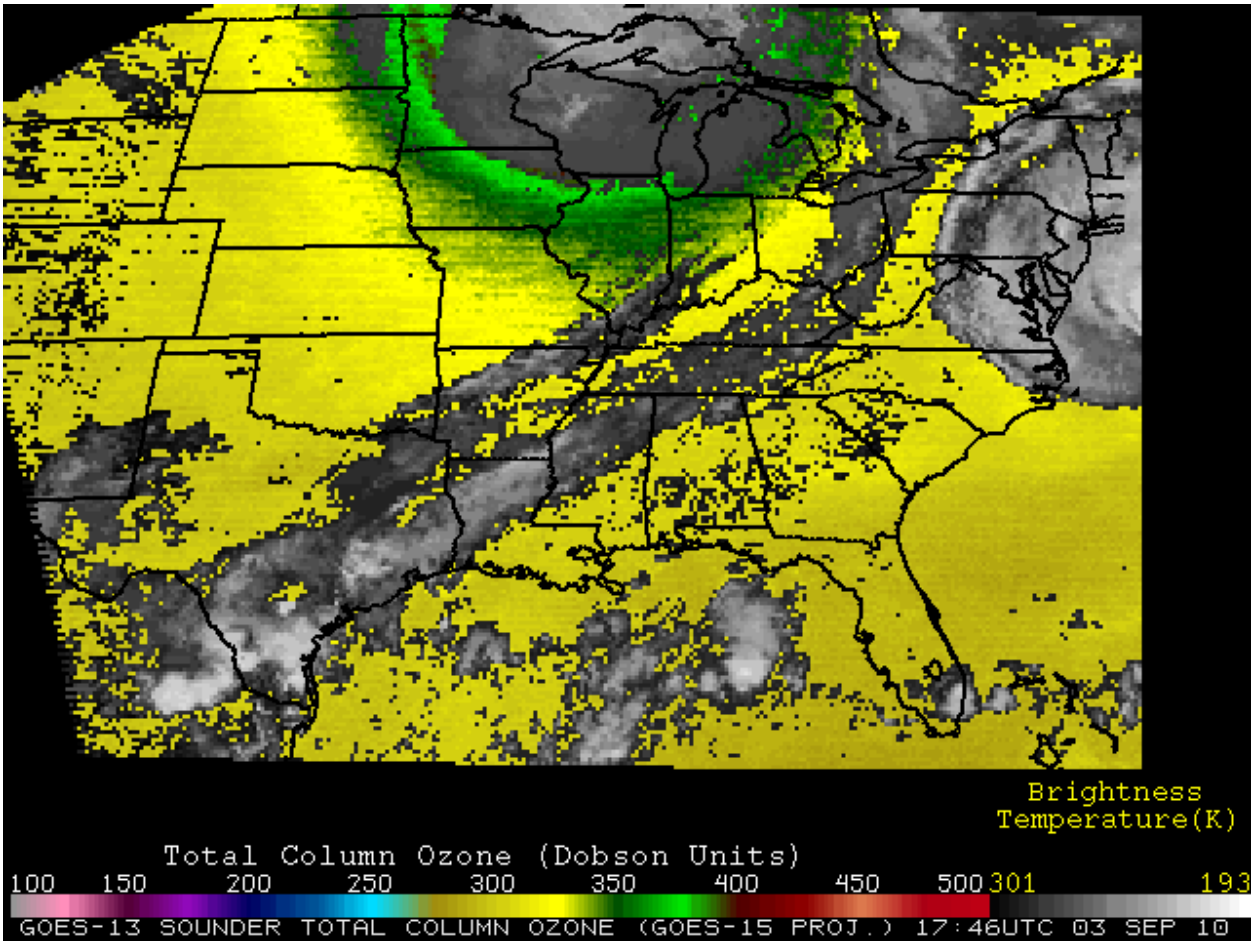

Figure 5.22: Example of GOES-13 Imager Total Column Ozone on 3 September 2010 at 1800 UTC.

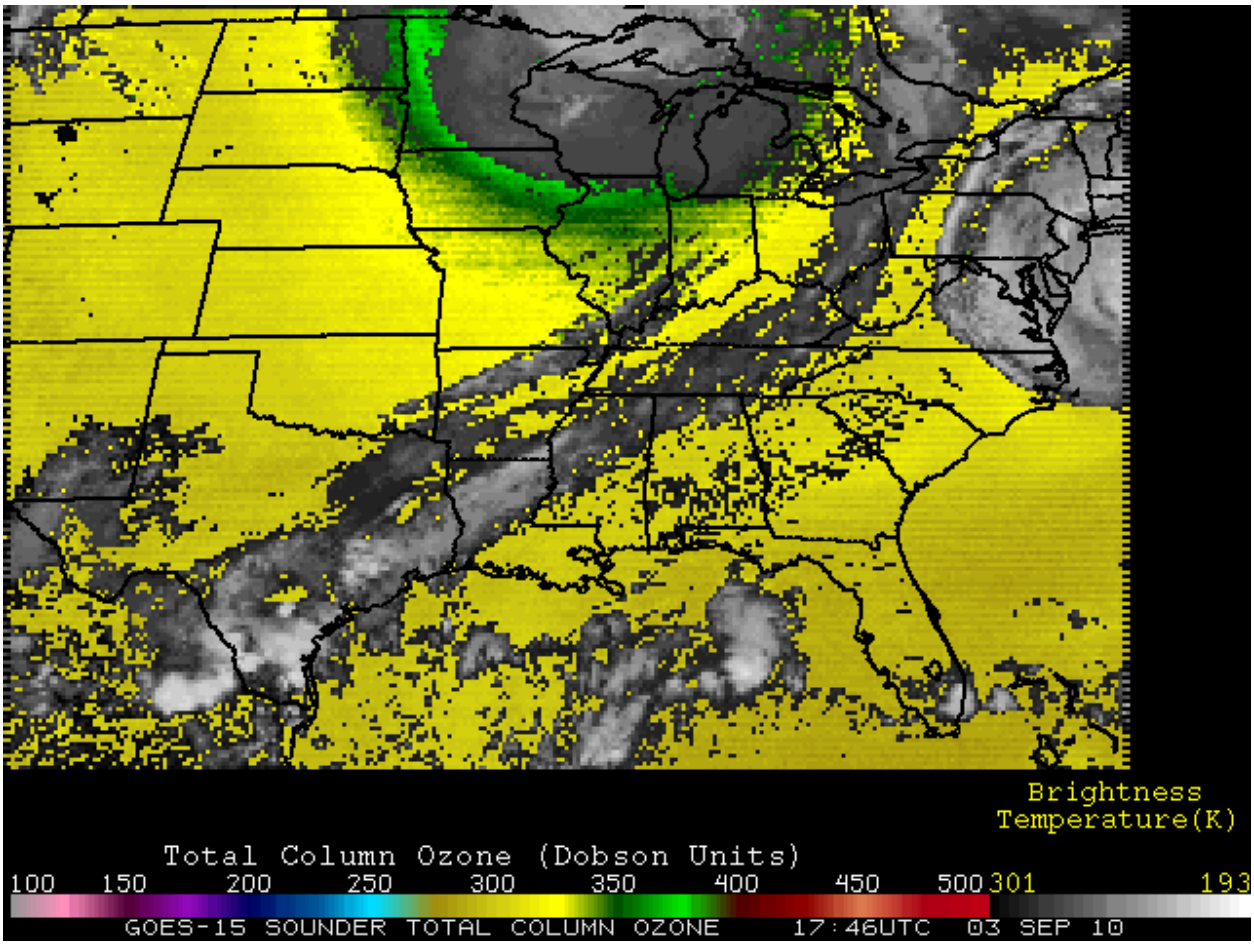

Figure 5.23: Example of GOES-15 Imager Total Column Ozone on 3 September 2010 at 1800 UTC. The image is displayed in the GOES-15 perspective.

5.10. GOES Surface and Insolation Product (GSIP)

The GOES Surface and Insolation Products (GSIP) system is operationally producing a suite of products relating primarily to upward and downward solar radiative fluxes at the surface and top of the atmosphere for the GOES series of satellites. As shown in Figures 5.24 and 5.25, the similarity of surface insolation derived from GOES-13 (the current GOES-EAST satellite) and GOES-15 data, as well as the other products, which are not shown, illustrates that GSIP is well on the way to continuing to produce a consistent dataset of the surface insolation products from the GOES-15 Imager.

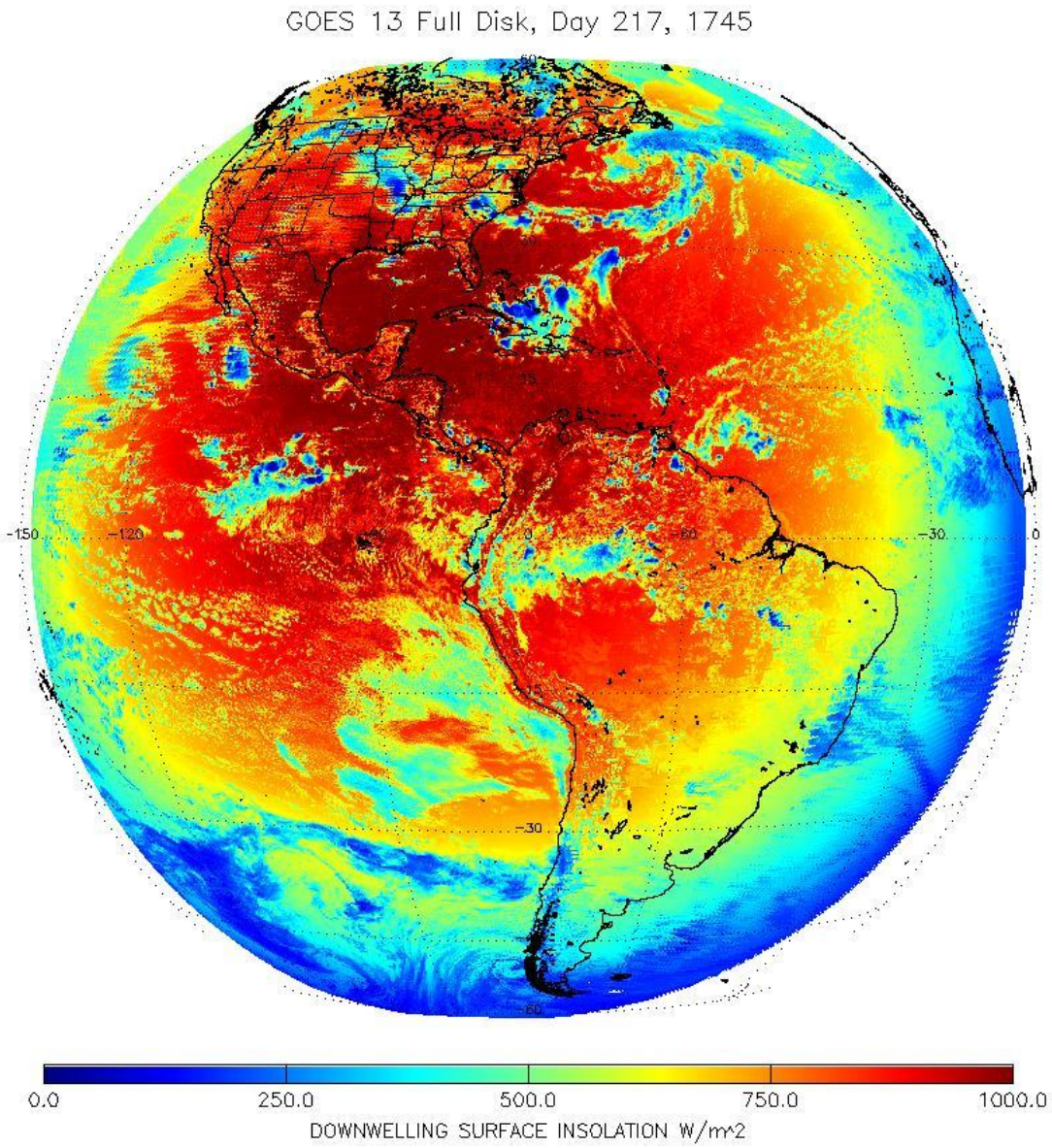

Figure 5.24: GOES-13 Imager downwelling surface insolation on 5 August 2011 beginning at 1745 UTC.

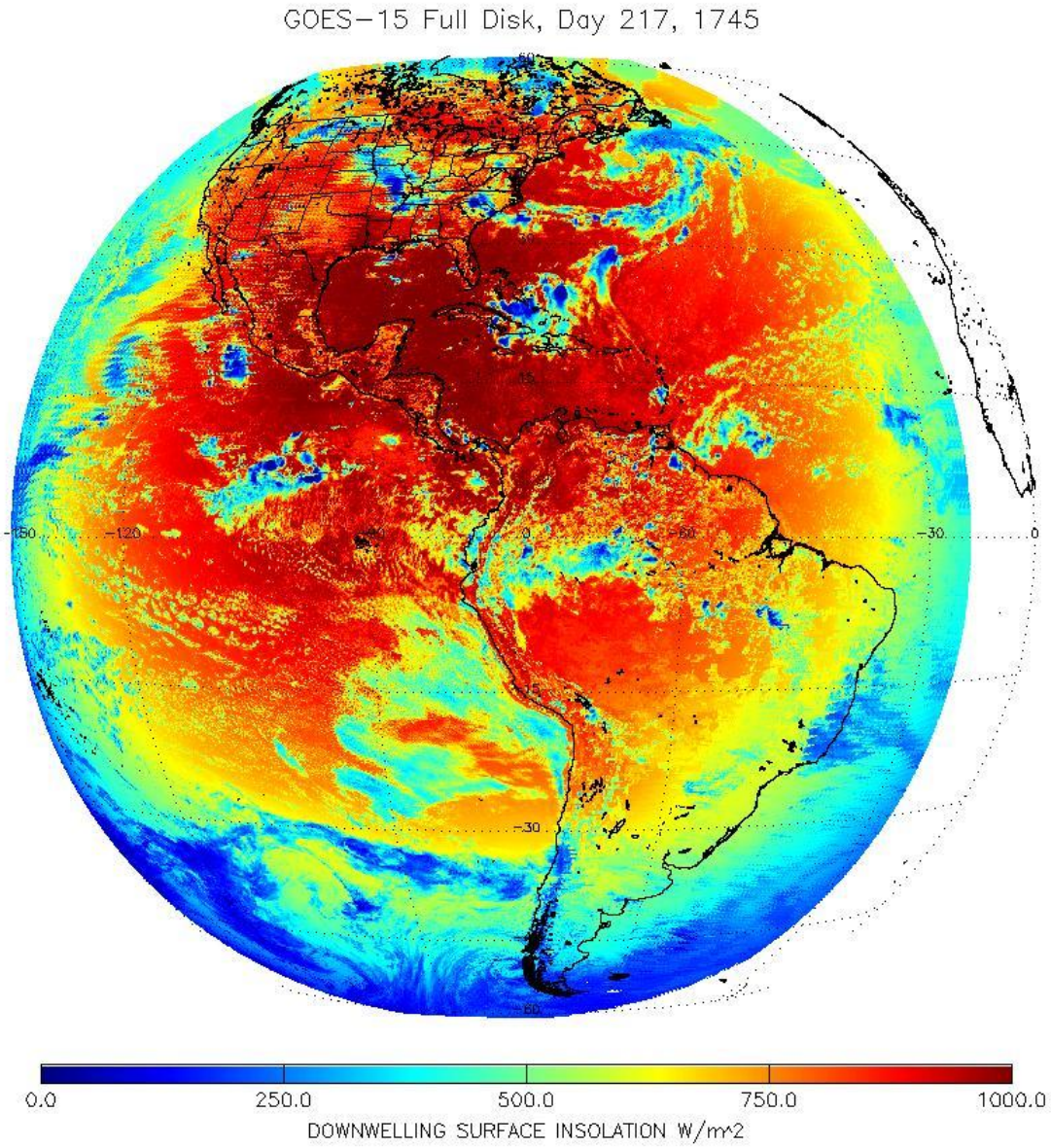

Figure 5.25: GOES-15 Imager downwelling surface insolation on 5 August 2011 beginning at 1745 UTC.

5.11. Precipitation and Tropical Applications

For precipitation, GOES-15 band-4 IR and band-1 visible imagery was compared to that of GOES-13 or GOES-11. Fourteen comparisons were completed involving a variety of meteorological events, including thunderstorms, stratiform rain events, and hurricanes. Cloud top temperatures for this wide variety of events ranged from +15°C (warm surface) to -82°C (near the eye of Hurricane Igor). Of these fourteen meteorological events, there were only minor differences observed in both band-4 IR and visible bands. Very small deviations of 1-2°C or less were occasionally noticed in the band-4 data but these deviations would not have affected or degraded precipitation operations in any way. Any subtle differences in measurements and/or

appearance were determined to be caused by the different viewing angles/parallax between GOES-15 and the comparison satellite (GOES-13 or 11).

With regard to tropical applications, similar minor discrepancies were observed in band-2 and band-4 IR imagery, with compared cloud top temperatures sometimes being slightly warmer and other times slightly colder. This result may be due to the viewing angle of the satellite, though it cannot be conclusively determined. Since the enhancement table used for the IR/SWIR (Split-Window InfraRed) is crucial to tropical cyclone intensity estimates, it is conceivable that these differences, though small, could have negatively impacted operations if they were to occur near the breaks between the various gray shades of the imagery enhancement. Note that the visible imagery from GOES-15 appeared slightly brighter than either GOES-13 or GOES-11, which is consistent as GOES-15 is a newer instrument and hence there has been less time for degradation in the visible bands.

6. Other Accomplishments with GOES-15

6.1. GOES-15 Imager Visible (band-1) SRF

A comparison of enhanced visible band images from GOES-11 and GOES-15 at 1500 UTC on 25 August 2010 is shown in Figures 6.1 and 6.2. Images from both satellites have been displayed in their native projections.

There are a couple of significant differences to note between the two visible images, while keeping in mind the very large difference in satellite view angles. GOES-15 is able to discern urban centers more readily than GOES-11 over this area, as well as variations in vegetation type. Examples of this ability are seen around the large metropolitan region of southeastern Wisconsin and northeastern Illinois (Milwaukee to Chicago). Also, both the Baraboo Range (located just to the northwest of Madison) and the "Military Ridge" (which runs east to west from Madison to Prairie du Chien) stand out more boldly in the GOES-15 image compared to the GOES-11 image. This difference is primarily due to the slight variation in the spectral width of the two visible bands on the GOES-11 and GOES-15 Imagers. A comparison of the visible band SRF for GOES-11 and GOES-15 shows that the sharper cutoff for wavelengths beyond 0.7 μm on the GOES-15 visible band makes it less sensitive to the signal from the mature corn crops, allowing greater contrast between the thick vegetation of the agricultural fields and the more sparsely vegetated cities, towns, and highway corridors.

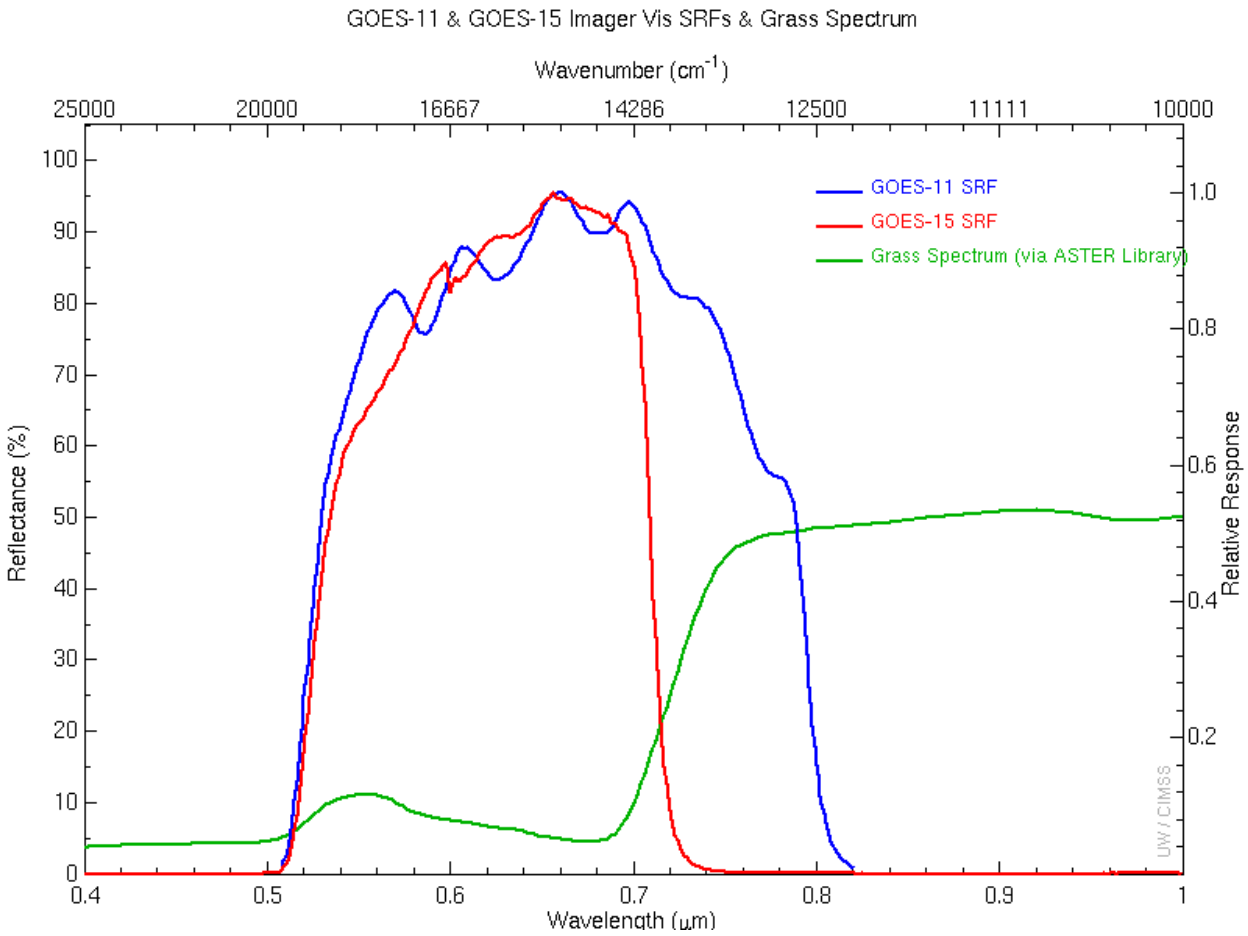

Figure 6.1: GOES-11 (blue) and GOES-15 (red) Imager visible (approximately 0.65 or 0.63 µm) band SRFs, with a representative spectrum for grass over-plotted (green).

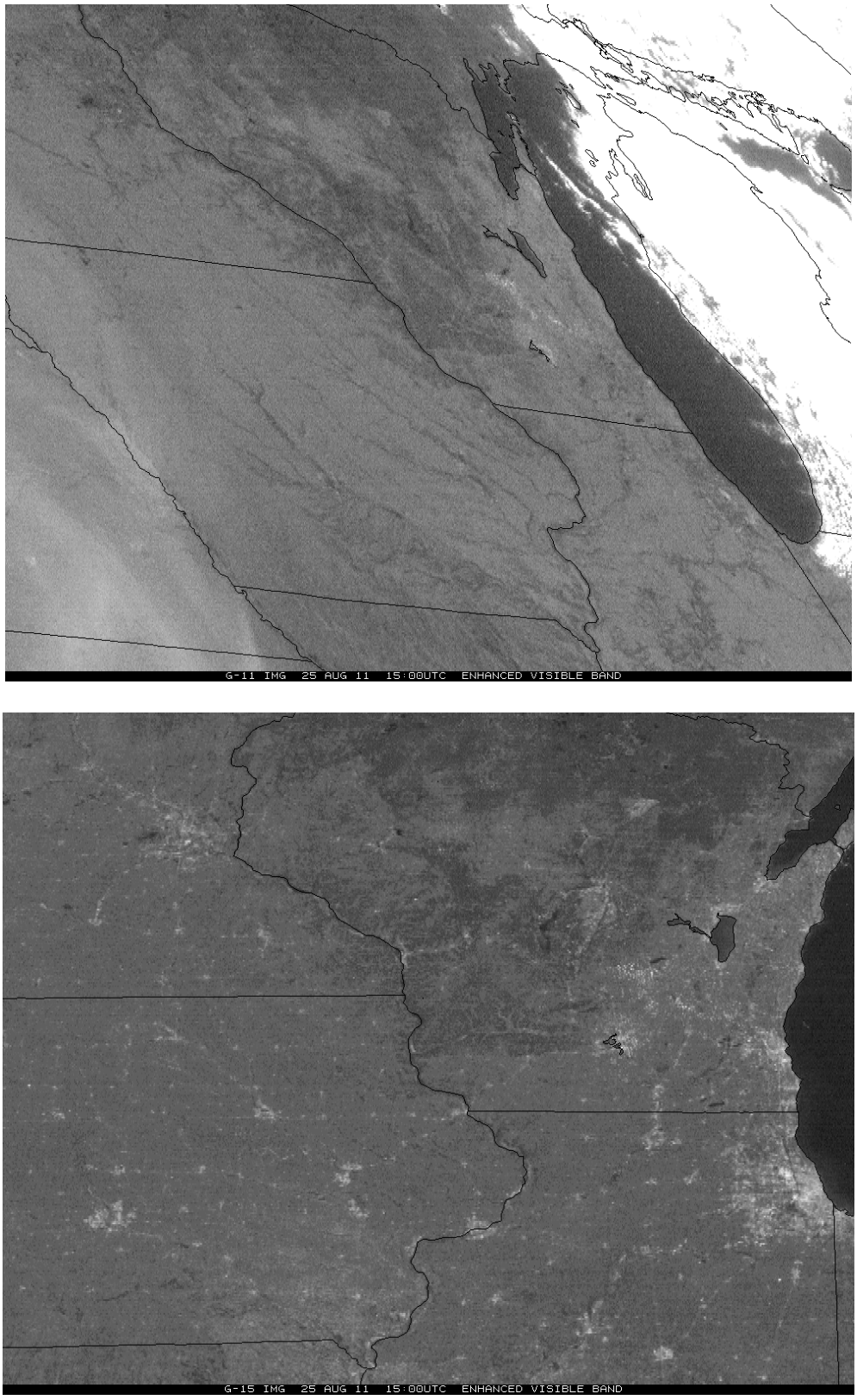

Figure 6.2: Comparison of the visible (0.65 µm) imagery from GOES-11 (top) and visible (0.63 µm) imagery from GOES-15 (bottom) on 25 August 2010 demonstrates how certain features, such as surface vegetation, are more evident with the GOES-15 visible data.

6.2. Lunar Calibration

Several GOES-15 Imager datasets were acquired during the PLT, so as to observe the lunar images as soon as possible in order to establish a baseline for future study of instrument degradation. While not intended, lunar images may allow an attempt on absolute calibration, although this theory has not been fully researched. Note that the image discontinuities are due to the relative changes in the satellite and moon geometry.

Figure 6.3: GOES-15 Imager visible (0.65 µm) band images of the moon from various dates.

The moon was intensively imaged on four different days during the PLT Science Test to investigate the scan-angle dependent reflectivity for the visible band: on 27 August 2011, in an upright position and on 22, 23 and 24 September 2010 in a yaw-flipped position. On each of these days between 13 and 84 consecutive Moon images were taken within 35 seconds of each other. Only the Moon images taken on 24 September 2010 (Julian Day 267) cover a large scan angle range from about 40.8^{o} to 49.8^{o}.

Although the Moon's surface is a good reference for the vicarious calibration of the visible band, the measured Moon irradiance can be affected by the moon surface BRDF, change in moon phase angle, and other sun-moon-satellite geometry relationships. However, the impact of these disturbances can be greatly reduced with the ratio of GOES-observed moon irradiance to the irradiance predicted with the USGS (U.S. Geological Survey) Robotic Lunar Observation (ROLO) model (Stone and Kieffer 2006). Figure 6.4 shows the observed and model irradiance ratio against the scan angle using the data obtained on 24 September 2010. The GOES moon irradiance was estimated by summing up all pixels within a lunar subset (Wu et al. 2006). It clearly shows that moon brightness decreases for angle of incidence (AOI) up to 43^{o}, peaks at approximately 45^{o}, then decreases to 47^{o}, beyond which it increases up to 50^{o}. Similar, but fractional, effects were observed on 22 and 23 September 2010 and 27 August 2010.

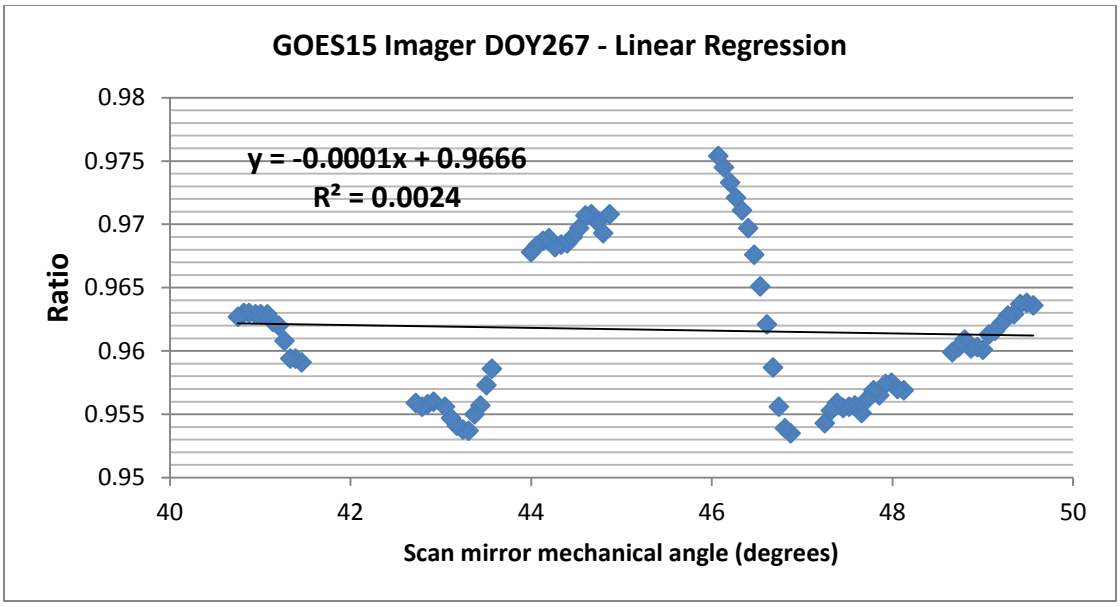

Figure 6.4: Ratio of observed and ROLO irradiance as a function of angle of incidence exhibits weak linear regression on 24 September 2010.

6.3. Improved Image Navigation and Registration (INR) with GOES-15

McIDAS images of GOES-15 visible band data show good INR performance. One example is the rapid development of a thunderstorm (along with several other storms across Arizona) on 17 August 2010. An animation can be found at http://cimss.ssec.wisc.edu/goes/blog/archives/6380.

6.4. Special 1-minute Scans

On 21 September 2010, 1-minute interval GOES-15 visible images centered on the Midwest offers a compelling demonstration of the value of frequent imaging for monitoring the development and evolution of convection. An animation of convection can be found at http://cimss.ssec.wisc.edu/goes/blog/archives/6849.

Another case was the special scans of Hurricane Igor, where a comparison of 1-minute interval GOES-15 SRSO images with the normal operational 30-minute interval GOES-13 visible images clearly demonstrates the advantage of higher temporal resolution for monitoring the evolution of the eye structure of the hurricane. More information can be found at: http://cimss.ssec.wisc.edu/goes/blog/archives/6790.

6.5. Special GOES-15 Scans

On 27 July 2011, when GOES-15 was out of storage and operating in a pre-operational mode, additional loops were made to show the GOES-15 Imager water vapor band and its 4 km resolution versus the 8 km resolution on GOES-11. In the loops, gradients are clearly depicted better (despite the vastly different view angles) as in the mid-level vortex. Animations showing these can be found at http://cimss.ssec.wisc.edu/goes/blog/archives/8529.

7. Super Rapid Scan Operations (SRSO)

During the GOES-15 Science Test, Super Rapid Scan Operations (SRSO) was called on seven separate days, typically corresponding to a meteorologically significant feature present on that day. As can be seen in Table 7.1, four of the seven calls were associated with active hurricanes in the Atlantic Ocean. On 11 September 2010, NASA/SPoRT in Huntsville requested SRSO over northern Alabama due to expected convection in the region so that they could make comparisons with their Total Lightning Mapping Array. In every case, real-time loops were created and made available over the Web to the appropriate forecasters, whether they be from the National Hurricane Center or local National Weather Service forecast offices.

Table 7.1: SRSO during the GOES-15 Science Test.

Date	Feature	Location
2010-08-24	Hurricane Danielle	18°N, 46°W
2010-09-03	Hurricane Earl	39°N, 72°W
2010-09-11	Lightning Monitoring over Huntsville AL	35°N, 87°W
2010-09-13	Hurricane Igor	18°N, 51°W
2010-09-17	Hurricane Karl	20°N, 96°W
2010-09-20	Western Fires and Fog Burnoff	39°N, 114°W
2010-09-21	Potential Severe Weather	41°N, 90°W

7.1. Overview of Operations, 11 September 2010, 1-minute SRSO, Southeast U.S.

NOAA GOES-15 SRSO were requested by the NASA/MSFC Earth Science Office to support research in algorithm development related to applications of future space-based geostationary lightning mapping systems (NOAA GOES-R Lightning Mapper (GLM)) in high-impact weather events. The satellite data combined with ground-based radar and lightning networks provide a robust means of examining cell evolution, including relationships among cloud kinematic, microphysics and lightning properties.

Operations on 11 September 2010 were centered over North Central Alabama with the goal of monitoring convective growth and decay. In particular, the objective of the day was to coordinate 1-minute GOES-15 scans with unique, high temporal, ground based measurements from the North Alabama Lightning Mapping Array (NALMA; Koshak et al. 2004), and the Advanced Radar for Meteorological and Operational Research (ARMOR; Petersen et al. 2007) C-band dual polarimetric radar.

Since most lightning casualties occur during the developing and dissipating portions of most thunderstorms, one important objective of current lightning research is better nowcasting of lightning initiation and cessation. Figures 7.1 and 7.2 display a small isolated thunderstorm located just west of Huntsville between 1810 and 1850 UTC. Figure 7.2 is a sequence of ARMOR images at an elevation of 11.4° (height ≈ 6 km and temperature ≈ -10°C at range of interest) using horizontal reflectivity (Z), differential reflectivity (ZDR) and correlation coefficient (ρ_{hv}) at 1817 (A-C), 1820 (D-F), and 1822 UTC (G-I). At 1817 UTC the cell of interest had a well developed ZDR column (4 dB), with a dip in ρ_{hv} (≈0.90) in a region of

moderate-to-high Z (35-50 dBZ), which is indicative of large supercooled rain drops, likely in the early stages of freezing. The cloud top temperature for this cell was near 261 K, and no lightning was present within the storm. At 1820 UTC, the ZDR column began to glaciate, as ZDR became smaller and a prominent lowering of ρ_{hv} continued, indicating mixed-phase precipitation (rain and frozen drops). By 1822 UTC, the glaciation of the supercooled raindrop column was likely complete, as suggested by the moderate Z (35-45 dBZ), low ZDR (< 1 dB) and high ρ_{hv} ($\geq$ 0.98).

During the period from 1820-1822 UTC, the cloud top temperature dropped 1 K to 260 K. Between 1822 and 1829 UTC the cloud top cooled at a more rapid rate, as the temperature dropped to 257 K. At 1829 UTC the first lightning flashes from the thunderstorm were observed by the NALMA. The cloud top temperature continued to fall over the next 12 minutes and reached a minimum of 238 K by 1841 UTC. During this period, the total flash rate for the thunderstorm peaked at 7 flashes per minute, and the thunderstorm top grew from 13 km to just below 15 km (Figure 7.1). At 1845 UTC the thunderstorm collapsed and the final two lightning flashes were observed soon after. Similar observations of decreasing cloud top temperatures prior to lightning initation were observed in several other thunderstorm cells from this day (e.g., Figure 7.3). Minimum temperatures observed just prior to the first flash in each storm ranged from 249-257 K.

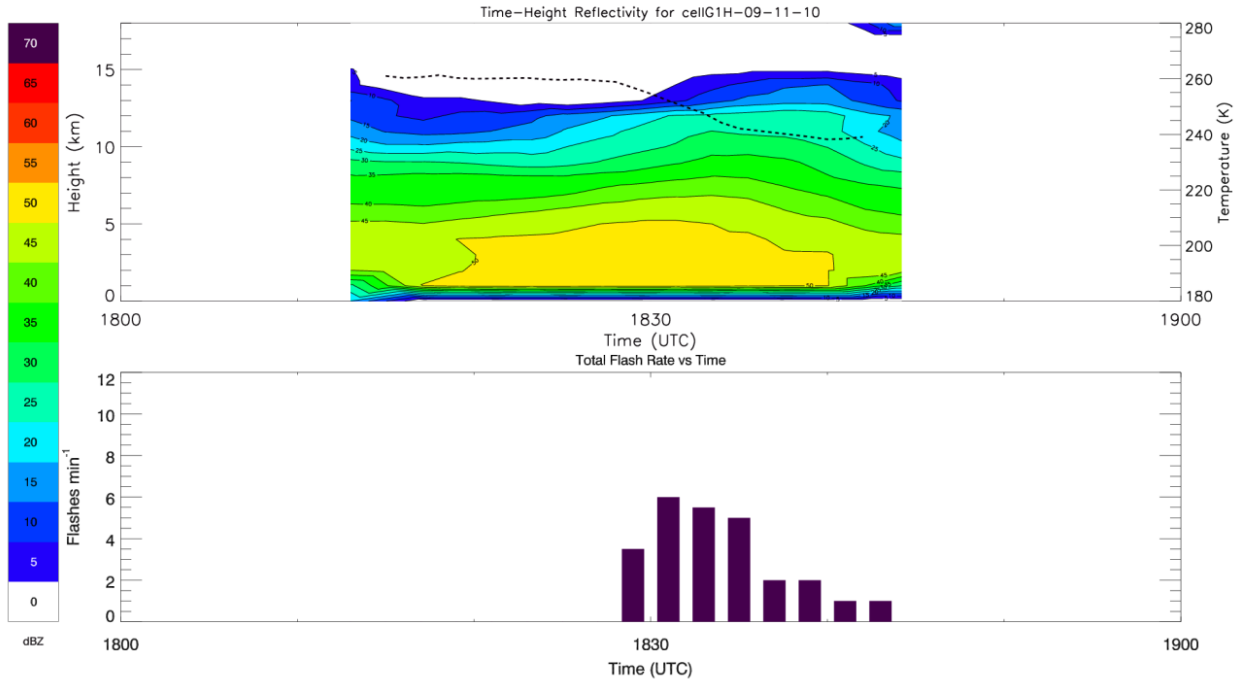

Figure 7.1: Time-height cross-section of maximum reflectivity vs. height (top), minimum cloud top temperature (dashed line, top) and total flash rate (bottom).

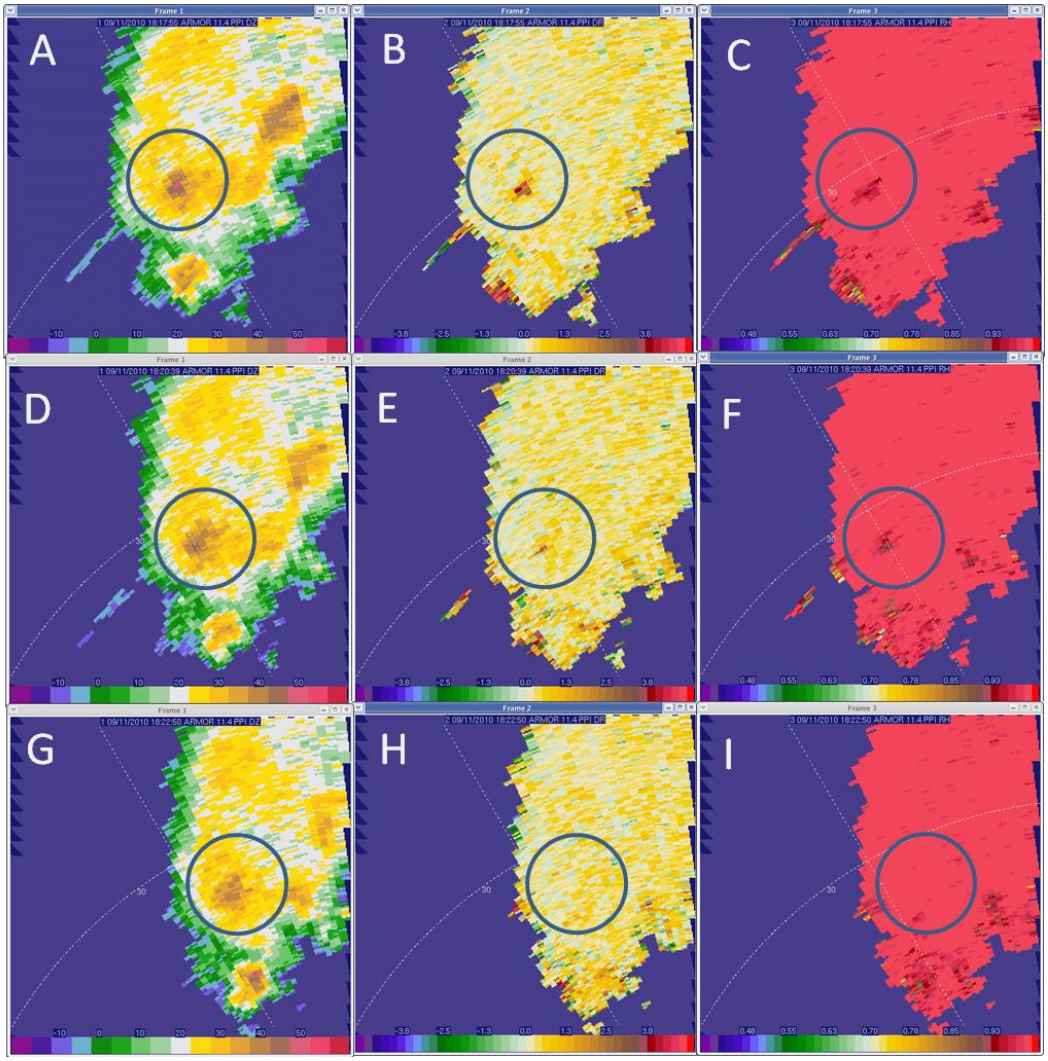

Figure 7.2: A series of Plan Position Indicator (PPI) images from ARMOR on 11 September 2010, between 1817 and 1822 UTC at 11.4° elevation (height ≈ 6 km and temperature ≈ -10°C at range of interest). Panels A-C are at 1817 UTC, D-F at 1820 UTC, and G-I at 1822 UTC. From left to right, radar fields presented here are horizontal reflectivity (Z), differential reflectivity (ZDR), and correlation coefficient (ρ_{hv}).

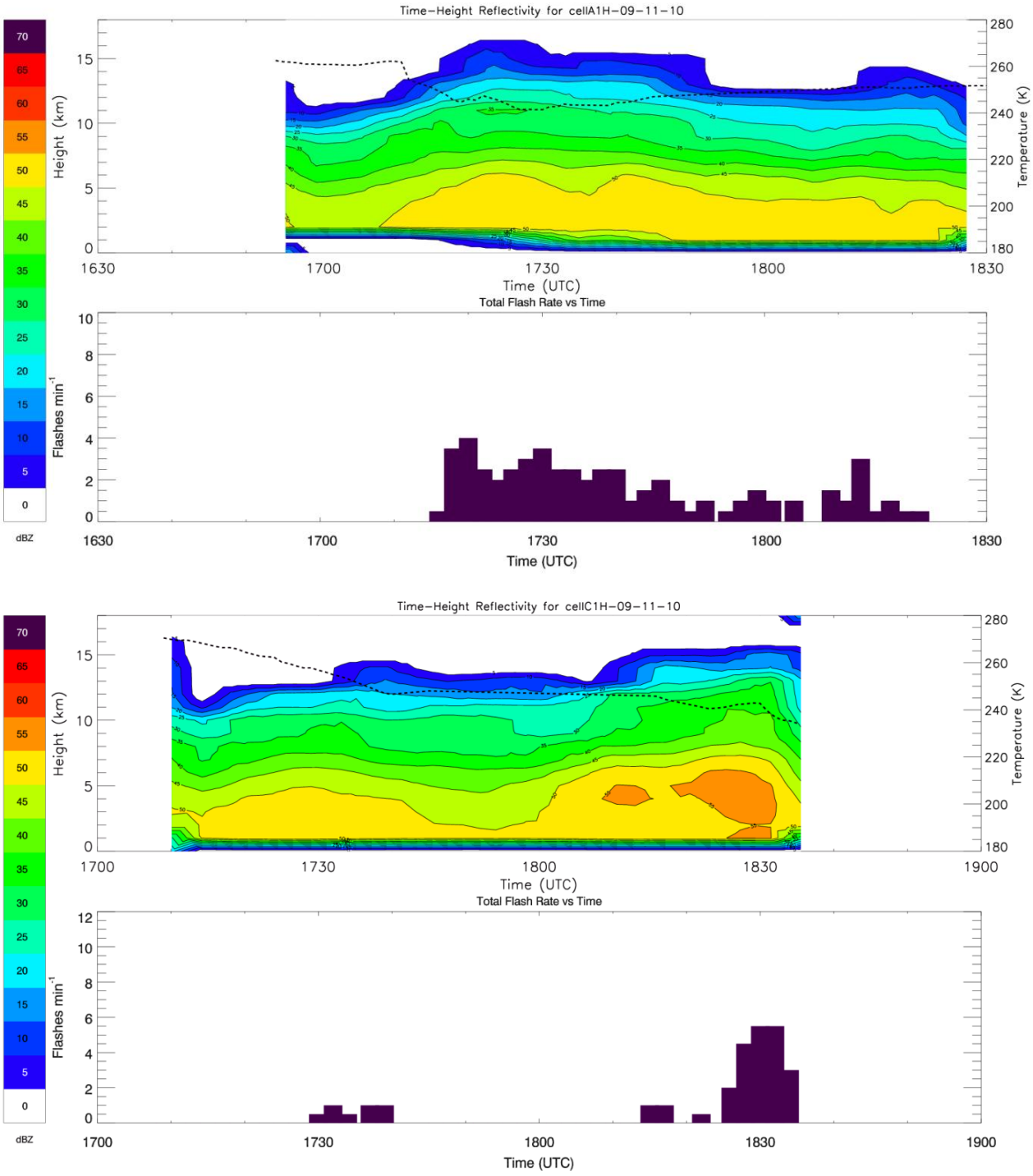

Figure 7.3: Time-height section of maximum reflectivity vs. height minimum cloud top temperature and total flash rate for two additional thunderstorms on 11 September 2010. Thunderstorm A (top) obtained a minimum temperature of 249 K before the first flash was observed, while thunderstorm C (bottom) had a minimum cloud top temperature of 256 K before the first flash was observed at 1728 UTC.

8. Overall Recommendations Regarding This and Future GOES Science Tests

The following conclusions and recommendations were drawn during the GOES-15 Science Test:

- Each of the four main goals of the GOES-15 Science Test were accomplished. The goals were to characterize the radiance integrity, generate products, acquire unique image sequences, and monitor instrument changes.

- The updated (Rev. H with the StAR correction) Imager and Sounder SRF should be used for any subsequent product generation. In the future, the latest system SRF should be made available well before the start of the Science Test.

- Science Tests should continue as a vital aspect of the checkout of each GOES satellite, as studying real-time data are an effective way to detect problems in the data stream, ground systems and product generation/use. To best test the overall system, the data should continue to flow via the operational path, even before the operation period.

- Science Test duration should be at least 5 weeks for 'mature' systems (and ideally should be during times with active convection over the continental U.S.). Much longer Science Tests will be needed for new systems such as GOES-R. It is expected on the order of a year will be needed for the many steps of engineering, science, products, validation and user readiness. This schedule could be split between a 6-month period of NASA-controlled time, followed by a 6-month period after the hand-over to NOAA. A longer period would also increase the odds of observing episodic events, such as volcanic activity.

- A Science Test could be preceded by several weeks of GOES-East and/or GOES-West schedule emulations. This plan would allow for more routine testing in operations, and then more flexibility during the Science Test itself. The Science Test should contain a mixture of the expected operational scan scenarios, along with any needed special scans.

- An additional aspect to the Science Test could involve yearly checkout of GOES data when individual spacecraft are taken out of storage and turned on for other purposes.

- While the GOES-15 GVAR data are captured and saved by a number of research groups, these unique and important pre-operational data should be part of the official GOES archive and be made available.

- Ideally, as many groups as possible should get access to the pre-operational images and products. This availability would help test the flow and quality of the information before operations, which is especially important for Numerical Weather Prediction (NWP) applications.

Acknowledgments

A large number of people played important roles in the success of the GOES-15 Science Test. The contributors listed on the front cover of this report provided analysis of GOES-15 radiance data and Imager and Sounder products. Yet, it takes many to accomplish the needed tasks to check-out a satellite. These include the government (NOAA, NASA), industry (Boeing, contractors, etc) and Universities (Cooperative Institutes, etc). Dan Lindsey and John Knaff (StAR/RAMMB), Gary Wade (StAR/ASPB), and Scott Bachmeier (UW/CIMSS) are specially thanked for their participation in the daily coordination where decisions were made to determine which Science Test schedules should be implemented in order to either capture interesting weather events, or to meet the requirements for the various data tests and generation of products. Scott is also thanked for his many informative satellite blog posts. Istvan Laszlo is thanked for his input on the GSIP images. In addition, thanks to Kevin Ludlum (GOES Scheduling Lead) and the rest of the GOES-15 Team at NOAA/NESDIS Office of Satellite and Product Operations (OSPO), for coordinating and establishing the numerous schedules and sectors used during the Science Test. Matt Seybold and Natalia Donoho of the Satellite Services Division User Services are also thanked. The entire SAB staff is thanked for their analysis with respect to the tropical, fire, volcano, and precipitation desks. Hyre Bysal, John Tsui, Ken Mitchell, J. Paul Douglas, Tom Renkevens and Mike Weinreb are thanked for their GOES engineering and calibration expertise.

The following are also acknowledged for their detailed reviews of the final document: Leanne Avila and Kate Maclay.

This project was funded by the NOAA/NESDIS Office of Systems Development (OSD) via the GOES I/M Product Improvement Plan (GIMPAP).

References / Bibliography

Daniels, J.M., T.J. Schmit, and D.W. Hillger, 2001: Imager and Sounder Radiance and Product Validations for the GOES-11 Science Test, *NOAA Technical Report NESDIS 103*, (August), 49 pp.

Eilers, P.H.C., and Goeman, J.J., 2004: Enhancing scatter plots with smoothed densities, *Bioinformatics*, **20**(5):623-628.

Gunshor, M., T. Schmit, W. Menzel, and D. Tobin, 2009: Inter-calibration of broadband Geostationary Imagers using AIRS, *J. Atmos. Oceanic Tech.*, **26**, 746-758.

Hillger, D.W., and T.J. Schmit, 2007: Imager and Sounder Radiance and Product Validation for the GOES-13 Science Test. *NOAA Technical Report, NESDIS 125*, (September), 75 pp.

Hillger, D.W., and T.J. Schmit, 2009: The GOES-13 Science Test: A Synopsis, *Bull. Amer. Meteor. Soc.*, **90**, 6-11.

Hillger, D.W., and T.J. Schmit, 2010: Imager and Sounder Radiance and Product Validation for the GOES-14 Science Test, *NOAA Technical Report, NESDIS 131*, (September), 105 pp.

Hillger, D.W., T.J. Schmit, and J.M. Daniels, 2003: Imager and Sounder Radiance and Product Validation for the GOES-12 Science Test, *NOAA Technical Report, NESDIS 115*, (September), 70 pp.

Hillger, D.W., and T.H. Vonder Haar, 1988: Estimating Noise Levels of Remotely Sensed Measurements from Satellites Using Spatial Structure Analysis, *J. Atmos. Oceanic Technol.*, **5**, 206-214.

Johnson, R., and M. Weinreb, 1996: GOES-8 Imager mid-night effects and slope correction. *Proc. SPIE*, Vol. **2812**, 596, dio:10.1117/12.254104.

Koshak, W.J., R.J. Solakiewicz, R.J. Blakeslee, S.J. Goodman, H.J. Christian, J.M. Hall, J.C. Bailey, E.P. Krider, M.G. Bateman, D.J. Boccippio, D.M. Mach, E.W. McCaul, M.F. Stewart, D.E. Buechler, W.A. Petersen, and D.J. Cecil, 2004: North Alabama Lightning Mapping Array (LMA): VHF source retrieval algorithm and error analysis, *J. Atmos. Ocean. Tech*., **21**, 543-558.

Li, Z., J. Li, W.P. Menzel, T.J. Schmit, J.P. Nelson III, J. Daniels, and S.A. Ackerman, 2008: GOES sounding improvement and applications to severe storm nowcasting, *Geophys. Res. Lett.*, **35**, L03806, doi:10.1029/2007GL032797.

Ma, X.L., T. Schmit, and W.L. Smith, 1999: A non-linear physical retrieval algorithm - its application to the GOES-8/9 Sounder, *J. Appl. Meteor.*, **38**, 501-513.

Menzel, W.P., F.C. Holt, T.J. Schmit, R.M. Aune, G.S. Wade, D.G. Gray, and A.J. Schreiner, 1998: Application of GOES-8/9 Soundings to weather forecasting and nowcasting, *Bull. Amer. Meteor. Soc.*, **79**, 2059-2078.

Merchant, C.J., A.R. Harris, E. Maturi, and S. MacCallum, 2005: Probabilistic physically-based cloud-screening of satellite infrared imagery for operational sea surface temperature retrieval, *Quart. J. Roy. Meteorol. Soc.*, **131**(611), 2735-2755.

Merchant, C.J., A.R. Harris, E. Maturi, O. Embury, S.N. MacCallum, J. Mittaz, and C.P. Old, 2009: Sea Surface Temperature Estimation from the Geostationary Operational Environmental Satellite 12 (GOES-12), *J. Atmos. Oceanic Technol*., **26**, 570-581.

Petersen, W.A., K.R. Knupp, D.J. Cecil, and J.R. Mecikalski, 2007: The University of Alabama Huntsville THOR Center instrumentation: Research and operational collaboration. Preprints, *33rd International Conf. Radar Meteorology*, Cairns, Australia, Amer. Meteor. Soc.

Schmit, T.J., E.M. Prins, A.J. Schreiner, and J.J. Gurka, 2002a: Introducing the GOES-M Imager, *Nat. Wea. Assoc. Digest*, **25**, 2-10.

Schmit, T.J., W.F. Feltz, W.P. Menzel, J. Jung, A.P. Noel, J.N. Heil, J.P. Nelson III, G.S. Wade, 2002b: Validation and Use of GOES Sounder Moisture Information, *Wea. Forecasting*, **17**, 139-154.

Stone, T.C., and H.H. Kieffer, 2006: Use of the Moon to support on-orbit sensor calibration for climate change measurements, *Proc. SPIE*, 6296 6296Y-1-9.

Tahara, Y., and K. Kato, 2009: New spectral compensation method for inter-calibration using high spectral resolution sounder, *Met. Sat. Center Technical Note*, No. 52, 1-37.

Weinreb, M.P., M. Jamison, N. Fulton, Y. Chen, J.X. Johnson, J. Bremer, C. Smith, and J. Baucom, 1997: Operational calibration of Geostationary Operational Environmental Satellite-8 and -9 Imagers and Sounders. *Appl. Opt.*, **36**, 6895-6904.

Wolfe, D., and S.I. Gutman, 2000: Developing an operational, surface-based, GPS, water vapor observing system for NOAA: Network design and results. *J. Atmospheric and Oceanic Tech*., **17**, 426-440.

Wu, X., and S. Sun, 2005: Post-launch calibration of GOES Imager visible band using MODIS, *Proc. SPIE*, Vol. **5882**, doi:10.1117/12.615401.

Wu, X., T. Schmit, and M. Gunshor, 2009: Correction for GOES-13 Imager 13.3 μm Channel Spectral Response Function, *NOAA/NESDIS/StAR Calibration Product Oversight Panel (CalPOP) Technical Memorandum*, 13 March, 9 pp.

Wu, X., T. Stone, F. Yu, and D. Han, 2006: Vicarious calibration of GOES Imager visible channel using the Moon, *Proc. SPIE*, 6296, doi:10.1117/12.681591.

Wu, X., and F. Yu, 2011: Personal communication.

Yu, F. and X. Wu, 2010: Instrument performance monitoring of GOES Imager and Sounder instruments, Calcon (http://www.sdl.usu.edu/conferences/calcon/previous), 23-26 August, Logan, UT.

Yu, F., X. Wu, M.K. Rama Varma Raja, L. Wang, Y. Li, and M. Goldberg, 2011. Evaluation of the diurnal and scan angle calibration variation of GOES Imager infrared instruments, submitted to *IEEE Transactions on Geosciences and Remote Sensing*.

Appendix A: Web Sites Related to the GOES-15 Science Test

GOES-15 NOAA/Science Post-Launch Test: http://rammb.cira.colostate.edu/projects/goes-p (updated daily during the Science Test)

GOES-15 RAMSDIS Online: http://rammb.cira.colostate.edu/ramsdis/online/goes-15.asp (contained real-time GOES-15 imagery and products during the Science Test)

CIMSS Satellite Blog: Archive for the 'GOES-15' Category: http://cimss.ssec.wisc.edu/goes/blog/archives/category/goes-15

NESDIS/StAR: GOES-15 First Images Transmitted: http://www.star.nesdis.noaa.gov/star/news2010_201004_GOES15.php

NOAA: GOES-15 Weather Satellite Captures Its First Image of Earth: http://www.noaanews.noaa.gov/stories2010/20100407_goes15.html

CIMSS GOES Calibration: http://cimss.ssec.wisc.edu/goes/calibration

NOAA: GOES Imager and Sounder SRF: http://www.oso.noaa.gov/goes/goes-calibration/goes-imager-srfs.htm http://www.oso.noaa.gov/goes/goes-calibration/goes-sounder-srfs.htm

GOES Imager Calibration: http://www.star.nesdis.noaa.gov/smcd/spb/fwu/homepage/GOES_Imager.php

Global Satellite Inter-Calibration System (GSICS) GEO-LEO baseline inter-calibration ATBD https://gsics.nesdis.noaa.gov/pub/Development/AtbdCentral/ATBD_for_NOAA_Inter-Calibration_of_GOES-AIRSIASI.2011.06.15.doc

NOAA, Office of Systems Development: The GOES-P Spacecraft: http://www.osd.noaa.gov/Spacecraft%20Systems/Geostationary_Sat/GOES_Sat_Info/goes_p_info.html (including GOES Data Book: http://goes.gsfc.nasa.gov/text/goes.databookn.html)

NASA GSFC: GOES-P Mission Overview video: http://www.youtube.com/watch?v=QpBSwwCPC94&list=PL05E2409F3516100B&index=6

NASA GSFC: GOES-O Project: GOES-O Spacecraft: http://goespoes.gsfc.nasa.gov/goes/spacecraft/goes_o_spacecraft.html

NASA-HQ: GOES-O Mission: http://www.nasa.gov/mission_pages/GOES-O/main/index.html

Boeing: GOES-N/P: http://www.boeing.com/defense-space/space/bss/factsheets/601/goes_nopq/goes_nopq.html

CLASS: http://www.class.ngdc.noaa.gov/saa/ products/welcome

Appendix B: Acronyms (and Abbreviations) Used in this Report

ABI	Advanced Baseline Imager (GOES-R)
AIRS	Atmospheric InfraRed Sounder
AMV	Atmospheric Motion Vector
AOI	Angle of Incidence
ARMOR	Advanced Radar for Meteorological and Operational Research
ASPB	Advanced Satellite Products Branch
ATBD	Algorithm Theoretical Basis Document
BB	Black Body
BRDF	Bi-directional Reflectance Distribution Function
CICS	Cooperative Institute for Climate Studies
CIMSS	Cooperative Institute for Meteorological Satellite Studies
CIRA	Cooperative Institute for Research in the Atmosphere
CLASS	Comprehensive Large Array-data Stewardship System
CON	CONUS (sector)
CONUS	Continental United States
CRTM	Community Radiative Transfer Model
CSBT	Clear Sky Brightness Temperature
dB	Decibel
dBZ	Decibels of Z (radar reflectivity)
DPI	Derived Product Image
ECMWF	European Centre for Medium-range Weather Forecasts
EMC	Environmental Modeling Center
EOS	Earth Observation System
EUMETSAT	European Organization for the Exploitation of Meteorological Satellites
FD	Full Disk (sector)
FOV	Field Of View
GEO	Geostationary Earth Orbit
GFS	Global Forecast System
GIMPAP	GOES I/M Product Improvement Plan
GLM	GOES-R Lightning Mapper
GOES	Geostationary Operational Environmental Satellite

GOES-R	Next generation GOES, starting with GOES-R
GRIP	Genesis and Rapid Intensification Processes
GPS	Global Positioning System
GSFC	Goddard Space Flight Center
GSICS	Global Space-based Inter-Calibration System
GSIP	GOES Surface and Insolation Product
GVAR	GOES Variable (data format)
hPa	Hectopascals (equivalent to *millibars* in non-SI terminology)
HUR	Hurricane (sector)
IASI	Infrared Atmospheric Sounding Interferometer
INR	Image Navigation and Registration
IPM	Instrument Performance Monitoring
IR	InfraRed
ITT	ITT Corporation
JMA	Japanese Meteorological Agency
KOZ	Keep Out Zone
LEO	Low Earth Orbit
LI	Lifted Index
LMA	Lightning Mapping Array
MAE	Mean Absolute Error
MBCC	Midnight Blackbody Calibration Correction
McIDAS	Man-Computer Interactive Data Access System
MetOp	Meteorological Operational (satellite)
MODIS	Moderate Resolution Imaging Spectroradiometer
MOON	Moon (sector)
MSFC	Marshall Space Flight Center
MVD	Mean Vector Difference
NALMA	North Alabama Lightning Mapping Array
NASA	National Aeronautics and Space Administration
NCEP	National Centers for Environmental Prediction
NEdR	Noise Equivalent delta Radiance (Sometimes given as NEdN)
NEdT	Noise Equivalent delta Temperature

NESDIS	National Environmental Satellite, Data, and Information Service
NHEM	Northern Hemisphere
NOAA	National Oceanic and Atmospheric Administration
NSF	National Science Foundation
NWP	Numerical Weather Prediction
OSD	Office of Systems Development
OPDB	Operational Products Development Branch
ORA	Office of Research and Applications (now StAR)
OSPO	Office of Satellite and Product Operations
PLT	Post-Launch Test
PPI	Plan Position Indicator
PREDICT	PRE-Depression Investigation of Cloud-systems in the Tropics
PRT	Platinum Resistance Thermometer
PSF	Point Spread Function
PW	Precipitable Water
RAMMB	Regional and Mesoscale Meteorology Branch
RAMSDIS	RAMM Advanced Meteorological Satellite Demonstration and Interpretation System
RAOB	Radiosonde Observation
Rev.	Revision
RMS	Root Mean Square
RMSE	Root Mean Square Error
ROLO	Robotic Lunar Observation
RT	Real Time
RTM	Radiative Transfer Model
RTN	Routine (sector)
SAB	Satellite Analysis Branch
SOCC	Satellite Operations Control Center
SOCD	Satellite Oceanography and Climatology Division
SC	Spacecraft
SPB	Sensor Physics Branch
SPEC	Specifications

SPoRT	Short-term Predication Research and Transition center
SPS	Sensor Processing System
SRF	Spectral Response Function
SRSO	Super Rapid Scan Operations
SSEC	Space Science and Engineering Center
SST	Sea Surface Temperature
StAR	SaTellite Applications and Research (formerly ORA)
stdv	Standard deviation
SWIR	Split-Window InfraRed
Tb	Brightness temperature
TCO	Total Column Ozone
THOR	Tornado and Hazardous weather Observations Research center
TOA	Top-of-Atmosphere
TPW	Total Precipitable Water
USGS	U.S. Geological Survey
UTC	Coordinated Universal Time
μm	Micrometers (*micron* was officially declared obsolete in 1968)
UW	University of Wisconsin (Madison)
WF_ABBA	Wildfire Automated Biomass Burning Algorithm
Z	Radar reflectivity
ZDR	Differential reflectivity